9th Edition

OPTICAL STIMULATION & IMAGING SYSTEMS
FOR BIOSCIENCES

PRODUCT CATALOG

MIGHTEX

Leader in All-Optical Cellular-Resolution
Optogenetics Photostimulation Calcium Imaging

Optical Stimulation & Imaging Systems for Biosciences
9th Edition
MIGHTEX

TABLE OF CONTENT

POLYGON DMD PATTERN ILLUMINATORS

Precise spatial, temporal, and/or spectral control of light is vital for many cutting-edge scientific applications (such as optogenetics, photostimulation, uncaging, etc.). Patterned illumination provides scientists with advanced capabilities that are not possible with wide-field illumination. In particular, precise 2D spatial control of light is crucial for the field of optogenetics, in which patterned illumination enables scientists to precisely deliver light of different colors, with high spatial and temporal resolution, to stimulate or silence cells or subcellular features. Such capabilities will facilitate functional understanding of single-cell activity and/or neural circuits in the brain, which otherwise impossible.

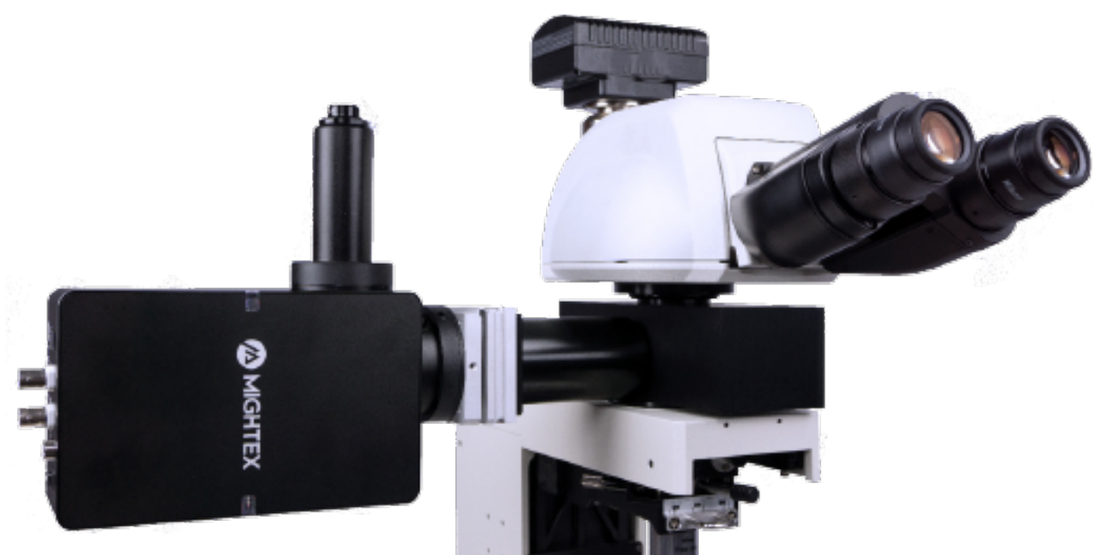

Overview

The requirement for precise spatial, temporal, and/or spectral control of light is vital for many cutting-edge scientific applications, such as optogenetics, photostimulation, and uncaging etc. Mightex's market-leading Polygon Patterned Illuminators enable bioscientists to selectively illuminate multiple cellular or subcellular targets with different wavelengths of light. The Polygon integrates state-ofthe-art digital micromirror (DMD) technology and high-power light sources to deliver high-intensity, high-uniformity illumination patterns with diffraction-limited resolution. With user-friendly software and hardware operation, the Polygon provides an optimized system for experiments requiring precisely targeted stimulation. Because each mirror in the array is individually addressable, users can simulteneously illuminate multiple spots that are sub-micron in size, depending on the microscope objective used. Users can also control a group of mirrors to deliver light in any custom-defined, unique shape with a very high resolution.

FEATURES

- Unlimited spatial & temporal control of light illumination: any size, any shape and anywhere
- Simultaneous illumination of multiple regions of interest
- High spatial resolution with over 1,000,000 pixels
- On-board memory capable of holding >2,000 patterns
- Frame rate up to 6,600Hz
- Uploading speed ~4ms (with USB3), enabling real-time projection and closed-loop control
- Large DMD chip capable of handling ultra high optical power for large-area illumination
- Compatible with all light sources: LEDs, lasers or arc lamps
- Interchangeable 1x and 2x front tubes for FoV and spatial resolution optimization
- Software compatibility: PolyScan, NIS Elements and MicroManager

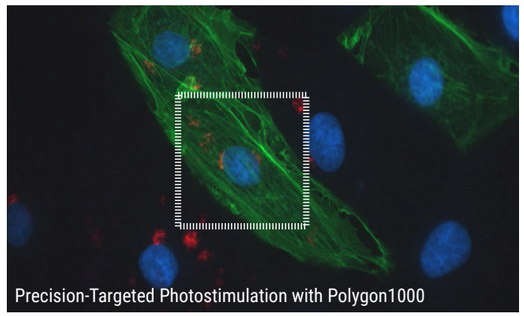
Precision-Targeted Photostimulation with Polygon1000

DMD Technology

The Polygon includes a DMD chip that is composed of more than one (1) million micromirrors that can be individually turned ON/OFF to reflect light onto the sample. Thus, you can assign each mirror to control the area(s) of illumination and create any number of different-sized ROIs simultaneously.

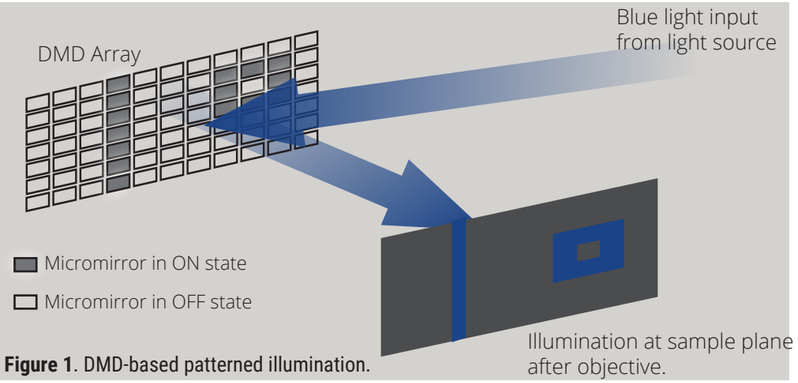

Figure 1. DMD-based patterned illumination.

Polygon Models

Mightex's Polygon pattern illuminators all use a DMD chip with approximately 1,000,000 pixels. Depending on the type of optical input port, the Polygon1000 product family can be generally grouped into two series: (1) Polygon1000-G with a lightguide input; and (2) Polygon1000-DL with a fiber input. Both Polygon1000-G and Polygon1000-DL are leading the market with a very high contrast ratio of 4,000:1. For those mission-critical bioscience applications that call for extremely high contrast ratio with any background completely eliminated, Mightex has developed the ground-breaking Polygon UHC pattern illuminator, which offers the cutting-edge contrast ratio of 10,000,000:1. See below for more.

Polygon1000-G

Model#: DSI-K3-000

- Accepts a 3mm-core lightguide input
- Compatible with any light source
- Wavelength range: 350nm-850nm
- High contrast ratio of 4,000:1
- Add-on front tube available for large field of view

Polygon1000-DL

Model#: DSI-K3-L00

- Accepts SMA-connectorized optical fiber (400μm, 0.22NA recommended)
- Compatible with laser sources
- Wavelength range: 400nm-850nm
- High contrast ratio of 4,000:1

Polygon1000-UHC

Model#: DSI-K3-UHC-000

- Accepts SMA-connectorized optical fiber (400μm, 0.22NA recommended)
- Compatible with laser sources
- Wavelength range: 400nm-850nm
- Super high contrast ratio of 10,000,000:1

Selection Guide

STEP 1

CHOOSE WAVELENGTH(S)

Choose the right light source(s) according to your specific application. For example, for optogenetics applications you may choose 470nm for ChR2 stimulation and 590nm for NpHR stimulation.

STEP 2

CHOOSE POLYGON MODEL

Determine which Polygon model will work best for your application. For UV (below 400nm) applications, our Polygon1000-G is recommended. For super-high power applications the Polygon1000-DL is recommended.

STEP 3

CHOOSE MICROSCOPE ADAPTOR

Choose the appropriate microscope adaptor for mounting the Polygon onto your specific microscope. The Polygon is compatible with upright or inverted microscopes from any commercial brand including (but not limited to) Leica, Nikon, Olympus and Zeiss.

Technical Specifications

ILLUMINATION FIELD OF VIEW AND RESOLUTION

Model	FOV	Projection Area	Commercial Microscope (1X Objective)[a]			
			Leica	Nikon	Olympus	Zeiss
POLYGON1000-G	Standard	Height | mm	6.2	6.2	5.5	5.1
		Width | mm	9.9	9.9	8.9	8.1
		Diagonal | mm	11.6	11.6	10.5	9.6
		Pixel Size | µm	7.6	7.6	6.9	6.3
	Large[c]	Height | mm	12.4	12.4	11	10.2
		Width | mm	19.8	19.8	17.8	16.2
		Diagonal | mm	23.2	23.2	21	19.2
		Pixel Size | µm	15.2	15.2	13.8	12.6
POLYGON1000-DL & POLYGON UHC	Standard	Diameter[b] | mm	12.4	12.4	11	10.2
		Pixel Size | µm	15.2	15.2	13.8	12.6

[a] To calculate illumination field-of-view and pixel resolution at the specimen, simply divide the above numbers by the magnification of the objective.
[b] Polygon1000-DL & Polygon UHC have a circular illumination field-of-view.
[c] 2X front tube lens sold separately.

CONTROL & TIMING

	1000 SERIES + Polygon UHC
Maximum Frame Rate[a] | fps	6,600
Input Trigger	TTL, BNC Connector
Input Trigger Delay | µs	50
Output Trigger	TTL, BNC Connector
Output Trigger Delay	User Programmable
Input Uploading Speed[b] | ms/frame	Up to 4 ms

[a] Values at 1bit depth. For grayscale features please contact Mightex for more information.
[b] USB3.0 version. Actual achievable speed is dependent on PC hardware performance.

SYSTEM & COMMUNICATION

Operating System[§]	Windows 7, 8, 10 and 11
Software	Nikon NIS Elements Micro-Manager PolyScan3 PolyScan4
Interface	SuperSpeed USB3.0
Power Supply	5Vdc 3A input power
Screen Resolution	1,366x768 or higher

[§] Polygon1000 supported by 64bit systems only.

Microscope Integration

The Polygon can be coupled to most commercially available inverted and upright microscopes (Nikon, Leica, Zeiss, Olympus) in the following configurations:

INFINITY PATH CONFIGURATION

This configuration projects the spatial patterns at infinity, and hence it is mounted directly into the infinity path of a microscope by using a beam combiner (for upright microscopes) along with an adaptor that matches the exact make/model of the microscope.

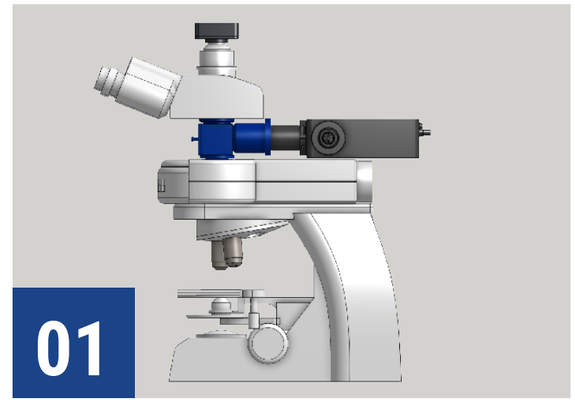

Upright Microscope

An adaptor (blue) is inserted in between the trinocular head and epi-illuminator of upright microscopes. Microscope adaptors are sold separately. A 45 degree mirror is mounted in the adaptor to guide the patterned illumination towards the objective.

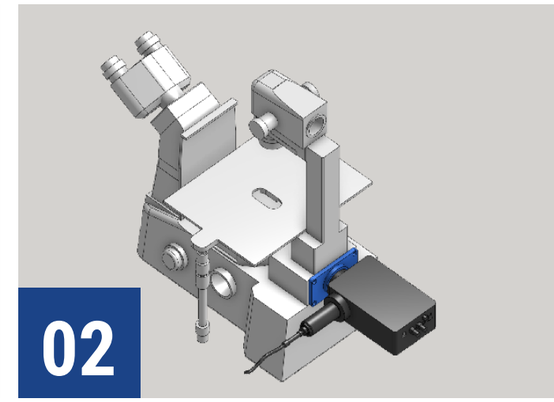

Inverted Microscope

The Polygon replaces the epi-illuminator at the back of inverted microscopes. Microscope adaptors are sold separately.

Please find more information regarding our mechanical microscope adaptors on page 13.

UNIQUE CONFIGURATIONS

If the infinity path of your microscope is unavailable, we also provide solutions that allow you to integrate the Polygon on your microscope system via non-standard ports as follows.

C-MOUNT CONFIGURATION	This configuration an be mounted onto one of the standard C-mount camera ports of your microscope. C-mount attachment sold separately.
LAPP CONFIGURATION	Do you have a Nikon microscope with a LAPP modular illumination system? We provide an attachment that is LAPP compatible. LAPP attachment sold separately.
SUBSTAGE MOUNT	Polygon can also be mounted sub-stage in place of the transmitted light source. Above-stage counterpart also available for inverted microscopes.

Infinity Port Expanders

Mightex's IPX expands an infinity-path port on a microscope into a maximum of 4 ports. There are two models of IPX expanders: (1) IPX4, which has 4 integrated ports; and (2) IPX2, which starts with 2 ports, but has a modular design and can be scaled up to 4 ports. Both IPX expanders are compatible with all Mightex Polygon models as well as with all Mightex's and any 3rd party widefield epi-fluorescent illumination sources via standard 3mm core liquid lightguide. It also supports cameras and laser scanners via appropriate adaptors. Ports 2, 3 and 4 feature pitch-yaw adjustable dichroic holders for centering FOV and each port can be mounted on either sides of the main IPX chassis, to avoid mechanical conflict with surrounding environment.

01

IPX2

02

IPX4

The photo below shows an IPX Infinity Port Expander installed on an inverted Zeiss microscope frame with a Polygon1000-G model mounted on Port 2 and an epi-illuminator with liquid lightguide interface mounted on Port 3. Dichroic mirrors, beamsplitters and optical filters are installed in the IPX to combine the illumination of the different devices.

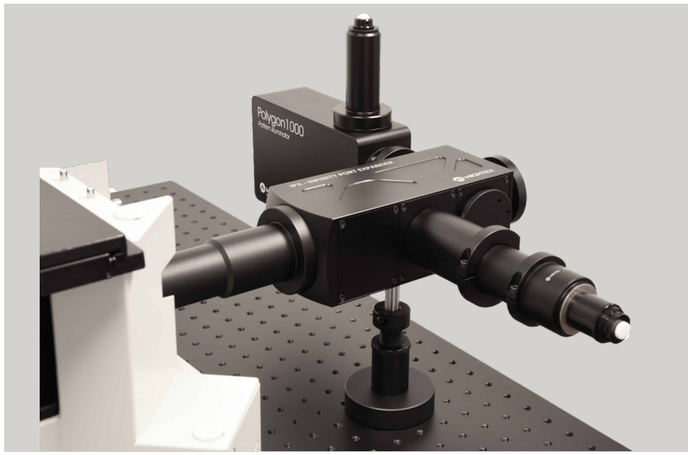

Microscope Adaptors

UPRIGHT MICROSCOPE ADAPTORS

With an upright microscope, the Polygon is usually coupled into the infinity path using a cube adaptor and a beam splitter. There are two options: (1) a cube adaptor with a single position; or (2) a 3-position filter holder/ adaptor. The former can only hold one mirror/dichroic. With the 3-position adaptor, one can hold up to three (3) mirrors/dichroics, and hence choose which filter to use by sliding the correct filter into the optical path. In addition, leaving one of the three positions blank will effectively remove the Polygon from the optical path, without having to physically remove it. Mightex's microscope adaptors now also come with an internal 2D tilt stage, which allows users to adjust the pitch and yaw of the Polygon projection via two fine-pitch screws. This enables the user to precisely center the Polygon field of view within the microscope's field of view. Allen wrench is included.

01

EXAMPLES

- Nikon Upright Microscopes (e.g., FN1)
- Leica Upright Microscopes
- Olympus Upright Microscopes (e.g., BX series)
- Zeiss Upright Microscopes (Axio Examiner A1, D1, Z1)

INVERTED MICROSCOPE ADAPTORS

Users with an inverted microscope can couple the Polygon into their microscope with a ring adaptor. The ring adaptor connects to the illuminator port at the back of the microscope. Please note that the epi-illuminator and accompanying tube lens and other additional optics need to be removed before coupling the Polygon into the backport. Please consult your microscope manufacturer for information on how to best remove the epi-illuminator of your specific microscope model. The user will need to utilize the filters/dichroics of the microscope to direct the illumination to the sample.

02

EXAMPLES

- Nikon TE2000, Eclipse Ti and Ti2
- Leica Inverted Microscopes
- Olympus IX Inverted Microscopes
- Zeiss Inverted Microscopes

CUSTOM IMAGING SYSTEMS ADAPTORS

Mightex has designed and developed mechanical Polygon mounting solutions for specialized microscopes and custom-built imaging solutions assembled with commercially available individual parts. If you have a custom-built imaging system and would like to integrate the Polygon onto your setup, please contact one of our Mightex representatives.

EXAMPLES

- Adaptor Ring for THT Macroscope
- Flange Adaptor for ASI Microscopes via 38mm Port
- Flange Adaptor with C-mount thread
- Flange Adaptor with M52x0.75 thread
- Flange Adaptor with external SM1 (1.035"-40) thread
- Flange Adater with external SM2 (2.035"-40) thread

Research Highlights

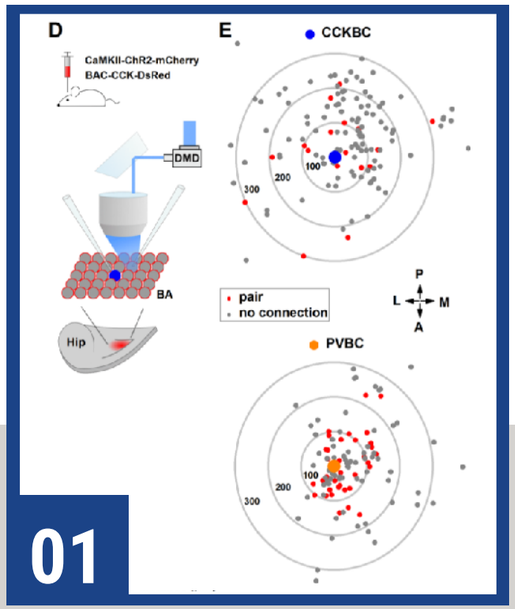

Circuit Mapping with Cellular-Resolution Optogenetics

Andrasi, T., Verses, J.M., Rovira-Esteban, L., Kozma, R., Vikor, A., Gregori, E., & Hajos, N. Differential excitatory control of 2 parallel basket cell networks in amygdala microcircuits. (2017) **PLoS Biology.**

Andrasi *et al.* 2017 investigated the connection between principal neurons and basket cells in the amygdala. Whole-cell slice electrophysiology was used to measure amygdala activity, and ChR2 was expressed to manipulate network activity. Mightex's Polygon was used to illuminate individual principal neurons expressing ChR2 and the activity elicited from a basket neuron was measured.

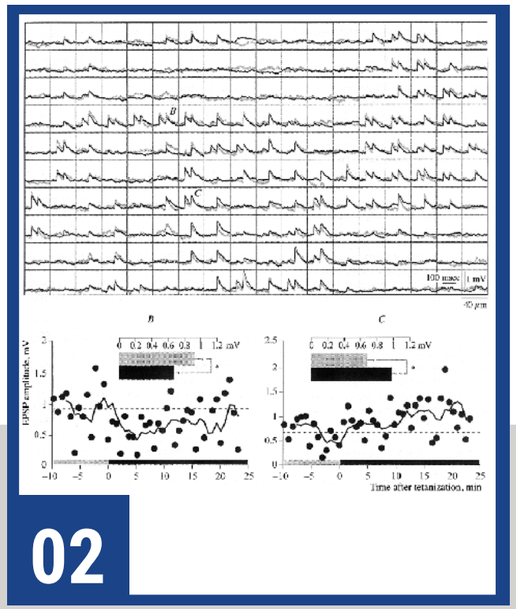

Grid-Scanning Optogenetics to Explore Neural Circuits

Simonova, N.A., Bal, N.V., Balaban, M.A., Volgushev, M.A., & Malyshev, A.Y. An Optogenetic Approach to Studies of the Mechanisms of Heterosynaptic Plasticity in Neocortical Neurons. (2019) **Neuroscience and Behavioural Physiology.**

Simonova *et al.* 2019 explored heterosynaptic plasticity in the neocortex. Whole-cell slice electrophysiology was used to record from layer 5 neurons, and ChR2 was expressed in layer 2/3 neurons to manipulate layer 5 activity. Mightex's Polygon was used to illuminate a randomized grid pattern across layer 2/3 neurons and the activity elicited from a layer 5 was measured.

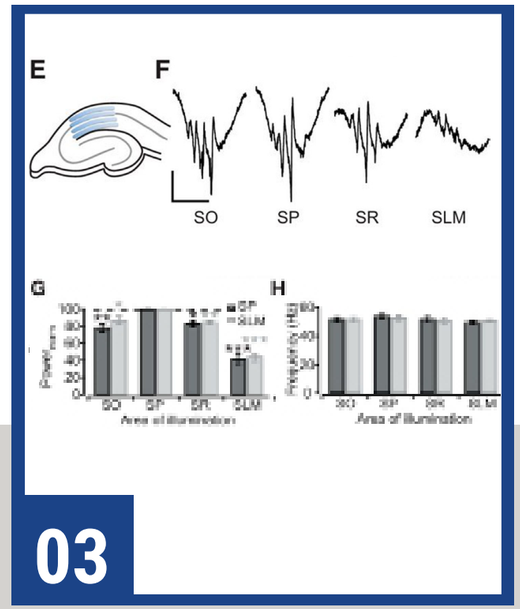

Layer-Specific Optogenetics in the Hippocampus

Butler, J.L., Mendonça, P.R. F., Robinson, H.P.C., & Paulsen, O. Intrinsic Cornu Ammonis Area 1 Theta-Nested Gamma Oscillations Induced by Optogenetic Theta Frequency Stimulation. (2016) **Journal of Neuroscience.**

Butler *et al.* 2016 explored intrinsic production of gamma oscillations in CA1 region of the hippocampus. Slice electrophysiology was used to measure hippocampal activity, and ChR2 was expressed to manipulate network activity. Mightex's Polygon was used to illuminate select layers of the hippocampus expressing ChR2 to measure the oscillatory activity produced.

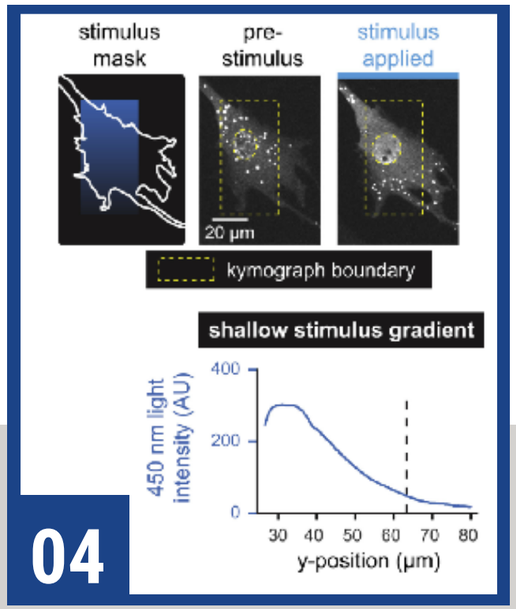

Studying Protein Phase Separation Using Optogenetics

Dine E., Gil G.A., Uribe G., Brangwynee C.P., & Toettcher J.E. Protein Phase Separation Provides Long-Term Memory of Transient Spatial Stimuli. (2018) **Cell Systems.**

Dine *et al.* 2018 set out to define how a physical interaction could play a significant role in the establishment and maintenance of asymmetry in living cells. They developed a novel optogenetic system called PixELLS. In the dark PixELLs undergo protein phase separation forming liquid-like clusters and upon 450 nm light PixELLs dissolve and become diffuse. Mightex's Polygon was used to draw an ROI on the cell to stimulate it with a gradient of blue light intensities.

Publications using Polygon

Below is a select list of recent peer-reviewed scientific publications from Mightex customers that include experiments performed with the Polygon. Please find a complete updated list of publications on our website including all of the 100+ publications.

1. Carlos A. Aguilar-Trigueros, Matthias C. Rillig, Jeff R. *Powell Symbiotic status alters fungal eco-evolutionary offspring trajectories* (2023) **Ecology Letters.**
2. Moawiah M. Naffaa, Rehan R. Khan, Chay T. Kuo, Henry H. Yin *Cortical regulation of neurogenesis and cell proliferation in the ventral subventricular zone* (2023) **Cell**
3. Alessandro Dema, Rabab Charafeddine, Shima Rahgozar, Jeffrey van Haren, Torsten Wittmann *Growth cone advance requires EB1 as revealed by genomic replacement with a light-sensitive variant* (2023) **eLife.**
4. Michael B. Sheets, Nathan Tague & Mary J. Dunlop *An optogenetic toolkit for light-inducible antibiotic resistance* (2023) **Nature.**
5. Xi Chen, Xiaowen Chen, Mohamed Elsayed, Wei Wang, and Aaron R. *Wheeler Steering Micromotors via Reprogrammable Optoelectronic Paths* (2023) **ACS Publications.**
6. Xinyu Xie, Fuqiang Hu, Dr. Yuqiao Zhou, Prof. Dr. Xiaohu Zhao, Prof. Dr. Zhipeng Yu *Photoswitchable Oxidopyrylium Ylide for Photoclick Reaction with High Spatiotemporal Precision: A Dynamic Switching Strategy to Compensate for Molecular Diffusion* (2023) **Angewandte Chemie.**
7. Wen Lu , Margot Lakonishok, and Vladimir I. *Gelfand Spatial Patterning of Micromotor Aggregation and Flux* (2023) **Chemnanomat.**
8. Stephen E. McGowan *Discoidin domain receptor-2 enhances secondary alveolar septation in mice by activating integrins and modifying focal adhesions* (2023) **American Journal of Physiology.**
9. Wen Zhong ,Wenhong Zheng and Xuying Ji *Spatial Distribution of Inhibitory Innervations of Excitatory Pyramidal Cells by Major Interneuron Subtypes in the Auditory Cortex* (2023) **Bioengineering.**
10. Thomas F. Mathejczyk, Mathias F. Wernet *Heading choices of flying Drosophila under changing angles of polarized light* (2023) **Nature.**
11. Joshua A. Riback, Jorine M. Eeftens,Daniel S.W. Lee, ..., Ralph Kleiner,Richard Kriwacki,Clifford P. Brangwynne *Viscoelasticity and advective flow of RNA underlies nucleolar form and function* (2023) **Molecular Cell.**
12. Wen Lu,Margot Lakonishok, and Vladimir I. Gelfand *The dynamic duo of microtubule polymerase Mini spindles/XMAP215 and cytoplasmic dynein is essential for maintaining Drosophila oocyte fate* (2023) **PNAS.**
13. Mitmoen M., Kedem O. *UV- and Visible-Light Photopatterning of Molecular Gradients Using the Thiol–yne Click Reaction.* (2022) **ACS Applied Materials and Interfaces.**
14. Ji, Xuying Liu, Wenhui, Xiao, Haoran, Xiao, Zhongju *The activated synaptic terminals beyond the light illumination range affect the results of optogenetics.* (2022) **Neuro Report.**
15. Tony Wang, Daasol Yang, Jiehao Chen, Jocelyn Chow. *Tetherless Microdriller for Maneuverability and On-Board Cargo Delivery Inside Viscoelastic Medi*. (2022) **MARSS.**
16. Lay Khoon Too, Weiyong Shen, So-Ra Lee, Ashish E. Mathai, Leszek Lisowski, John Y. Lin, Mark C. Gillies & Matthew P. Simunovic. *Optogenetic restoration of high sensitivity vision with bReaChES, a red-shifted channelrhodopsin.* (2022) **Nature.**
17. Sant Kumar, Mustafa Khammash. *Platforms for Optogenetic Stimulation and Feedback Control.* (2022) **Frontiers.**
18. Martinetti L.E., Bonekamp K.E., Autio D.M., Kim H., Crandall S.R. *Short-Term Facilitation of Long-Range Corticocortical Synapses Revealed by Selective Optical Stimulation.* (2022) **Cerebral Cortex.**
19. Dema A., van Haren J., Wittmann T. *Optogenetic EB1 inactivation shortens metaphase spindles by disrupting cortical force-producing interactions with astral microtubules.* (2022) **Current Biology.**
20. Gruber A., Edri O., Glatstein S., Goldfracht I., Huber I., Arbel G., Gepstein A., Chorna S., Gepstein Li. *Optogenetic Control of Human Induced Pluripotent Stem Cell Derived Cardiac Tissue Models.* (2022) **Journal of the American Heart Association.**
21. Galloni A.R., Ye Z., Rancz E. *Dendritic Domain-Specific Sampling of Long-Range Axons Shapes Feedforward and Feedback Connectivity of L5 Neurons.* (2022) **Journal of Neuroscience.**
22. Jing Liu, Cassidy Enloe, Katie D. Li-Oakey, and John Oakey. *Optimizing Immunofunctionalization and Cell Capture on Micromolded Hydrogels via Controlled Oxygen-Inhibited Photopolymerization.* (2022) **ACS Publications.**
23. Shimba K., Asahina T., Sakai K., Kotani K., Jimbo Y. *Recording Saltatory Conduction Along Sensory Axons Using a High-Density Microelectrode Array.* (2022) **Frontiers in Neuroscience.**
24. Yueqin Liu, Sitong Li, Xinxin Zhang, Laijian Wang, Xi Kuang, Fei Yin, Qianhui Xia , Bin Jiang , Yupeng Yang. *Corticotropin releasing factor neurons in the visual cortex mediate long-term changes in visual function induced by early adversity.* (2022) **Neurobiology of Stress.**
25. Jocelyn Y. Kishi, Ninning Liu, Matthew Serrata, Constance L. Cepko, Sinem K. Saka & Peng Yin. *Light-Seq: light-directed in situ barcoding of biomolecules in fixed cells and tissues for spatially indexed sequencing.* (2022) **Nature Methods.**
26. Zhang S., Elsayed M., Peng R., Chen Y., Zhang Y., Neale S.L., Wheeler A.R. *Influence of light pattern thickness on the manipulation of dielectric microparticles by optoelectronic tweezers.* (2022) **Photonics Research.**
27. Shuailong Zhang, Mohamed Elsayed, Ran Peng, Yujie Chen, Yanfeng Zhang, Steven L. Neale, and Aaron R. Wheeler. *Influence of light pattern thickness on the manipulation of dielectric microparticles by optoelectronic tweezers.* (2022) **Photonics Research.**
28. Jack A., Kim Y., Strom A.R., Lee D.S.W., Williams B., Schaub J.M., Kellogg E.H., Finkelstein I.J., Ferro L.S., Yildiz A., Brangwynne C.P. *Compartmentalization of telomeres through DNA-scaffolded phase separation.* (2022) **Developmental Cell.**

29. Sengupta M., Daliparthi V., Roussel Y., Bui T.V., Bagnall M.W. *Spinal V1 neurons inhibit motor targets locally and sensory targets distally.* (2021) **Current Biology.**
30. Gruber A., Edri O., Huber I., Arbel G., Gepstein A., Shiti A., Shaheen N., Chorna S., Landesberg M., Gepstein L. *Optogenetic modulation of cardiac action potential properties may prevent arrhythmogenesis in short and long QT syndromes.* (2021) **JCI Insight.**
31. Honda M., Oki S., Kimura R., Harada A., Maehara K., Tanaka K., Meno C., Ohkawa Y. *High-depth spatial transcriptome analysis by photo-isolation chemistry.* (2021) **Nature Communications.**
32. Dine E., Reed E.H., Toettcher J.E. *Positive feedback between the T cell kinase Zap70 and its substrate LAT acts as a clustering-dependent signaling switch.* (2021) **Cell Reports.**
33. Lemaire L., Desroches M., Krupa M., Pizzamiglio L., Scalmani P., Mantegazza M. *Modeling NaV1.1/SCN1A sodium channel mutations in a microcircuit with realistic ion concentration dynamics suggests differential GABAergic mechanisms leading to hyperexcitability in epilepsy and hemiplegic migraine.* (2021) **PLOS Computational Biology.**
34. Chua C.J., Han J.L., Li W., Liu W., Entcheva E. *Integration of Engineered "Spark-Cell" Spheroids for Optical Pacing of Cardiac Tissue.* (2021) **Frontiers in Bioengineering and Biotechnology.**
35. Jiang H., Guo A., Chiu A., Li H., Lai C.S.W., Lau C.G. *Target-specific control of piriform cortical output via distinct inhibitory circuits.* (2021) **The FASEB Journal.**
36. McFann S., Dutta S., Toettcher J.E., Shvartsman S.Y. *Temporal integration of inductive cues on the way to gastrulation.* (2021) **PNAS.**
37. Zhang S., Li W., Elsayed M., Peng J., Chen Y., Zhang Y., Sun Y., Kherani N.P., Neale S.L., Wheeler A.R. *Integrated Assembly and Photopreservation of Topographical Micropatterns.* (2021) **Nano Micro Small.**
38. Zhang S., Elsayed M., Peng R., Chen Y., Wheeler A.R. *Reconfigurable multi-component micromachines driven by optoelectronic tweezers.* (2021) **Nature Communications.**
39. Bellot-Saez A., Stevenson R., Kekesi O., Samokhina E., Ben-Abu Y., Morley J.W., Buskila Y. *Neuromodulation of Astrocytic K+ Clearance.* (2021) **International Journal of Molecular Sciences.**
40. Chenais N.A.L., Leccardi M.J.I.A., Ghezzi D. *Photovoltaic Retinal Prosthesis Restores High-Resolution Responses to Single-Pixel Stimulation in Blind Retinas.* (2021) **Communications Materials.**
41. Ruan H., Wang L., Yuan F., Weng S., Zhong Y. *Orexin-A Differentially Modulates Inhibitory and Excitatory Synaptic Transmission in Rat Inner Retina.* (2021) **Neuropharmacology.**
42. Lee D.S.W, Wingreen N.S., Brangwynne C.P. *Chromatin Mechanics Dicates Subdiffusion and Coarsening Dynamics of Embedded Condensates.* (2021). **Nature Physics.**
43. Lu M., van Tartwijk F.W., Lin J.Q., Nijenhuis W., Kaminski C.F. *The Structure and Global Distribution of the Endoplasmic Reticulum Network are Actively Regulated by Lysosomes.* (2021) **Science Advances.**
44. Geisterfer Z.M., Oakley J., Gatlin J.C. *Microfluidic Encapsulation of Xenopus laevis Cell-Free Extracts Using Hydrogel Photolithography.* (2020) **STAR Protocols.**
45. Tabarean I.V. *Activation of Preoptic Arginine Vasopressin Neurons Induces Hyperthermia in Male Mice.* (2020) **Endocrinology.**
46. Chenais N.A.L., Leccardi M.J.I.A., Ghezzi D. *Naturalistic Spatiotemporal Modulation of Epiretinal Stimulation Increases the Response Persistence of Retinal Ganglion Cell.* (2020) **Journal of Neural Engineering.**
47. Wei L., Li W., Entcheva E., Li Z. *Microfluidics-Enabled 96-Well Perfusion System for High-Throughput Tissue Engineering and Long-Term All-Optical Electrophysiology.* (2020) **Lab on a Chip**.
48. Kastli R., Vighagen R., van der Bourg A., Argunsah A.O.,Aguzzi A., Helmchen F., Karayannis T. *Developmental Divergence of Sensory Stimulus Representation in Cortical Interneurons.* (2020) **Nature Communications.**
49. Anastasiades P.G., Collins D.P., Carter A.G. *Mediodorsal and Ventromedial Thalamus Engage Distinct L1 Circuits in the Prefrontal Cortex.* (2020) **Neuron.**
50. Liu X., Dimidschstein J., Fishell G., Carter A.G. *Hippocampal Inputs Engage CCK+ Interneurons to Mediate Endocannabinoid-Modulated Feed-Forward Inhibition in the Prefrontal Cortex. (2020) eLife. Optogenetic Sensor: A Glutamine Lever Induces Unfolding of the Ja Helix.* (2020) **ACS Chemical Biology.**
51. Fattahi N., Nieves-Otero P.A., Masigol M., van der Vlies A.J., Jensen R.S., Hansen R.R., Platt T.G. *Photodegradable Hydrogels for Rapid Screening, Isolation, and Genetic Characterization of Bacteria with Rare Phenotypes.* (2020) **BioMacromolecules.**
52. Lindner M., Gilhooley M.J., Peirson S.N., Hughes S., Hankins M.W. *The Functional Characteristics of Optogenetic Gene Therapy for Vision Restoration.* (2020)**Cellular and Molecular Life Sciences.**
53. Johnson H.E., Djabrayan N.J.V., Shvartsman S.Y., Toettcher J.E. *Optogenetic Rescue of a Patterning Mutant.* (2020) **Current Biology.**
54. Ravindran P.T., Wilson M.Z., Jena S.G., Toettcher J.E. *Engineering Combinatorial and Dynamic Decoders Using Synthetic Immediate-Early Genes.* (2020)**Communications Biology.**
55. Carrasco-Lopez C., Alam N., Toettcher J.E., Avalos J.L. *Development of Light-Responsive Protein Binding in the Monobody Non-Immunoglobulin Scaffold.* (2020) **Nature Communications.**
56. Murphy C.A., Raz A., Grady S.M., Banks M.I. *Optogenetic Activation of Afferent Pathways in Brain Slices and Modulation of Responses by Volatile Anesthetics.* (2020) **JOVE.**
57. Cheng C., Harpster M.H., Oakey J. *Convection-Driven Microfabricated Hydrogels for Rapid Biosensing.* (2020) **Analyst.**
58. Sulerud T., Sami A.B., Li G., Kloxin A., Oakey J., & Gatlin J. *Microtubule-Dependent Pushing Forces Contribute to Long-Distance Aster Movement and Centration in Xenopus Laevis Egg Extracts.* (2020) **Molecular Biology of the Cell.**
59. Iuliano J.N., Collado J.T., Gil A.A., Ravindran P.T.,Gardner K.H., Simmerling C.L., Meech S.R., Tonge P.J. *Unraveling the Mechanism of a LOV Domain Optogenetic Sensor: A Glutamine Lever Induces Unfolding of the Ja Helix.* (2020) **ACS Publications.**
60. Wang L., Guo W., Shen X.,Lyu Q., Herbison A.E., Kuang Y. *Different Dendritic Domains of the GnRH Neuron Underlie the Pulse and Surge Modes of GnRH Secretion in Female Mice.* (2020) **eLife.**
61. Liu S. *Dopamine Suppresses Synaptic Responses of Fan Cells in the Lateral Entorhinal Cortex to Olfactory Bulb Input in Mice.* (2020) **Frontiers in Cellular Neuroscience.**
62. Chong E., Moroni M., Wilson C., Shoham S., Panzeri S., Rinberg D. *Manipulating Synthetic Optogenetic Odors Reveals the Coding Logic of Olfactory Perception.*(2020) **Science.**
63. Geisterfer Z.M., Zhu D.Y., Mitchison T.J., Oakey J., Gatlin J.C. *Microtubule Growth Rates Are Sensitive to Global and Local Changes in Microtubule Plus-End Density.* (2020) **Current Biology.**
64. Kauvar I.V., Machado T.A., Yuen E., Kochalka J., Choi M., Allen W.E., Wetzstein G., Deisseroth K. Cortical *Observation by Synchronous Multifocal Optical Sampling Reveals Widespread Population Encoding of Actions.* (2020) **Neuron.**
65. Mu M., Geng H., Rong K., Peng R., Wang S., Geng L., Qian Z., Yung W., Ke Ya. A Limbic *Circuitry Involved in Emotional Stress-Induced Grooming.* (2020) **Nature Communications**
66. Song Y., Hwang Y., Kim K., Lee H.,Jung M.W., Petersen C.C.H., Knott G., Lee S., Lee S. *Somatostatin Enhances Visual Processing and Perception by Suppresing Excitatory Inputs to Parvalbumin-positive Interneurons in V1.* (2020) **Science Advances**

67. Kissinger S.T., Anderson A.K., Pak A., & Chubykin A.A. *Visual Experience-Dependent Oscillations and Underlying Circuit Connectivity Changes Are Impaired in Fmr1 KO Mice*. (2020) **Cell Reports**
68. Oboti L. & Sokolowski K. *Gradual Wiring of Olfactory Input to Amygdala Feedback Circuits.* (2020) **Scientific Reports**
69. Goglia A.G., Wilson M.Z., Sibert J., Basta L.P., Deveport D., & Toettcher J.E. *A Live-Cell Screen for Altered Erk Dynamics Reveals Principles of Proliferative Control.* (2020) **Cell Systems**
70. Jiang Z., McBride R., Jiang K., Oakey J. Crosslinker *Length Dictates Step-Growth Hydrogel Network Formation Dynamics and Allows Rapid On-Chip Photoencapsulation.* (2020) **Biofabrication**
71. Chung H., Park K., Jang H.J., Kohl M.M., & Kwag J. *Dissociation of Somatostatin and Parvalbumin Interneurons Circuit Dysfunctions Underlying Hippocampal Theta and Gamma Oscillations Impaired by Amyloid β Oligomers In Vivo.* (2020) **Brain Structure and Function**
72. Nijenhuis W., Grinvsven M.M.P., & Kapitein L.C. *An Optimized Toolbox for the Optogenetic Control of Intracellular Transport.* (2020) **Journal of Cell Biology**
73. Papasavvas C.A., Parrish R., & Trevelyan A.J. *Propagating Activity in Neocortex, Mediated by Gap-Junctions and Modulated by Extracellular Potassium.* (2020) **eNeuro**
74. Callahan R.A., Roberts R., Sengupta M., Kimura Y., Higashijima S. & Bagnall M.W. *Spinal V2b Neurons Reveal a Role for Ipsilateral Inhibition in Speed Control.* (2020) **eLife**
75. Murphy C., Krause B., & Banks M. *Selective Effects of Isoflurane on Cortico-Cortical Feedback Afferent Responses in Murine Non-Primary Neocortex.* (2019) **British Journal of Anaesthesia.**
76. Dorsey P.J., Rubanov M., Wang W., & Schulman R. *Digital Maskless Photolithographic Patterning of DNA-Functionalized Poly(ethylene glycol) Diacrylate Hydrogels with Visible Light Enabling Photodirected Release of Oligonucleotides.* (2019) **ACS Macro Letters.**
77. Petrovskaya L.E., Roshchin M.V., Smirnova G.R., Kolotova D.E., Balaban P.M., Ostrovsky M.A., & Malyshev A.Y. *Bicistronic Construct for Optogenetic Prosthesis of Ganglion Cell Receptive Field of Degenerative Retina.* (2019) **Doklady Biochemistry and Biophysics.**
78. Yoon J.Y., Lee H.R., Ho W.K., & Lee S.H. *Disparities in Short-Term Depression Among Prefrontal Cortex Synapses Sustain Persistent Activity in a Balanced Network.* (2019) **Cerebral Cortex.**
79. Noren B.E., Shaha R.K., Stenquist A.T., Frick C.P., & Oakey J.S. *Cell Printing in Complex Hydrogel Scaffolds.* (2019) **IEEE Transactions of Nanobioscience.**
80. Wei Q., Krolewski D.M., Moore S., Kumar V., Li F., Martin B., Tomer R., Murphy G.G., Deisseroth K., Watson Jr S.J., & Akil H. *Uneven Balance of Power Between Hypothalamic Peptidergic Neurons in the Control of Feeding.* (2018) **Proceedings of the National Academy of Sciences.**
81. Moscato L., Montagna I., De Propris L., Tritto S., Mapelli L., & D'Angelo E. *Long-Lasting Response Changes in Deep Cerebellar Nuclei in vivo Correlate with Low-Frequency Oscillations.* (2019) **Frontiers in Cellular Neuroscience.**
82. Johnson H.E. & Toettcher J.E. *Signaling Dynamics Control Cell Fate in the Early Drosophila Embryo.* (2019) **Developmental Cell.**
83. Simonova N.A., Bal N.V., Balaban P.M., Volgushev M.A., & Malyshev A.Y. *An Optogenetic Approach to Studies of the Mechanisms of Heterosynaptic Plasticity in Neocortical Neurons.* (2019) **Neuroscience and Behavioral Physiology.**
84. Shen C., Zheng D., Li K., Yang J., Pan H., Yu X., Fu J., Zhu Y., Sun Q., Tang M., Zhang Y., Sun P., Xie Y., Duan S., Hu H., & Li X. *Cannabinoid CB1 Receptors in the Amygdalar Cholecystokinin Glutamatergic Afferents to Nucleus Accumbens Modulate Depressive-Like Behavior.* (2019) **Nature Medicine.**
85. Li Y., Li C., Xi W., Jin S., Wu Z., Jiang P., Dong P., He X., Xu F., Duan S., Zhou Y., & Li X. *Rostral and Caudal Ventral Tegmental Area GABAergic Inputs to Different Dorsal Raphe Neurons Participate in Opioid Dependence.* (2019) **Neuron.**
86. van Der Vlies J.A., Barua, N., Nieves-Otero P.A., Plat T.G., & Hansen R.R. *On Demand Release and Retrieval of Bacteria from Microwell Arrays Using Photodegradable Hydrogel Membranes.* (2018) **ACS Applied Bio Materials.**
87. Ogasawara, S. *Transcription Driven by Reversible Photocontrol of Hyperstable G-Quadruplexes.* (2018) **ACS Synthetic Biology.**
88. Konetski D., Zhang D., Schwartz D.K., & Bowman C.N. *Photo-induced Pinocytosis for Artificial and Proto-Cell Systems.* (2018) **Chemistry of Materials.**
89. Majumder R., Feola I., Teplenin A.S., de Vries A.A., Panfilov A.V., & Pijnappels D. *Optogenetics Enables Real-Time Spatiotemporal Control Over Spiral Wave Dynamics in an Excitable Cardiac System.* (2018) **eLife.**
90. Tabor, K.M., Smith, T.S., Brown, M., Bergeron, S.A., Briggman, K.L., & Burgess H.A. *Presynaptic Inhibition Selectively Gates Auditory Transmission to the Brainstem Startle Circuit.* (2018) **Current Biology.**
91. Virag, T.T., Cserep, C., Schlingloff, D., Posfai, B., Szonyi, A., Sos, K.E., Kornyei, Z., Denes, A., Gulyas, A.I., Freund, T.F., & Nyiri, G. *Co-Transmission of Acetlycholine and GABA Regulates Hippocampal States.* (2018) **Nature Communications.**
92. Rhomberg, T., Rovira-Esteban, L., Vikor, A., Paradiso, E., Kremser C., Nagy-Pal, P., Papp, O.I., Tasan, R., Erdelyi, F., Szabo, G., Ferraguit, F. & Hajor, N. *VIP-Immunoreactive Interneurons Within Circuits of the Mouse Basolateral Amygdala.* (2018) **Journal of Neuroscience.**
93. Teplenin, A.S., Dierckx, H., de Vries, A.A.F., Pijnappels, D.A., & Panfilov, A.V. *Paradoxical Onset of Arrhythimic Waves from Depolarizes Areas in Cardiac Tissue Due to Curvature-Dependent Instability.* (2018) **Physical Review X.**
94. Che, A., Babij, R., Iannone, A.F., Fetcho, R.N., Ferrer, M., Liston, C., Fishell, G., & De Marco Garcia, N.V. *Layer I Interneurons Sharpen Sensory Maps during Neonatal Development.* (2018) **Neuron.**
95. Johnson H.E., Djabrayan N.J.V., Shvartsman S.Y., Toettcher J.E. *Optogenetic Rescue of a Patterning Mutant.* (2020) **Current Biology.**
96. Fattahi N., Nieves-Otero P.A., Masigol M.,Jensen R.S., Hansen R.R., Platt T.G. *Photodegradable Hydrogels for Rapid Screening, Isolation, and Genetic Characterization of Bacteria with Rare Phenotypes.* (2020) **BioMacromolecules.**
97. Wang L., Guo W., Shen X., Yeo S., Long H., Wang Z., Lyu Q., Herbison A.E., Kuang Y. *Different Dendritic Domains of the GnRH Neuron Underlie the Pulse and Surge Modes of GnRH Secretion in Female Mice.* (2020) **eLife.**

98. Liu S. *Dopamine Suppresses Synaptic Responses of Fan Cells in the Lateral Entorhinal Cortex to Olfactory Bulb Input in Mice.* (2020) **Frontiers in Cellular Neuroscience.**
99. Chong E., Moroni M., Wilson C., Shoham S., Panzeri S., Rinberg D. *Manipulating Synthetic Optogenetic Odors Reveals the Coding Logic of Olfactory Perception.* (2020) **Science.**
100. Geisterfer Z.M., Zhu D.Y., Mitchison T.J., Oakey J., Gatlin J.C. *Microtubule Growth Rates Are Sensitive to Global and Local Changes in Microtubule Plus-End Density*. (2020) **Current Biology.**
101. Kauvar I.V., Machado T.A., Yuen E., Kochalka J., Choi M., Allen W.E., Wetzstein G., Deisseroth K. *Cortical Observation by Synchronous Multifocal Optical Sampling Reveals Widespread Population Encoding of Actions.* (2020) **Neuron.**
102. Mu M., Geng H., Rong K., Peng R., Wang S., Geng L., Qian Z., Yung W., Ke Ya. *A Limbic Circuitry Involved in Emotional Stress-Induced Grooming.* (2020) **Nature Communications**
103. Song Y., Hwang Y., Kim K., Lee H., Kim J., Maclachlan C., Dubois A., Jung M.W., Petersen C.C.H., Knott G., Lee S., Lee S. *Somatostatin Enhances Visual Processing and Perception by Suppresing Excitatory Inputs to Parvalbumin-positive Interneurons in V1.* (2020) **Science Advances**
104. Kissinger S.T., Wu Q., Quinn C.J., Anderson A.K., Pak A., & Chubykin A.A. *Visual Experience-Dependent Oscillations and Underlying Circuit Connectivity Changes Are Impaired in Fmr1 KO Mice.* (2020) **Cell Reports**
105. Oboti L. & Sokolowski K. *Gradual Wiring of Olfactory Input to Amygdala Feedback Circuits.* (2020) **Scientific Reports**
106. Callahan R.A., Roberts R., Sengupta M., Kimura Y., Higashijima S. & Bagnall M.W. *Spinal V2b Neurons Reveal a Role for Ipsilateral Inhibition in Speed Control.* (2020) **eLife**
107. Dorsey P.J., Rubanov M., Wang W., & Schulman R. *Digital Maskless Photolithographic Patterning of DNA-Functionalized Poly(ethylene glycol) Diacrylate Hydrogels with Visible Light Enabling Photodirected Release of Oligonucleotides.* (2019) **ACS Macro Letters.**
108. Petrovskaya L.E., Roshchin M.V., Smirnova G.R., Kolotova D.E., Balaban P.M., Ostrovsky M.A., & Malyshev A.Y. *Bicistronic Construct for Optogenetic Prosthesis of Ganglion Cell Receptive Field of Degenerative Retina.* (2019) **Doklady Biochemistry and Biophysics.**
109. Goglia A.G., Wilson M.Z., Sibert J., Basta L.P., Deveport D., & Toettcher J.E. *A Live-Cell Screen for Altered Erk Dynamics Reveals Principles of Proliferative Control.* (2020) **Cell Systems**
110. Jiang Z., Shaha R., McBride R., Jiang K., Tang M., Xu B., Goroncy A.K., Frick C., & Oakey J. *Crosslinker Length Dictates Step-Growth Hydrogel Network Formation Dynamics and Allows Rapid On-Chip Photoencapsulation.* (2020) **Biofabrication**
111. Chung H., Park K., Jang H.J., Kohl M.M., & Kwag J. *Dissociation of Somatostatin and Parvalbumin Interneurons Circuit Dysfunctions Underlying Hippocampal Theta and Gamma Oscillations Impaired by Amyloid β Oligomers In Vivo.* (2020) **Brain Structure and Function**
112. Nijenhuis W., Grinvsven M.M.P., & Kapitein L.C. *An Optimized Toolbox for the Optogenetic Control of Intracellular Transport.* (2020) **Journal of Cell Biology**
113. Papasavvas C.A., Parrish R., & Trevelyan A.J. *Propagating Activity in Neocortex, Mediated by Gap-Junctions and Modulated by Extracellular Potassium.* (2020) **eNeuro**
114. Yoon J.Y., Lee H.R., Ho W.K., & Lee S.H. *Disparities in Short-Term Depression Among Prefrontal Cortex Synapses Sustain Persistent Activity in a Balanced Network.* (2019) **Cerebral Cortex.**
115. Noren B.E., Shaha R.K., Stenquist A.T., Frick C.P., & Oakey J.S. *Cell Printing in Complex Hydrogel Scaffolds.* (2019) **IEEE Transactions of Nanobioscience.**
116. Moscato L., Montagna I., De Propris L., Tritto S., Mapelli L., & D'Angelo E. *Long-Lasting Response Changes in Deep Cerebellar Nuclei in vivo Correlate with Low-Frequency Oscillations.* (2019) **Frontiers in Cellular Neuroscience.**
117. Murphy C., Krause B., & Banks M. *Selective Effects of Isoflurane on Cortico-Cortical Feedback Afferent Responses in Murine Non-Primary Neocortex*. (2019) **British Journal of Anaesthesia.**
118. Johnson H.E. & Toettcher J.E. *Signaling Dynamics Control Cell Fate in the Early Drosophila Embryo.* (2019) **Developmental Cell.**
119. Simonova N.A., Bal N.V., Balaban P.M., Volgushev M.A., & Malyshev A.Y. *An Optogenetic Approach to Studies of the Mechanisms of Heterosynaptic Plasticity in Neocortical Neurons.* (2019) **Neuroscience and Behavioral Physiology.**
120. Shen C., Zheng D., Li K., Yang J., Pan H., Tang M., Zhang Y., Sun P., Xie Y., Duan S., Hu H., & Li X. *Cannabinoid CB1 Receptors in the Amygdalar Cholecystokinin Glutamatergic Afferents to Nucleus Accumbens Modulate Depressive-Like Behavior.* (2019) **Nature Medicine.**
121. Li Y., Li C., Xi W., Jin S., Wu Z., Jiang P., Dong P., He X., Xu F., Duan S., Zhou Y., & Li X. *Rostral and Caudal Ventral Tegmental Area GABAergic Inputs to Different Dorsal Raphe Neurons Participate in Opioid Dependence.* (2019) **Neuron.**
122. van Der Vlies J.A., Barua, N., Nieves-Otero P.A., Plat T.G., & Hansen R.R. *On Demand Release and Retrieval of Bacteria from Microwell Arrays Using Photodegradable Hydrogel Membranes.* (2018) **ACS Applied Bio Materials.**
123. Konetski D., Zhang D., Schwartz D.K., & Bowman C.N. *Photo-induced Pinocytosis for Artificial and Proto-Cell Systems.* (2018) **Chemistry of Materials.**
124. Ogasawara, S. *Transcription Driven by Reversible Photocontrol of Hyperstable G-Quadruplexes.* (2018) **ACS Synthetic Biology.**
125. Wei Q., Krolewski D.M., Moore S., Kumar V., Li F., Martin B., Tomer R., Murphy G.G., Deisseroth K., Watson Jr S.J., & Akil H. *Uneven Balance of Power Between Hypothalamic Peptidergic Neurons in the Control of Feeding.* (2018) **Proceedings of the National Academy of Sciences.**
126. Majumder R., Feola I., Teplenin A.S., de Vries A.A., Panfilov A.V., & Pijnappels D. *Optogenetics Enables Real-Time Spatiotemporal Control Over Spiral Wave Dynamics in an Excitable Cardiac System.* (2018) **eLife.**
127. Tabor, K.M., Smith, T.S., Brown, M., Bergeron, S.A., Briggman, K.L., & Burgess H.A. *Presynaptic Inhibition Selectively Gates Auditory Transmission to the Brainstem Startle Circuit.* (2018) **Current Biology.**
128. Virag, T.T., Cserep, C., Schlingloff, D., Posfai, B., Szonyi, A., Sos, K.E., Kornyei, Z., Denes, A., Gulyas, A.I., Freund, T.F., & Nyiri, G. *Co-Transmission of Acetlycholine and GABA Regulates Hippocampal States.* (2018) **Nature Communications.**
129. Rhomberg, T., Rovira-Esteban, L., Vikor, A., Paradiso, E., Kremser C., Nagy-Pal, P., Papp, O.I., Tasan, R., Erdelyi, F., Szabo, G., Ferraguit, F. & Hajor, N. *VIP-Immunoreactive Interneurons Within Circuits of the Mouse Basolateral Amygdala.* (2018) **Journal of Neuroscience.**
130. Teplenin, A.S., Dierckx, H., D.A., & Panfilov, A.V. *Paradoxical Onset of Arrhythimic Waves from Depolarizes Areas in Cardiac Tissue Due to Curvature-Dependent Instability.* (2018) **Physical Review X.**
131. Che, A., Babij, R., Iannone, A.F., Fetcho, R.N., Ferrer, M., Liston, C., Fishell, G., & De Marco Garcia, N.V. L*ayer I Interneurons Sharpen Sensory Maps during Neonatal Development. (2018)* **Neuron.**

OASIS *IN VIVO* IMAGING SYSTEMS

01.

Recent development of cutting edge neuroscientific techniques to image (calcium) and manipulate neural activity (optogenetics) *in vivo* have significantly shifted forward how neuroscientists examine the brain. Moreover, combining these imaging and manipulation techniques with single-cell resolution offers researchers unique abilities to uncover even deeper understanding of the brain, and how neural processes impact behaviour.The OASIS platform combines these two techniques in a unique fashion, allowing simultaneous all-optical imaging and manipulation of neurons *in vivo* using patterned photostimulation. Mightex is proud to offer two powerful systems to meet researchers' needs:

01. OASIS Implant Capable of imaging and manipulation of neuronal populations across deep brain and cortical regions with sub cellular resolution in awake, freely-behaving animals.

02. OASIS Macro and Micro A modular macroscope or microscope solution for head fixed experiments: Macro offers extra large F0V (e.g.) covering the entire mouse's brain, while Micro enables high-resolution imaging.

A key feature of both OASIS platforms is modularity, affording researchers flexibility and easy system reconfiguration to accommodate a wide range of requirements from subcellular to brainwide experiments.

02.

OASIS In Vivo Imaging Systems

OASIS Implant

Mightex's OASIS Implant is a ground-breaking microendoscopic system that is capable of all optical simultaneous imaging and manipulation of neural activity (with single-cell resolution), both in the deep brain and the cortical region, of freely-behaving animals. Its modular design allows for a wide-range of calcium imaging (e.g. GCaMP or RCaMP) and optogenetic applications with both wide-field and patterned illumination capabilities (when combined with Mightex's market-leading Polygon). Patterned illumination allows researchers to target specific regions or cells of interest in freelybehaving animals.

The OASIS implant features an extremely compact and lightweight headmount design, weighing only 0.3g (compact) to 0.7g (standard) compared to ~2g for a miniscope. This feature minimises behavioural constraints and experimental confounds while optimising and broadening the scope of possible behavioural measures. Lastly, the OASIS Implant system affords researchers high quality deep brain data collection (imaging) due to the compatibility of our platform with high sensitivity, scientific-grade cameras.

Together the modular, light weight, and high quality data acquisition features of the OASIS implant make it an ideal neuroscience tool for examining neural circuits and processes in awake, freely-behaving animals.

FEATURES

- *In vivo* recording and manipulation of neural circuit activity in the brain
- Cellular resolution, high-quality imaging for quantitative analysis
- Multiwavelength illumination allows a wide-range of calcium imaging and optogenetic applications
- Multi brain region imaging and stimulation
- Futureproof, modular syste, reconfigurable by users for different research needs

Cellular-Resolution Optogenetics

Super lightweight and super compact headmounts

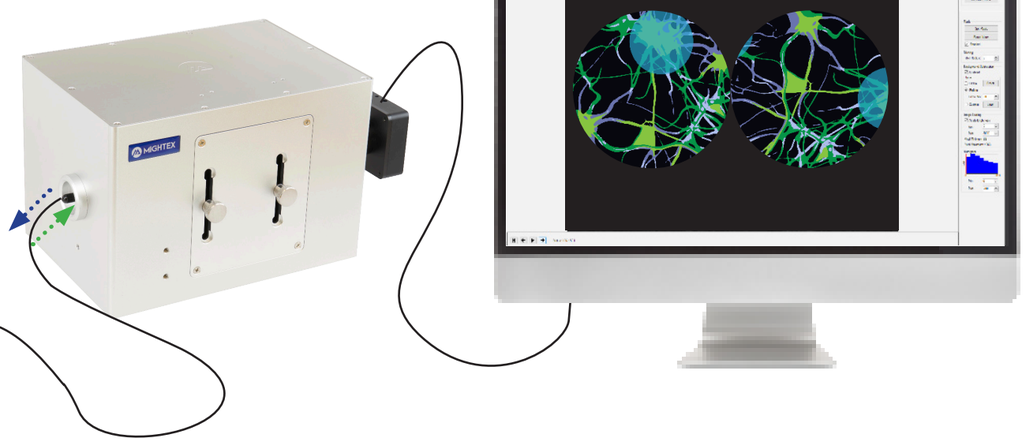

Freely-Behaving, Cellular-Resolution, Multi-Region Optogenetics and Calcium Imaging

The OASIS Implant Platform

Multiple components make part of the OASIS Implant platform to allow the system to perfom its many functions.

RECONFIGURABLE ILLUMINATION PORTS

The two (2) illumination ports at the back of the OASIS Implant main chassis allows the introduction of multiple light sources, either via an epi-fluorescent illuminator that accepts a 3mm-core lightguide input or by coupling Mightex's Polygon DMD for maximum illumination control. This flexibility allows researchers the ability to use the light sources and wavelenghts that will suit their specific imaging and optogenetic applications.

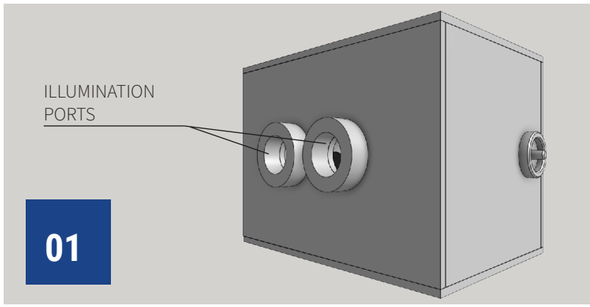

SWITCHABLE FILTER SETS

Each of the two (2) illumination ports on the OASIS Implant contains a filter holder that can hold up to three (3) filter sets, allowing researchers to easily switch between filters to meet their unique imaging and optogenetic stimulation needs.

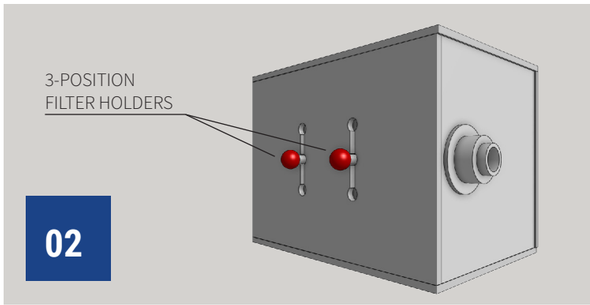

INTERCHANGEABLE IMAGING FIBERS

The OASIS Implant uses a flexible imaging fiber to transmit and collect light from the deep-brain or the cortex of a freely-behaving animal for imaging and optogenetics. A standard SMA multimode fiber is also compatible with the OASIS Implant for fiber photometry experiments.

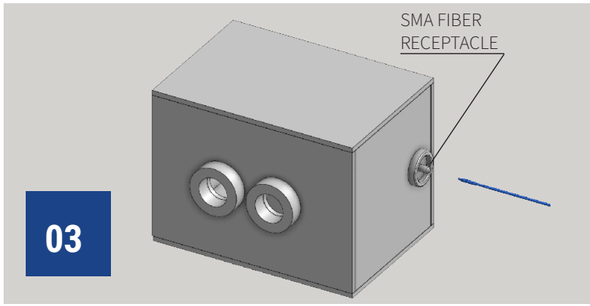

SCIENTIFIC-GRADE CAMERAS

Equipped with a standard C-mount camera port, the OASIS Implant system works with any low-noise, high-sensitivity, good-linearity and high-speed scientific camera, enabling high-quality image acquisition and high-precision quantitative data analysis. Multiple cameras can also be supported.

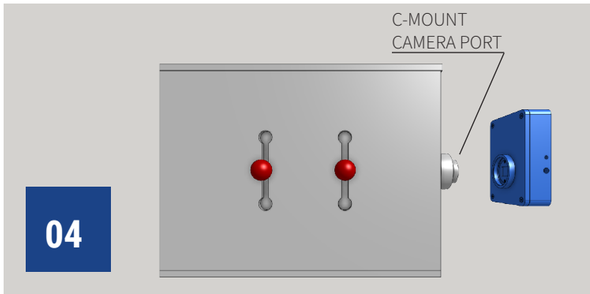

Research Highlights

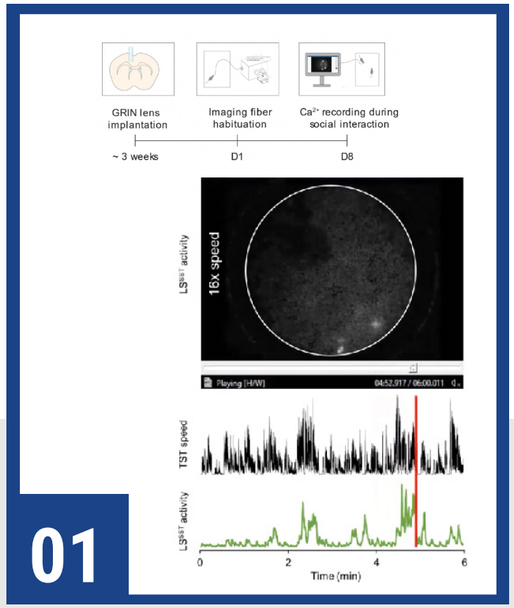

In Vivo Calcıum Imaging of Somatostatin Positive Neurons During Social Interaction Tasks

Huanhuan Li, Hyun Hailey Sung and Chunyue Geoffrey Lau. Activation of Somatostatin-Expressing Neurons in the Lateral Septum Improves Stress-Induced Depressive-like Behaviors in Mice. (2022) **Pharmaceutics.**

The cingulate cortex (CC) is a key brain region in the limbic system that coordinates actions and motivational behaviors. Somatostatin-expressing GABAergic neurons in the cingulate cortex (CCSST) can provide powerful inhibition to the CC circuitry through high basal firing activity and synchronized firing.
The video shows Ca2+ activity of somatostation-expressing cingulate cortex neurons during social interaction collected using the Mightex OASIS Implant system.

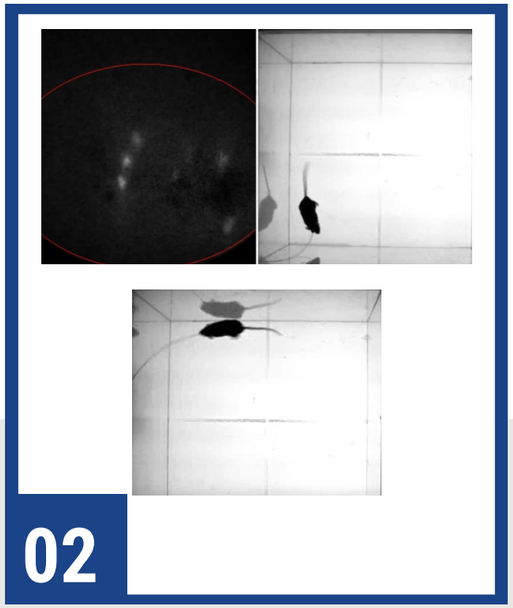

Elucidating Dynamic Intracellular Sıgnalling Pathways of Hippocampus-Dependent Memory with the OASIS Implant

Jayant Rai, a 4th year PhD student in the Department of Molecular Genetics at the University of Toronto. He is co-supervised by Dr. Kenichi Okamoto and Dr. Mei Zhen. Jay recently received the first prize in our Mightex Annual Research Excellence Award for the research outlined above.

Utilizing advanced techniques like the Mightex OASIS Implant micro-endoscopy system, Jay is exploring the neural dynamics of hippocampal neurons during memory tasks in freely moving mice. His goal is to link specific neuronal activity patterns with distinct mouse behaviors, paving the way for a deeper understanding of learning and memory mechanisms.

Cellular-Resolution Optogenetics

The OASIS Implant imaging fiber cables provide bi-directional optical transmission. That is, it is capable of transmitting light from the OASIS Implant to the brain for optical stimulation for excitation of indicators and opsins, and transmitting emitted light from the brain back to the OASIS system to record fluctuation in indicator signals. Individual pixels within the image can be individually addressed for patterned illumination with Mightex's Polygon for cellular resolution optogenetic stimulation. Our imaging fiber cables are also highly durable and flexible, and can withstand the many forces involved in freely-behaving experiments.

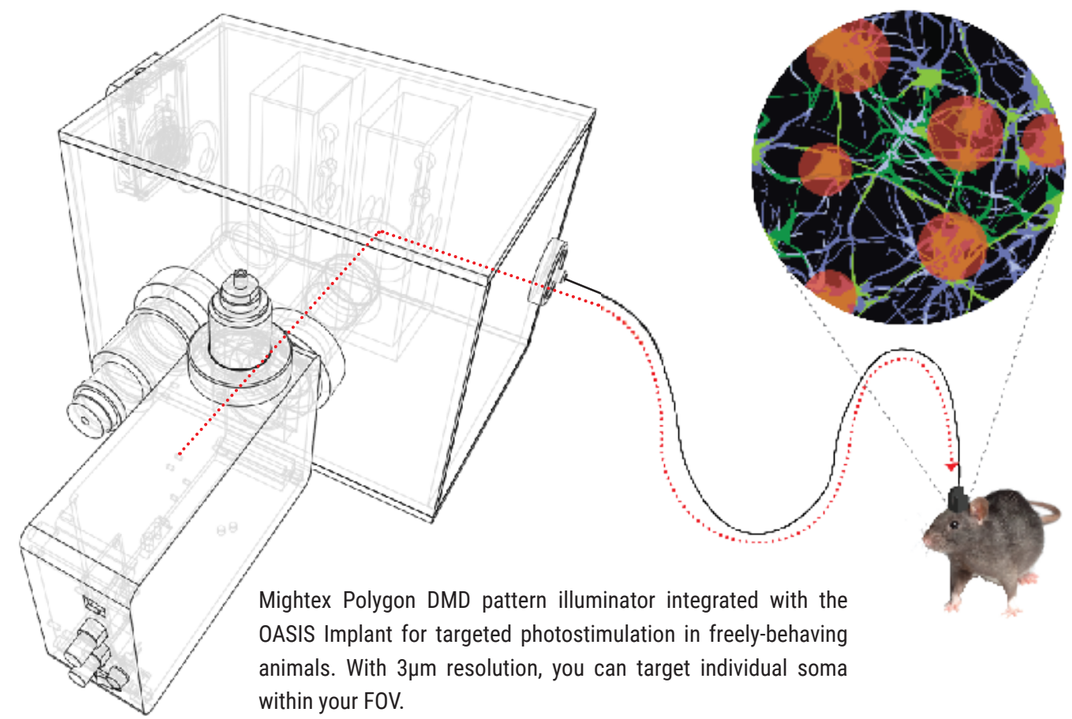

Mightex Polygon DMD pattern illuminator integrated with the OASIS Implant for targeted photostimulation in freely-behaving animals. With 3μm resolution, you can target individual soma within your FOV.

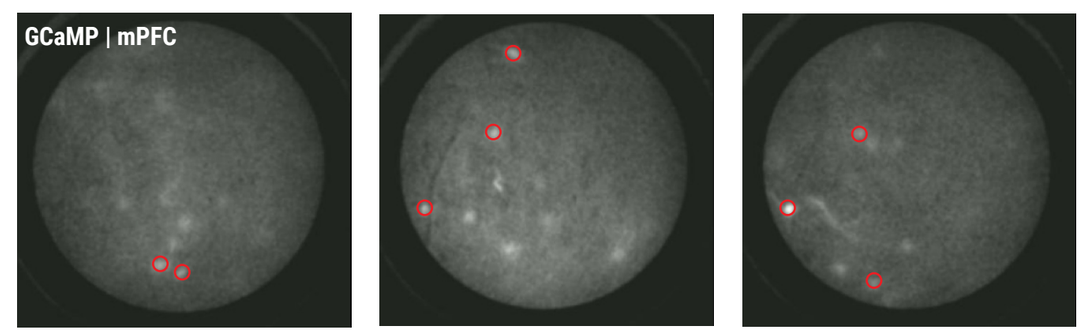

Imaging Fibers and Headmounts

The OASIS implant platform is capable of imaging and stimulating cortical and deep brain regions and spinal cord, allowing for data acquisition from anywhere within the central nervous system. To access deep brain regions, the OASIS implant headmount interfaces with an implantable gradient index (GRIN) lens. This headmount allows for accurate positioning and focus of the fiber relative to the GRIN to maximise data quality. The total weight of headmount can be as low as 0.3g, depending on components. These ultra light weight options maximise naturalistic behaviour while maintaining high quality data collection. Our headmounts also feature focus and orientation lock mechanisms to maxmise reproducbility of data collection parameters across multiple sessions.

HEADMOUNTS

Standard Headmount

Up to 3X lighter than miniscope alternatives. Provides focusing adjustment and ability to lock both focusing and orientation

7mm x 8mm base; height-15mm

Compact Headmount

This headmount is designed for multi-region or experiments requiring a smaller footprint on the surface of the head. Total weight 0.3g.

3mm x 4mm base; height- 5mm

IMAGING FIBERS

Deep-Brain Imaging Fibers

This flexible imaging probe is designed for deep-brain applications by using a fiber coupled to an implanted GRIN lens.

Part Number	Resolution	Field-of-View	Length
FBR-0350-10K-XXX-XXP	3μm	350	1-3 meters
FBR-0650-30K-XXX-XXP	3μm	650	1-3 meters

Cortical Imaging Fibers

These are designed for large field of view applications by using a fiber with an increased field of view through a cortical window.

Part Number	Resolution	Field-of-View	Length
FBR-0650-30K-XXX-10X	3μm	0.65mm	1-3 meters
FBR-0650-30K-XXX-34X	10.2μm	2.2mm	1-3 meters
FBR-0650-30K-XXX-50X	15μm	3.2mm	1-3 meters

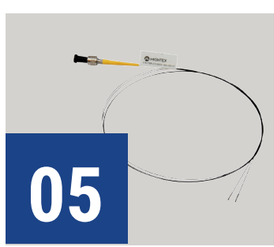

Multi-Region Imaging Fibers

Designed for multi-region imaging and optogenetics applications by using a split-fiber coupled to multiple implanted GRIN lenses.

Soft Imaging Fibers

For applications requiring increased mobility, such as with songbirds. Extra malleable fiber coupled to an implanted GRIN lens.

OASIS Implant ROAM

For experiments involving rotational behaviours, the OASIS Implant with Rotation Adaptive Mechanism (ROAM) provides the same cutting edge technology and high quality data acquisition as the OASIS Implant while accommodating high degrees of animal movement. When studying behavior paradigms that require constant animal movement and multiple changes of direction, the OASIS Implant ROAM will be the perfect solution.

FEATURES

Bi-directional
360-degree Fiber Rotation

Adaptive Rotation For
Photostimulation Tracking

- Interchangeable imaging fiber probes to accomodate different imaging/ stimulation experiments
- Furcated fiber probes for multi-region stimulation and imaging
- Interchangeable cameras, compatible with both GECI and GEVI imaging
- Motorized stand for easy height adjustment to further enhance freedom of movement
- Super-light head mounted fixture (0.7g)
- Futureproof, modular system design

OASIS Implant Systems Configurations

These are just a few ways the OASIS Implant can be configured for your experiments. However, the OASIS platform is modular and reconfigurable. Please contact a sales representative to tailor a system to meet your unique requirements.

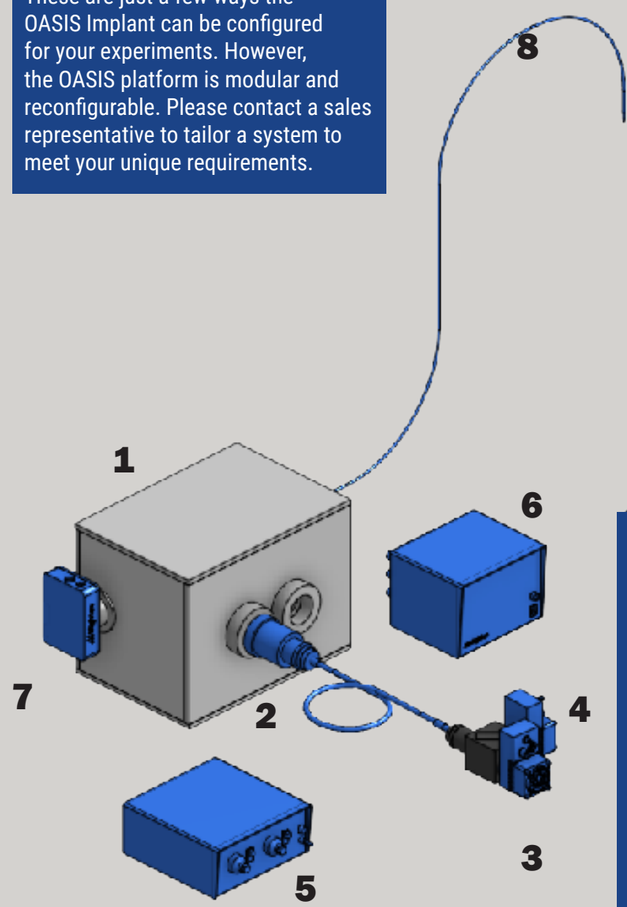

FIBER PHOTOMETRY

COMPONENTS

1. OASIS Implant Platform
   GCAMP Filter Set
   90R/10T Beam Splitter
2. Epi Widefield Illuminator
3. 405nm LED light source
4. 470nm LED light source
5. 2-channel LED Controller
6. BLS Analog & Digital Input/Output Module
7. High-sensitivity Camera
8. Fiber Patchcord
   Mating sleeves
   Cannulas

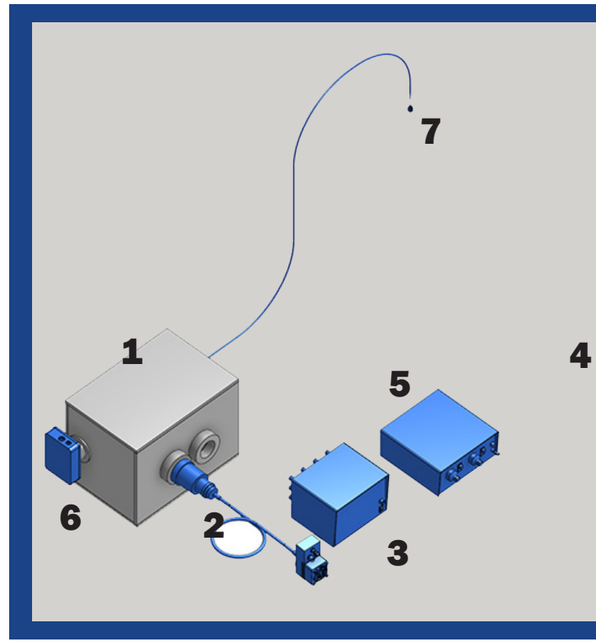

CALCIUM IMAGING

COMPONENTS

1. OASIS Implant Platform
   GCAMP Filter Set
   90R/10T Beam Splitter
2. Epi Widefield Illuminator
3. 470nm Lightguide-coupled LED source
4. LED Controller
5. BLS Analog & Digital Input/Output Module
6. High-sensitivity Camera
7. Imaging Fiber
   GRIN Implant
   Headmounts

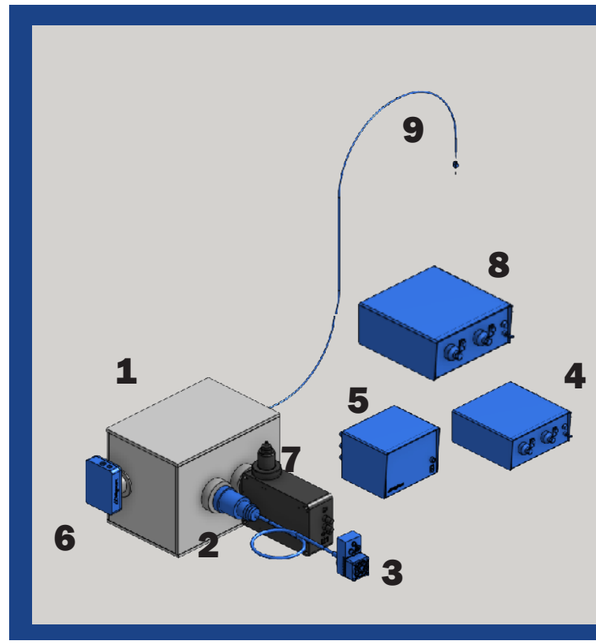

CALCIUM IMAGING & OPTOGENETICS

COMPONENTS

1. OASIS Implant Platform
   GCAMP Filter Set
   90R/10T Beam Splitter
2. Epi Widefield Illuminator
3. 470nm Lightguide-coupled LED source
4. LED Controller
5. BLS Analog & Digital Input/Output Module
6. High-sensitivity Camera
7. Polygon DMD Pattern Illuminator
8. 635nm Laser Source
9. Imaging Fiber
   GRIN Implant
   Headmounts

OASIS Macro & Micro

OASIS Macro and Micro are designed to provide researchers with a scalable/reconfigurable optical system for cellular-resolution imaging and stimulation experiments in head-fixed experimental preparations. Unlike traditional micro/macroscopes, the OASIS platforms provide ample space for working with fixed animals and the platforms' position can be easily adjusted around the animal. The modularized design of the OASIS platform allows for the final system to be tailored to the researcher's specific experimental requirements to image or illuminate a large or small field of view. The addition of Mightex's Polygon to our OASIS platform enables targeted patterned illumination of regions or cells of interest. As well, major features, such as adding a second or a third illumination source, and fine details, such as adaptors for a particular make of microscope objectives, can be adjusted. Overall, the flexible OASIS platform can facilitate the unique and diverse research endeavors of the scientific community.

FEATURES

50mm Tube Lens for Large Field of View

Futureproof Modular Design

- Patterned (with a Polygon) and/or wide-field illumination
- High optical power over a large field of view
- Heavy duty precision manual or motorized XYZ stage
- Tilt mechanism to rotate the system relative to a tilted specimen surface
- Options available to include additional wide-field illumination or multiple cameras
- Accepts any C-mount camera
- Software platform available

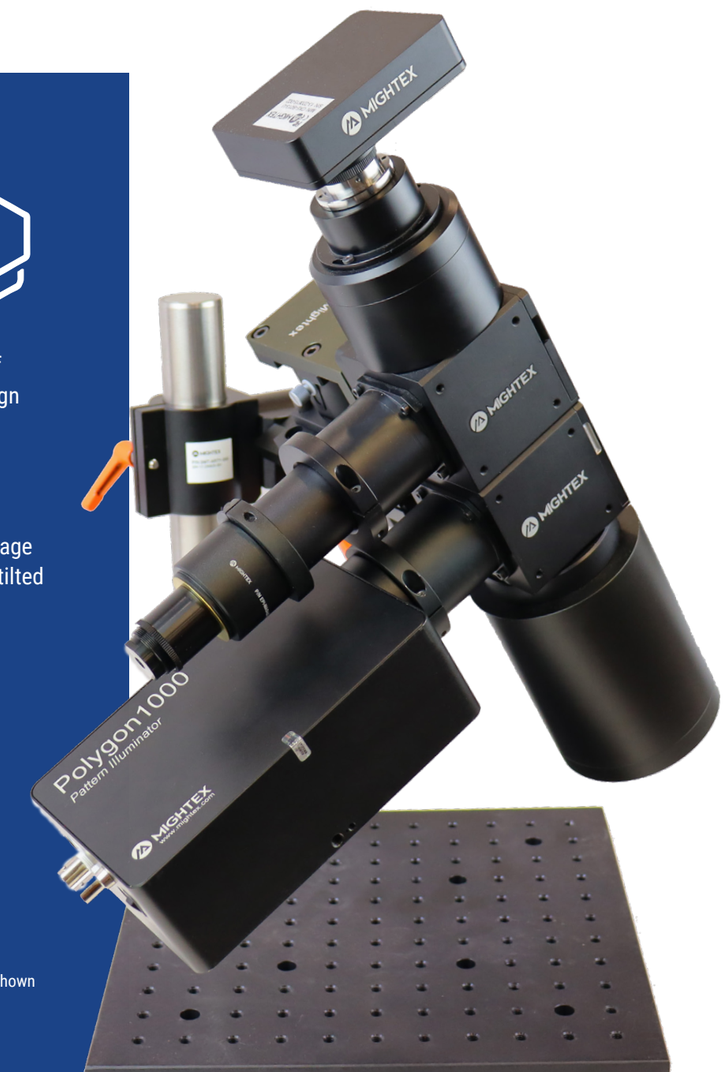

OASIS Macro System shown

OASIS Macro & Micro Platforms

The OASIS Macro & Micro platforms are made up of multiple components that provide great versatility to researchers.

MULTI-PORT ILLUMINATION

The OASIS Micro and Macro can be modified to accomodate multiple light sources, depending on the imaging and/or optogenetic application. Either via an epi-fluorescent illuminator that accepts a 3mm-core liquid lightguide input or by coupling Mightex's Polygon pattern illuminator for maximum illumination control, the researcher has full control of illumination with the the OASIS Micro and Macro.

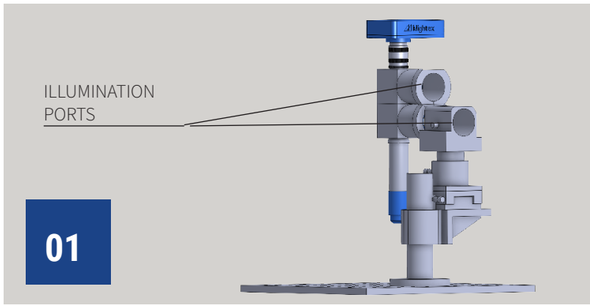

MULTIPLE OBJECTIVES

The OASIS Micro can be used with different commercially availble objectives from the major microscope brands (Olympus, Nikon, Zeiss, Leica). The OASIS Macro on the other hand should be used with our macro objective lenses (1X, 2X, and 4X). These lenses are interchangeable.

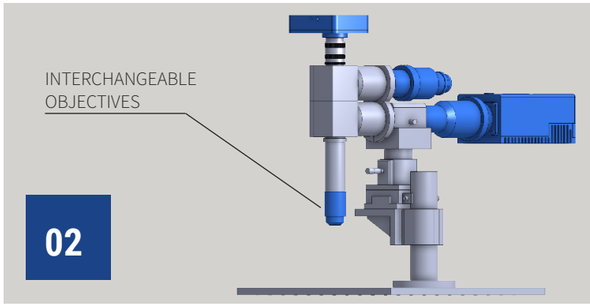

TRANSLATIONAL OR STEREOTAXIC

Two (2) different stage options are available depending on the animal model and region of interest of the researcher. The standard translation stage allows for adjustments in the XYZ. The stereotaxic stage provides an extra two axes of tilt allowing the objective to be adjusted around the animal from multiple angles to obtain maximum control of imaging location.

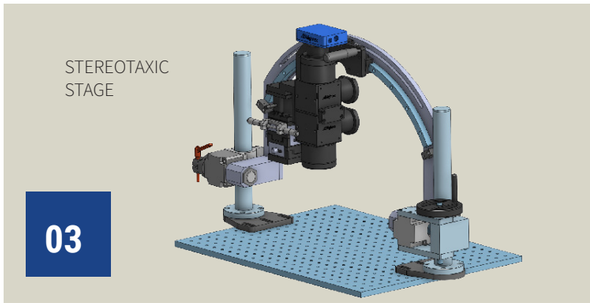

SCIENTIFIC-GRADE CAMERAS

The OASIS Macro and Micro come with a standard C-mount port that is compatible with any C-mount camera.Researchers can use high-speed, high-sensitivity cameras to capture better quality images for reliable quantitative analysis.

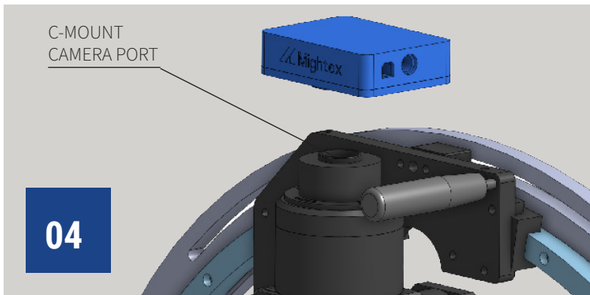

Research Highlights

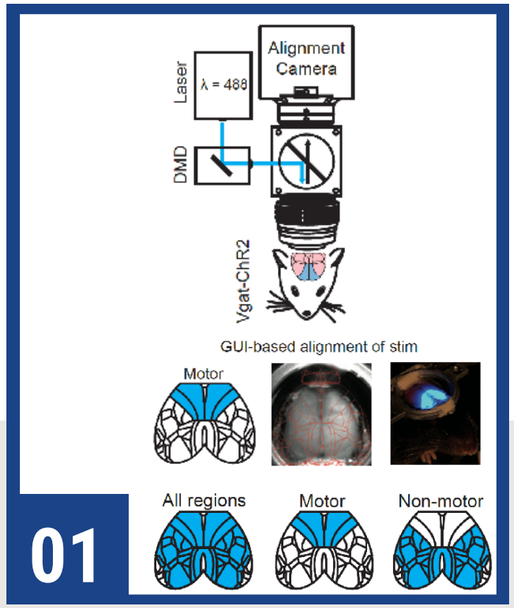

Targeted Optogenetic Stimulation of Motor and Non-Motor Cortices

Kauvar I.V., Machado T.A., Yuen E., Kochalka J., Choi M., Allen W.E., Wetzstein G., Deisseroth K. Cortical Observation by Synchronous Multifocal Optical Sampling Reveals Widespread Population Encoding of Actions. (2020) **Neuron.**

Kauvar *et al.* 2020 used the Polygon DMD illuminator together with Mightex's large field-field-of-view OASIS Macro imaging system to simultaneously optogenetically inhibit multiple regions of the mouse's whole brain cortex. They provide evidence that cortical non-motor areas may play a causal role in motor plan execution.

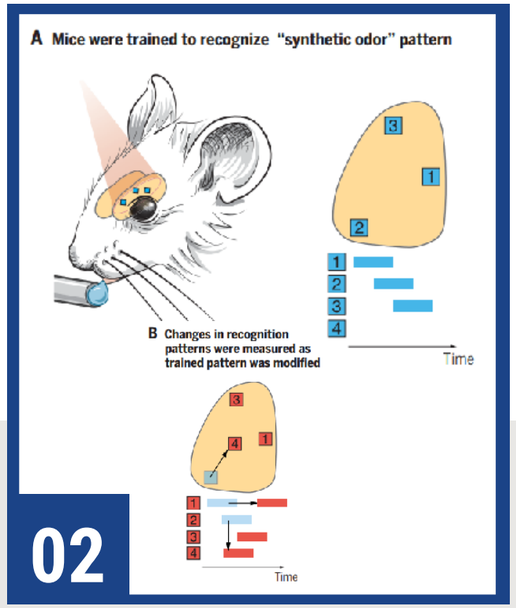

Perceptual Invariance to the Olfactory Spatio-temporal Code

Chong E., Moroni M., Wilson C., Shoham S., Panzeri S., Rinberg D. Manipulating Synthetic Optogenetic Odors Reveals the Coding Logic of Olfactory Perception (2020) **Science.**

Chong *et al.* 2020 utilized the Polygon integrated into our OASIS Micro modular microscope platform to deliver coded spatial and temporal illumination patterns to produce synthetic optogenetic odors in the olfactory bulb of live and awake mice to uncover new information and priciples governing the spatio-temporal code of olfactory perception.

OASIS Macro & Micro Systems Configurations

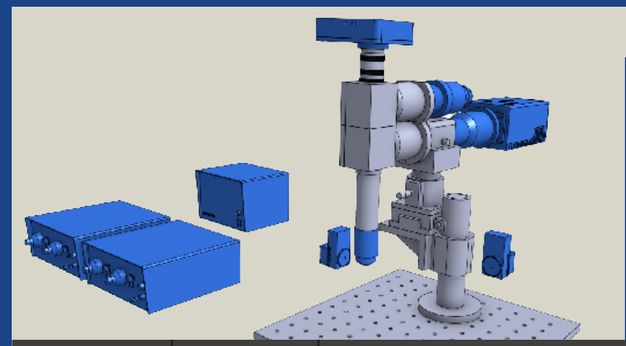

CALCIUM IMAGING & TARGETED OPTOGENETICS

OASIS MICRO

OASIS Micro Platform
XYZ Translational Stage
GCAMP Filter Set
90R/10T Beam Splitter

Epi Widefield Illuminator
BLS-Series Lightguide-coupled LED sources
LED Controllers
BLS Analog & Digital Input/Output Module
High-sensitivity Camera
Polygon DMD Pattern Illuminator

Model	Projection Area	Commercial Microscope (1X Objective)[a]			
		Leica	Nikon	Olympus	Zeiss
POLYGON1000-G LARGE FOV	Height | mm	12.4	12.4	11	10.2
	Width | mm	19.8	19.8	17.8	16.2
	Diagonal | mm	23.2	23.2	21	19.2
	Pixel Size | µm	15.2	15.2	13.8	12.6
POLYGON1000-DL	Diameter[b] | mm	12.4	12.4	11	10.2
	Pixel Size | µm	15.2	15.2	13.8	12.6

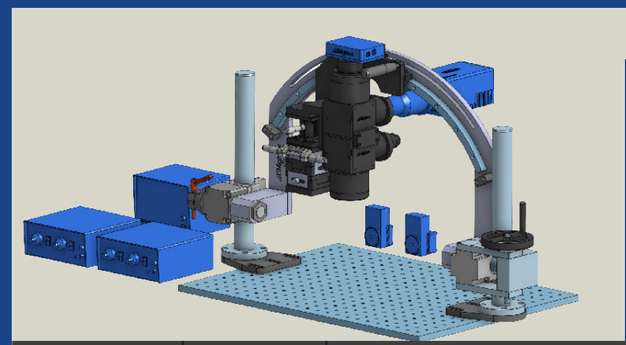

CALCIUM IMAGING & TARGETED OPTOGENETICS

OASIS MACRO

OASIS Macro Platform
XYZ Stereotaxic Stage
GCAMP Filter Set
90R/10T Beam Splitter

Epi Widefield Illuminator
BLS-Series Lightguide-coupled LED sources
LED Controllers
BLS Analog & Digital Input/Output Module
High-sensitivity Camera
Polygon DMD Pattern Illuminator

Model	Projection Area	Objective		
		4X	2X	1X
POLYGON1000-G LARGE FOV	Height | mm	3.1	6.2	12.4
	Width | mm	4.9	9.9	19.8
	Diagonal | mm	5.8	11.6	23.2
	Pixel Size | µm	3.8	7.6	15.2
POLYGON1000-DL	Diameter[b] | mm	3.1	6.2	12.4
	Pixel Size | µm	3.8	7.6	15.2

SYSTEM CONTROL & DATA ACQUISITION

Mightex offers complete system solutions for hardware synchronization and device management control to enable researchers to program and customize their experimental parameters to optimize the collection and interpretation of experimental results.

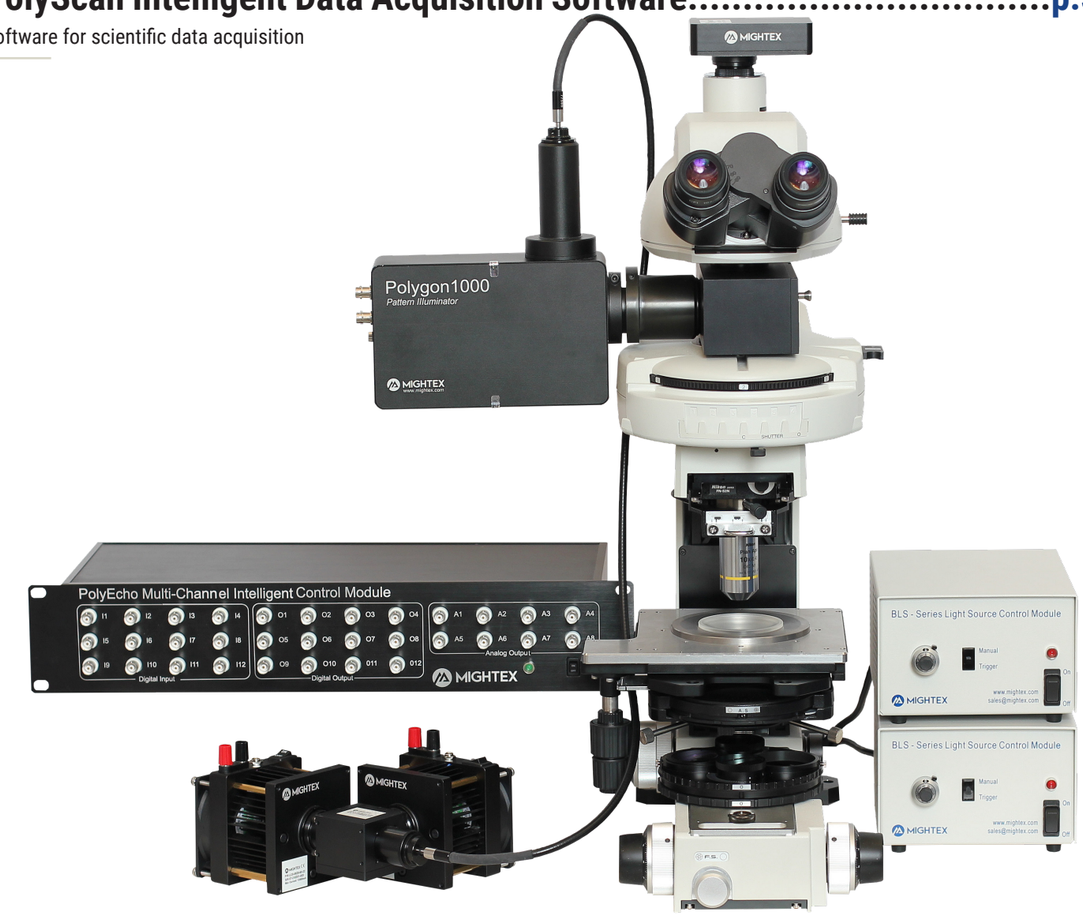

PolyEcho Multi-Channel Intelligent Control Module

In multi-threaded, event-driven experiments including in freely-behaving neuroscience animal research, there is a need for the data-acquisition system to react to different triggering events with different user-defined responses, in which cameras, light sources, or other devices are activated in a pre-programmed fashion. In such experiments, triggering events usually do not occur in a predefined sequence but rather in a largely random manner. Multiple hardware- or software-trigger signals, each corresponding to a specific event, are fed to the system and all devices must be properly coordinated and synchronized, not only to generate & send optical and/or electrical signals/stimulations to the specimen, but also to collect data from the specimen. There is also a need to accurately record the timing ("time-stamping") of those events and actions, in order to ensure reliable post-acquisition data processing and analysis. Our Mightex PolyEcho intelligent control module is designed to enable such event-driven experiments. The goal is not only to reliably record the timing of all events using timestamps generated by the same clock inside the PolyEcho device, but also to coordinate different devices in order to properly synchronize signal/stimulation generation and data collection.

01

PolyEcho | PEC-CM12-U

KEY FEATURES

- 12 TTL inputs, 12 TTL outputs and 8 analog outputs
- Each TTL input can be programmed to control any combination of TTL & analog outputs
- Unified time-stamping for all input and output ports
- Port configuration software programmable by user
- Control parameters uploadable from PC to PolyEcho for real-time operation
- Trigger delay <20ms
- Support both hardware/TTL and software triggers

This schematic illustrates a typical data acquisition system which may include a wide range of equipment. The system may receive multiple hardware/TTL and software triggers, in response to which, it will activate data acquisition as per the trigger-specific workflow defined by the researcher through Mightex's PolyScan software. At the heart of the system is the PolyEcho Multi-Channel Intelligent Control Module, which is capable of not only handling up to 12 hardware/TTL and up to 32 software triggers, but also synchronizing and controlling all hardware devices in the system. In addition, PolyEcho is also able to send out additional TTL and analog signals to control other equipment outside the Data Acquisition System. Last but not least, all incoming trigger events and all control signals sent to the devices are logged with precise and unified time stamps.

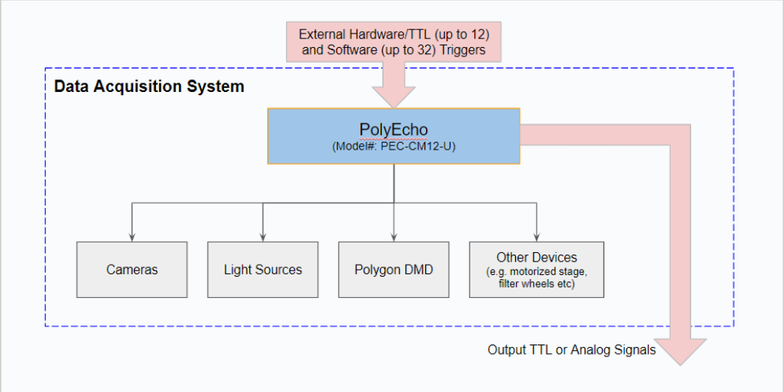

Figure 1. Data acquistion system control with Mightex PolyEcho

PERFORMANCE SPECIFICATIONS

Models	PEC-CM12-U
Current Accuracy | mA	±3%
Number of Channels	12x Digital Inputs 12x Digital Outputs 8x Analog Outputs
Power Supply Input Voltage (V_{dc}) | V	24
Channel Connector Type	BNC
Analog Channel Output Voltage Resolution | %	0.1
Analog Channel Output Voltage Range | V	0 - 5V or 0 - 10V*
Analog Channel Output Voltage Accuracy | V	+/-0.5% (or +/-3mV)**
Digital and Analog Channel Output Time Resolution | µs	20
Input Trigger Current Requirement | mA	2-20

[a] When forward voltage of LED load is greater than 8V, 24V DC input might be used.
[b] External analog voltage source should have 8+ mA of current driving capability.
[c] The input current should be greater than the combined output current of the two channels.

DIMENSIONS

Models	Weight |g	Size (lxwxh) |mm
PEC-CM12-U		485(L) x 220(W) x 89(H)

PolyScan Intelligent Data Acquisition Software

PolyScan is a turn-key data acquisition software for scientific research. It provides highly flexible system wiring & configuration, device parameter settings, experimental workflow programming, as well as hardware synchronization and control for scientific experiments. PolyScan paves the way for the future of scientific data collection, providing an easily navigable and flexible platform for efficient and reliable experimental control, as well as data collection and review.

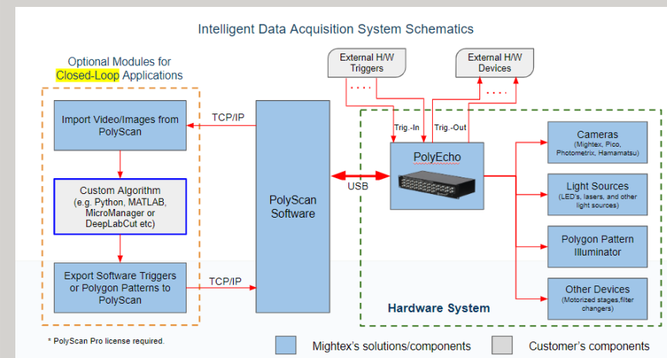

Figure 2. Data acquistion system control with Mightex PolyScan and PolyEcho

The schematic diagram shows a typical data acquisition system based on PolyScan software and PolyEcho multi-channel intelligent control module. In such a system, PolyScan and PolyEcho can be considered as the 'soul' and the 'brain' of the system, respectively, and the user can use PolyScan to set all control parameters of all devices (including cameras, light sources, Polygon pattern illuminator, and other devices) and use PolyEcho to synchronize/control all devices through TTL and analog control signals.

KEY FEATURES

- Support of a wide range of Mightex hardware devices such as cameras, light sources, light source drivers, and Polygon DMD pattern illuminators.
- Fully customizable system configuration and device wiring
- Unified time stamping for all devices and all triggers (with PolyEcho)
- Capable of handling both TTL and software triggers (with PolyEcho)
- Programmable system response and experimental workflow, tailorable for each trigger source and/or for each trigger pulse
- Sharable experimental template containing system wiring, device settings, and experimental workflow
- Data review during and post data acquisition
- (Pro license) Support 3rd-party non-Mightex hardware devices
- (Pro license) Closed-loop control capabilities
- (Pro license) Support custom algorithms and data exchange with external programs such as Python, MATLAB, MicroManager and DeepLabCut.

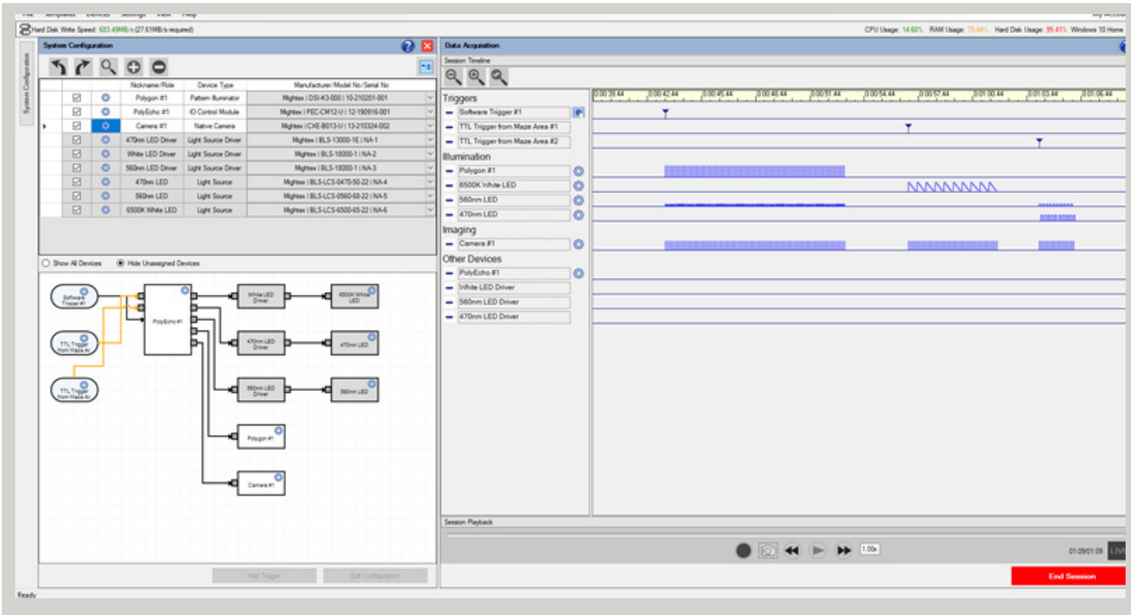

The main GUI of the PolyScan software as shown above is composed of three sections: (1) a list of hardware devices in the data acquisition system; (2) a wiring diagram illustrating how the devices are connected/wired; and (3) a timing diagram showing how each and every device responds to hardware and software triggers during the data acquisition.

Please visit **www.mightex.com** for more information regarding:

- Mightex PolyScan software
- Software license options
- Supported hardware
- Complete list of features

LIGHT SOURCES

Mightex offers the widest collection of bioscience LED and laser solutions. With hundreds of wavelengths and beam format options to choose from our portfolio can provide the right illumination solution for any experiment.

LED Light Source Selection Guide

Mightex has developed the most comprehensive LED source solutions in the market. In order to make it easier for our customers to choose the best LED solutions for their specific applications, below is a brief LED source selection guide:

STEP 1 Choose your desired wavelengths based on the charts below

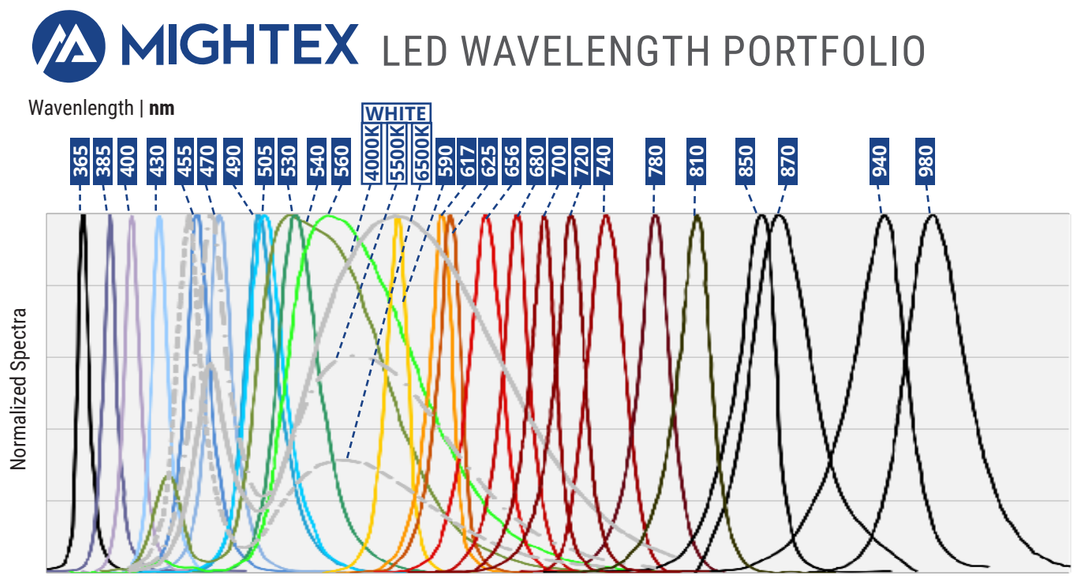

New LED wavelengths are continually added to the portfolio. Please visit **www.mightex.com** for updated list.

STEP 2 Choose the best beam format for your application

MICROSCOPY LEDS	FIBER-COUPLED LEDS	LIGHTGUIDE-COUPLED LEDS	UNIFORM PRECISION LEDS
Collimated output	Coupled into fiber with 200-1000μm diameters	Coupled into lightguides with 3-5mm diameter	Highly uniform illumination
Attachable to epi-port	Fiber optics implants	Optional collimator	Free space illumination
Modular multiwavelength concept	Multiwavelength	Compatible with commercial microscopes	Ideal for uniform illumination of cell culture plates and multi-well dishes

Microscopy LEDs

Mightex has developed the LCS-series high-power LED turn-key systems to produce homogeneous, high-intensity, wide-field illumination under a microscope objective. In addition to the superb optical performances, the LED systems also feature ultra fast switching & quick response times, as well as advanced software and/or synchronization capabilities such that users can easily integrate the LED source into a larger system.

LCS-series microscopy LED turn-key systems feature a modular design that is both scalable and reconfigurable. Such a design enables customers to re-use their previously purchased LED modules, expand a single-wavelength system into a multiwavelength one, add new wavelength(s), or remove/ replace old wavelength(s) from an existing multiwavelength system, leading to significant cost savings in both materials and labor.

A basic LCS-series microscopy LED turn-key system consists of (1) an LED control module, (2) a BLS-series highpower LED collimator source, and (3) a microscope adaptor, as illustrated below.

EXAMPLE CONFIGURATION

Type J LCS-Series Collimated LED directly coupled to microscope's epi-illuminator port.

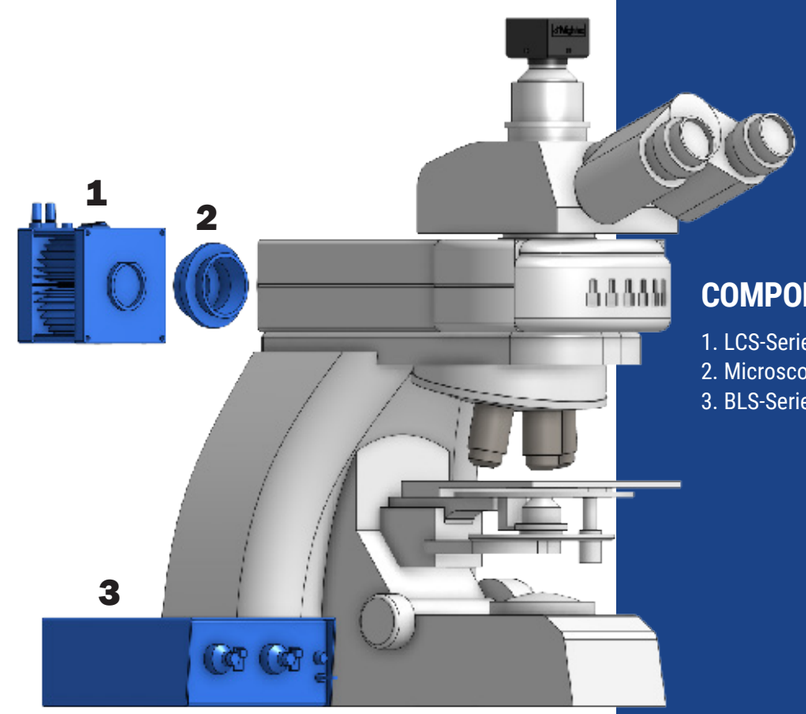

COMPONENTS

1. LCS-Series Collimated LED
2. Microscope Adaptor
3. BLS-Series LED Controller

01

Type-A LCS Collimated LED

- Passively cooled via a integrated heat sink
- 22mm aperture for standard microscopy applications
- Adjustable focus
- Aspherical collimating lens

Part Number	Nominal Wavelength (nm)	Half Diverging Angle (Deg.) φ22mm[1]	I_{op} (mA)	V_{op} (V)	Typical Output Power[2] (mW)
BLS-LCS-0365-04-22	365	3.4	1000	3.65	500
BLS-LCS-0400-01-22	400	2.5	350	3.5	100
BLS-LCS-0395-03-22	395	1.7	1000	3.1	270
BLS-LCS-0400-01-22	400	2.5	350	3.5	100
BLS-LCS-0400-03-22	400	1.7	1000	3.1	265
BLS-LCS-0400-04-22	400	1.7	1000	3.5	750
BLS-LCS-0405-03-22	405	1.7	1000	3	325
BLS-LCS-0410-03-22	410	1.7	1000	3	315
BLS-LCS-0415-03-22	415	1.7	1000	3	310
BLS-LCS-0430-02-22	430	1.7	500	3.8	190
BLS-LCS-0455-03-22	455	1.7	1000	3	500
BLS-LCS-0470-03-22	470	1.7	1000	3.9	200
BLS-LCS-0471-02-22	471	1.7	350	3	140
BLS-LCS-0490-01-22	490	1.7	350	3.5	140
BLS-LCS-0505-03-22	505	1.7	1000	3.9	135
BLS-LCS-0560-03-22	560 broadband	2.2	1000	2.9	240
BLS-LCS-0585-03-22	585 broadband	2.2	700	2.9	82
BLS-LCS-0590-03-22	590	1.7	1000	3.9	65
BLS-LCS-0617-03-22	617	1.7	1000	3.9	150
BLS-LCS-0625-03-22	625	1.7	1000	3.9	280
BLS-LCS-0656-03-22	656	1.7	1000	3.1	280
BLS-LCS-0680-02-22	680	1.7	600	2.7	75
BLS-LCS-0700-01-22	700	1.7	500	2.1	51
BLS-LCS-0720-01-22	720	1.7	600	2.2	73
BLS-LCS-0740-03-22	740	2.5	1000	2.5	200
BLS-LCS-0780-02-22	780	1.7	800	2.5	110
BLS-LCS-0810-02-22	810	1.7	800	2.2	120
BLS-LCS-0850-03-22	850	1.7	1000	3	430
BLS-LCS-0870-01-22	870	1.7	700	1.9	110
BLS-LCS-0910-02-22	910	1.7	1000	1.9	120
BLS-LCS-0940-02-22	940	1.7	1000	1.8	200
BLS-LCS-0980-01-22	980	1.7	500	1.4	30
BLS-LCS-3000-03-22	warm white 3,000K	1.7	1000	2.8	150

Type-A LCS | *continued*

Part Number	Nominal Wavelength (nm)	Half Diverging Angle (Deg.) φ22mm[1]	I_{op} (mA)	V_{op} (V)	Typical Output Power[2] (mW)
BLS-LCS-4000-03-22	warm white 4,000K	1.7	1000	3.9	180
BLS-LCS-5500-03-22	cool white 5,500K	1.7	1000	3.9	170
BLS-LCS-6500-03-22	glacier white 6,500K	1.7	1000	3.6	180

[1] Clear aperture diameter. Use these two-digit numbers to replace xx in the part number.
[2] Due to variations in the manufacturing process and operating parameters such as temperature and current, the actual output of any given LED may vary. Specifications are intended to be used as a guideline.

02

Type-J LCS Collimated LED

- High Power (>7W models)
- Passively cooled via a integrated heat sink
- 22mm aperture for standard microscopy applications
- Adjustable focus
- Aspherical collimating lens

Part Number	Nominal Wavelength (nm)	Half Diverging Angle (Deg.) φ22mm[1]	I_{op} (mA)	V_{op} (V)	Typical Output Power[2,3] (mW)
LCS-0365-13-22-J	365	3.4	3500	3.85	1200
LCS-0470-14-22-J	470	1.7	3000	4.6	860
LCS-0530-13-22-J	530	1.4	2400	4.9	290
LCS-0540-14-22-J	540	2.2	3000	4.6	500
LCS-0625-07-22-J	625	1.4	2400	2.9	260

[1] Clear aperture diameter. Use these two-digit numbers to replace xx in the part number.
[2] Maximum CW output achievable with a BLS-3000-2 BioLED control module.
[3] Due to variations in the manufacturing process and operating parameters such as temperature and current, the actual output of any given LED may vary. Specifications are intended to be used as a guideline.

LED Microscope Adaptors

Our mechanical adaptors connect our microscopy collimated LEDs and beam combiners to different models, allowing integration into virtually any microscopy system.

MODELS

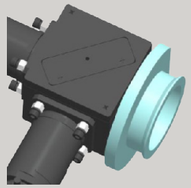

01

Leica DMI Microscope Adaptor

ACC-BC25-LC1

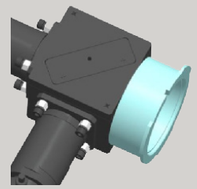

02

Nikon Eclipse Microcope Adaptor

ACC-BC25-NK1

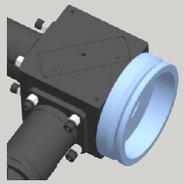

03

Olympus IX & BX Microscope Adaptors

ACC-BC25-OL1

04

Olympus MLS Adaptor

ACC-BC25-OL2

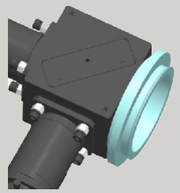

05

Zeiss Axioskop Microscope Adaptor

ACC-BC25-ZS1

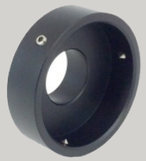

06

Transmission Port Nikon Adaptors

ACC-BC25-NK-LV-UEPI

Multiwavelength Microscopy LEDs

Mightex offers a uniquely versatile high-power multiwavelength microscopy LED system. The LCS modular “building blocks” construction system allows users to assemble an LED solution with two (2) or more light sources coupled together with beam combiners with high efficiency dichroics.

In addition to the superb optical output power, the LCS series allows users to rapidly change (in the order of microseconds) between different LEDs, or illuminate multiple wavelengths simultaneously. The LCS-Series utilizes advanced LED controllers with software, analog, and TTL synchronization capabilities, enabling customers to easily integrate the LED system into their experimental setup. LCS-series microscopy LEDs are designed to provide maximum flexibility and versatility. For example, a three wavelength system can easily be expanded into a four-wavelength solution to suit changing requirements of an application.

EXAMPLE CONFIGURATION

Multiwavelength Type-A LCS-Series Collimated LEDs directly coupled to microscope’s epi-illuminator port.

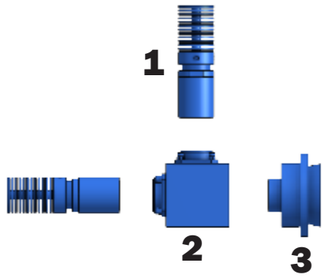

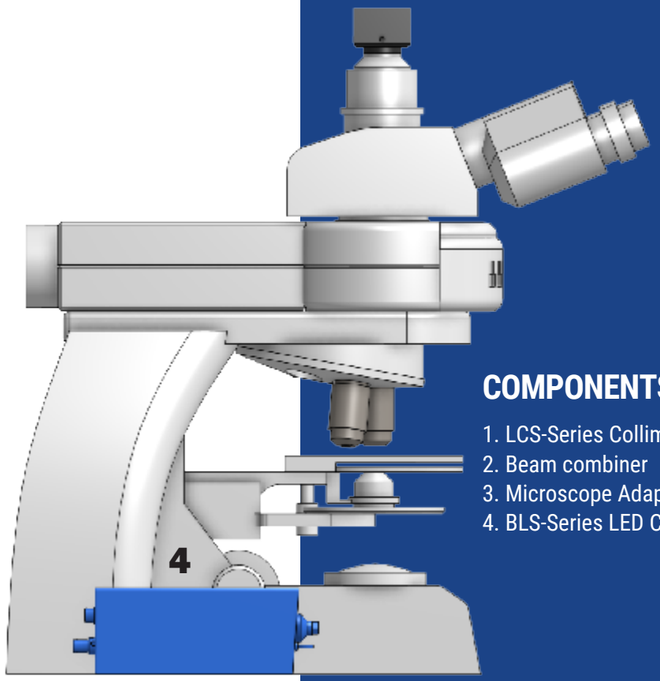

COMPONENTS

1. LCS-Series Collimated LED
2. Beam combiner
3. Microscope Adaptor
4. BLS-Series LED Controller

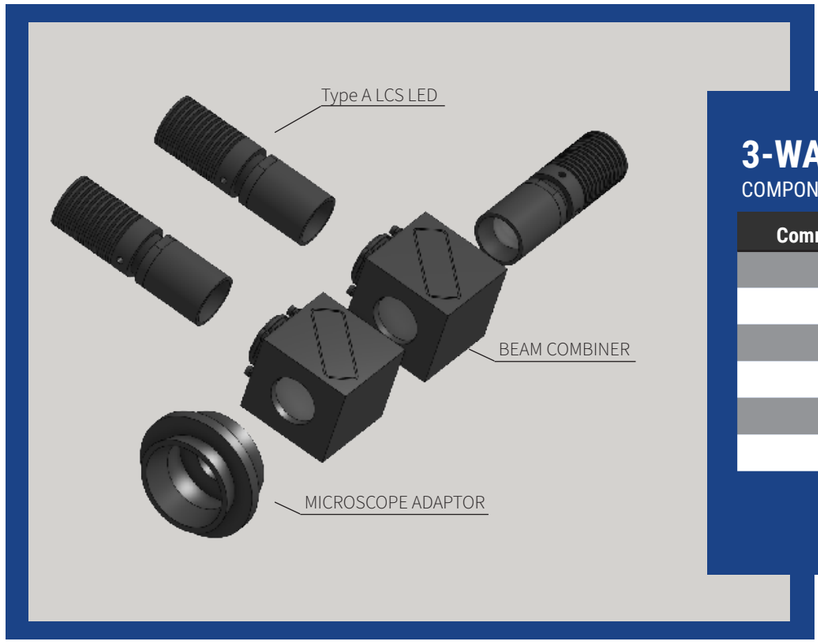

3-WAVELENGTH
COMPONENTS

Common Wavelength Combinations
365nm / 400nm / 470nm
385nm / 470nm / 530nm
400nm / 470nm / 530nm
470nm / 530nm / 625nm
470nm / 590nm / 617nm
470nm / 590nm / 625 nm

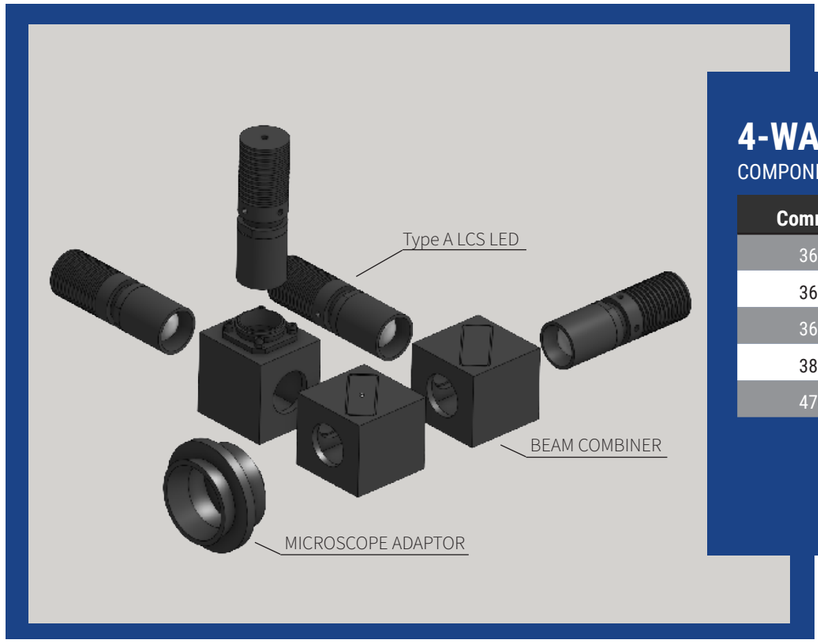

4-WAVELENGTH
COMPONENTS

Common Wavelength Combinations
365nm / 400nm / 470nm / 530nm
365nm / 470nm / 530nm / 590nm
365nm / 470nm / 530nm / 625nm
385nm / 470nm / 530nm / 625nm
470nm / 530nm / 625nm / 740nm

WheeLED Wavelength-Switchable LED Sources

Mightex's WheeLED™ wavelength-switchable LED light source combines multiple LEDs into a single chassis. Up to nine (9) different LEDs from UV-NIR, including a number of white LEDs, can be mounted into a single chassis to form a cost-effective solution to meet the wide wavelength range that your microscopy application demands. The WheeLED™ wavelength-switchable LED sources let users manually switch between a selection of LED sources with different wavelengths and/or white LEDs.
A high-NA aspherical collimating optics is included for precision collimation and high light throughput. Clear aperture of the optics is 22mm in diameter. Under a microscope, the WheeLED™ produce homogeneous, high-intensity, wide-field illumination. Howevre, other optional optics are available and may be added for fiber/ lightguide coupling and other functions. The light sources can be driven by Mightex LED controllers or other LED controllers and current sources. Only a single driving channel is required because at any time only one wavelength is powered up. Over-current protection is built into the light source to prevent potential damage during switching.

EXAMPLE CONFIGURATION

Wavelength-Switchable WLS Series Collimated LED directly coupled to microscope's epi-illuminator port.

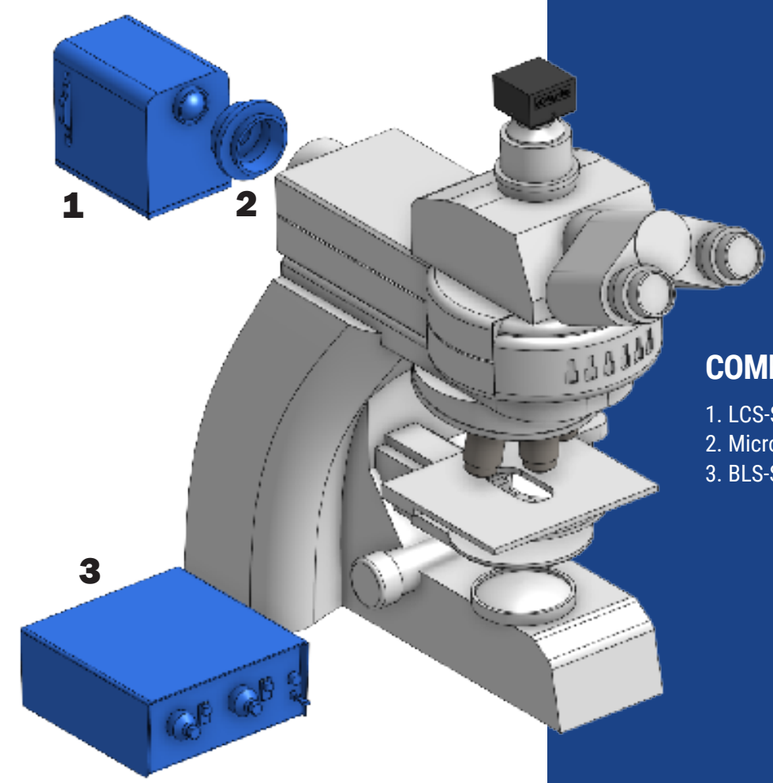

COMPONENTS

1. LCS-Series Collimated LED
2. Microscope Adaptor
3. BLS-Series LED Controller

01

WheeLED Collimated LED

- Wavelength Switchable
- Up to 9 wavelengths
- Rapid on/off timing
- High-power, homogeneous illumination
- Low cost multiwavelength solution

Part Number	Wavelength (nm)	Half Diverging Angle (deg.)	I_{op} (mA)	V_{op} (V)	Typical Output Power[1] (mW)
WLS-LED-0340-02	340	3.4	500	4.3	23
WLS-LED-0365-04	365	3.4	1000	3.65	500
WLS-LED-0385-04	385	3.4	1000	3.65	500
WLS-LED-0400-01	400	2.5	350	3.5	100
WLS-LED-0400-04	400	1.7	1000	3.5	750
WLS-LED-0405-03	405	1.7	1000	3	325
WLS-LED-0410-03	410	1.7	1000	3	315
WLS-LED-0415-03	415	1.7	1000	3	310
WLS-LED-0420-03	420	1.7	1000	3	310
WLS-LED-0425-03	425	1.7	1000	3	290
WLS-LED-0455-03	455	1.7	1000	3.9	280
WLS-LED-0470-03	470	1.7	1000	3.9	200
WLS-LED-0490-01	490	1.7	350	3.5	140
WLS-LED-0505-03	505	1.7	1000	3.9	135
WLS-LED-0530-03	530	1.7	1000	3.9	100
WLS-LED-0560-02	560 broadband	1.7	700	2.9	180
WLS-LED-0560-03	560 broadband	2.2	1000	2.9	240
WLS-LED-0590-03	590	1.7	1000	3.9	65
WLS-LED-0617-03	617	1.7	1000	3.9	150
WLS-LED-0625-03	625	1.7	1000	3.9	280
WLS-LED-0656-03	656	1.7	1000	2.7	280
WLS-LED-0680-02	680	1.7	600	2.7	75
WLS-LED-0740-03	740	2.5	1000	2.5	200
WLS-LED-0780-02	780	1.7	800	2.5	110
WLS-LED-0810-02	810	1.7	800	2.2	120
WLS-LED-0850-03	850, 3W	1.7	1000	3	430
WLS-LED-0870-01	870	1.7	700	1.9	110
WLS-LED-0940-01	940	1.7	700	1.5	100
WLS-LED-0940-02	940	1.7	1000	1.8	200
WLS-LED-0980-01	980	1.7	500	1.4	30
WLS-LED-4000-03	warm white 4,000K	1.7	1000	3.9	180
WLS-LED-5500-03	cool white 5,500K	1.7	1000	3.9	170
WLS-LED-6500-03	glacier white 6,500K	1.7	1000	3.6	180

[1] Due to variations in the manufacturing process and operating parameters such as temperature and current, the actual output of any given LED may vary. Specifications are intended to be used as a guideline.

Fiber-Coupled LED Sources

Mightex fiber-coupled LED light sources employ the latest high-power LED technologies and proprietary coupling optics to achieve maximum optical output power through a fiber optic cable. Optical output is coupled into a fiber through a standard SMA fiber adaptor port (SMA fiber patch cords are sold separately), allowing users to use Mightex LEDs with any SMA fiber they choose. Output power and beam properties will depend on the core diameter and NA of the fiber chosen. All modules also feature a locking electrical connector for secured connection and are compatible with any Mightex BLS Series controller. Single wavelength (FCS) and multiwavelength (WFC) units are available in any wavelength within Mightex's wavelength portfolio. Single wavelength LEDs (FCS series) are ideal for applications where the required working wavelength is known and switching wavelengths without switching the fiber is not required. The FCS series features precise proprietary coupling optics for maximum output power intensity. The FCS series is available in type A configuration with optimized thermal dissipation passive cooling housing, and a type B configuration with higher power LED emitters. Type B configuration LEDs feature an active cooling fan to ensure proper heat dissipation.

01

Type-A FCS Fiber-Coupled LED

- Passively cooled via an integrated heat sink
- UV/VIS/NIR wavelengths
- SMA fiber receptacle
- No moving parts in optical path
- Locking electrical connector

Part Number	Description	Nominal Wavelength (nm)	I_{op} (mA)	V_{op} (V)	Typical Radiant Flux[1,2] (mW) With 400µm 0.22NA Fiber	Typical Radiant Flux (mW) With 400µm 0.39NA Fiber
BLS-FCS-0000-000	Cool White	5,500K	1000	3.9	3.2	6.4
BLS-FCS-0001-000	Warm White	4,000K	1000	3.9	3.2	6.4
BLS-FCS-0002-000	Glacier White	6,500K	1000	3.6	3.2	6.4
BLS-FCS-0003-000	Warm White	3,000K	1000	2.8	2.8	5.6
BLS-FCS-0265-001	Deep UV	265	350	6.3	400µW	N/A
BLS-FCS-0275-001	Deep UV	275	600	6		N/A
BLS-FCS-0280-002	Deep UV	280	800	6.5	600µW	N/A
BLS-FCS-0310-001	Deep UV	310	600	5.8	360µW	N/A
BLS-FCS-0325-001	Deep UV	325	350	5.4	220µW	N/A
BLS-FCS-0340-002	Deep UV	340	350	4.3	0.6	1.1
BLS-FCS-0365-001	UV 365nm	365	1000	3.65	4.3	8.6
BLS-FCS-0380	UV 380nm	380	1000	3.2	2.8	5.6
BLS-FCS-0385-001	UV 385nm	385	1000	3.65	5.8	11.6
BLS-FCS-0395	UV 395nm	395	1000	3.1	6.2	12.4
BLS-FCS-0400-002	UV 400nm, 3W	400	1000	3.1	6.1	12.2

Type-A FCS | *continued*

Part Number	Description	Nominal Wavelength (nm)	I_{op} (mA)	V_{op} (V)	Typical Radiant Flux[1,2] (mW) With 400µm 0.22NA Fiber	Typical Radiant Flux (mW) With 400µm 0.39NA Fiber
BLS-FCS-0405	UV 405nm	405	1000	3	7.5	15
BLS-FCS-0410	410nm	410	1000	3	7.3	14.6
BLS-FCS-0415	415nm	415	1000	3	7.2	14.4
BLS-FCS-0430	430nm	430	500	3.8	2.9	5.8
BLS-FCS-0455	455nm	455	1000	3.0	18	36
BLS-FCS-0470	470nm	470	1000	3.9	7	14
BLS-FCS-0471	471nm	471	350	3	2.1	4.2
BLS-FCS-0490	490nm	490	350	3.5	3.2	6.4
BLS-FCS-0505	505nm	505	1000	3.9	3.5	7
BLS-FCS-0530	530nm	530	1000	2.85	7	14
BLS-FCS-0560	560nm broadband	560	700	2.9	5.5	11
BLS-FCS-0590	590nm	590	1000	3.2	1.2	3.8
BLS-FCS-0617	617nm	617	1000	3	6.5	13
BLS-FCS-0625	625nm	625	1000	3	6.5	13
BLS-FCS-0656	656nm	656	1000	3.1	6.5	13
BLS-FCS-0680	680nm	680	600	2.7	1.4	2.8
BLS-FCS-0700	700nm	700	500	2.1	0.6	1.2
BLS-FCS-0720	720nm	720	600	2.2	0.9	1.8
BLS-FCS-0740	740nm	740	1000	2.9	3.6	7.2
BLS-FCS-0780	NIR 780nm	780	800	2.5	2.2	4.4
BLS-FCS-0810	NIR 810nm	810	800	2.2	1.5	3
BLS-FCS-0850-001	NIR 850nm, 3W	850	1000	3	6	12
BLS-FCS-0870	NIR 870nm	870	700	1.9	1.4	2.8
BLS-FCS-0910	NIR 910nm	910	1000	1.9	1.5	3
BLS-FCS-0940	NIR 940nm	940	1000	2.4	4	8

[1] Measured with a 400µm core 0.22 numerical aperture (NA) fiber. Output optical power scales approximately linearly with fiber core area and NA^2.
[2] Due to variations in the manufacturing process and operating parameters such as temperature and current, the actual output of any given LED may vary. Specifications are intended to be used as a guideline.

02

Type-B FCS Fiber-Coupled LED

- Acitvely cooled via a fan
- Higher Power (>7W models)
- VIS wavelengths
- SMA fiber receptacle
- No moving parts in optical path

Part Number	Description	Nominal Wavelength (nm)	I_{op} (mA)	V_{op} (V)	Typical Radiant Flux[1,2] (mW) With 400µm 0.22NA Fiber	Typical Radiant Flux (mW) With 400µm 0.39NA Fiber
BLS-FCS-0470-101	Blue	470	3000	4.6	19	38
BLS-FCS-0530-100	Green	530	2400	4.9	8	15
BLS-FCS-0540-100	Broadband Green	540	3000	4.6	10	20
BLS-FCS-0625-100	Red	625	2400	2.9	9	22

[1] Measured with a 400µm core 0.22 numerical aperture (NA) fiber. Output optical power scales approximately linearly with fiber core area and NA^2.
[2] Due to variations in the manufacturing process and operating parameters such as temperature and current, the actual output of any given LED may vary. Specifications are intended to be used as a guideline.

03

Type-H FCS Fiber-Coupled LED

- Acitvely cooled via a fan
- Super High Power (>38W models)
- SMA fiber receptacle
- No moving parts in optical path

Part Number	Description	Nominal Wavelength (nm)	I_{op} (mA)	V_{op} (V)	Typical Radiant Flux[1,2] (mW) With 1000µm 0.22NA Fiber	Typical Radiant Flux (mW) With 1000µm 0.39NA Fiber
BLS-FCS-0365-201	UV	365	18	4.2	200	140
BLS-FCS-0405-201	UV	405	18	3.6	70	220
BLS-FCS-0470-200	Blue, 50W	470	13	3.8	90	280
BLS-FCS-0470-201	Blue, 60W	470	18	3.4	105	330
BLS-FCS-0525-200	Green, 60W	525	13	4.6	50	160
BLS-FCS-0525-201	Green, 80W	525	18	4.4	60	190
BLS-FCS-0560-200	560 broadband	560	18	3.8	90	280
BLS-FCS-0625-200	Red, 38W	625	13	2.9	40	130
BLS-FCS-0625-201	Red, 42W	625	18	2.3	45	150
BLS-FCS-0730-200	NIR	730	18	5.9	90	170
BLS-FCS-0850-200	NIR	850	18	3.75	110	340
BLS-FCS-6500-200	Glacier White, 30W	6500K	9	3.7	60	180
BLS-FCS-6500-201	Glacier White, 65W	6500K	18	3.7	100	280

[1] Measured with a 1000µm core 0.22 numerical aperture (NA) fiber. Output optical power scales approximately linearly with fiber core area and NA^2.
[2] Due to variations in the manufacturing process and operating parameters such as temperature and current, the actual output of any given LED may vary. Specifications are intended to be used as a guideline.
* Estimated

Multiwavelength Fiber-Coupled LED

Mightex multiwavelength fiber-coupled light sourcesare enabled by the latest LED technologies andMightex's proprietary beam combining and couplingoptics. Up to eight (8) LEDs are coherently combined into a single multi-mode fiber with the highest efficiency possible. Each LED can be powered independently and simultaneously, making the WFC-series a new class of light sources with a tunable spectrum. The light sources are offered in two configurations: the standard configuration and the high-power configuration. Neutral beam combiners are used in the standard configuration. The standard configuration has the advantage of low cost and the most flexible wavelength plans. Any wavelength and white color may be combinedin the standard configuration. For applications that require the highest possible output power, one shouldchoose the high-power configuration where high-efficiency dichroic beam splitters are used to combine different wavelengths. Because not all possible dichroic beamsplitters are in stock, some wavelength combinations may require customization. Please contact us with your detailed wavelength plan to obtain a quotation for custom higher-power configurations.

01

WFC High-Power Fiber-Coupled LED

- Multiwavelength with up to 8 wavelengths in one unit
- Combined single fiber output
- Interchangeable fiber with SMA receptacle
- Cooling fan for maximum intensity stability
- High Power Configuration

Wavelength Code	Wavelength (nm)	I_{op} (mA)	V_{op} (V)	Typical Radiant Flux[1,2] (mW)					
				2-Wavelength		4-Wavelength		6 or 8-Wavelength	
				400µm 0.22NA fiber	400µm 0.39NA fiber	400µm 0.22NA fiber	400µm 0.39NA fiber	400µm 0.22NA fiber	400µm 0.39NA fiber
0365	365	1000	3.65	3.6 (7.2)	3.2 (6.4)	2.9 (5.8)	6.4	2.9	5.8
0380	380	1000	3.2	2.3 (4.6)	1.9 (3.8)	1.7 (3.4)	3.8	1.7	3.4
0385	385	1000	3.65	4.8 (9.6)	4.3 (8.6)	3.9 (7.8)	8.6	3.9	7.8
0390	390	1000	3.1	4.8 (9.6)	4.3 (8.6)	3.9 (7.8)	8.6	3.9	7.8
0395	395	1000	3.1	5.1 (10.2)	4.1 (8.2)	3.7 (7.4)	8.2	3.7	7.4
0400	400	1000	3.8	4.4 (8.8)	4.0 (8.0)	2.0 (4.0)	8.0	2	4.0
0405	405	1000	3	6.2 (12.4)	5.0 (10.0)	4.5 (9.0)	10	4.5	9
0410	410	1000	3	6.2 (12.4)	5.0 (10.0)	4.5 (9.0)	10	4.5	9
0415	415	1000	3	6.1 (12.2)	4.9 (9.8)	4.4 (8.8)	9.8	4.4	8.8
0425	425	1000	3	5.3 (10.6)	4.3 (8.6)	3.8 (7.6)	10.2	4.5	9.0
0455	455	1000	3.9	5.6 (11.2)	5.1 (10.2)	4.5 (9.0)	10.8	4.9	9.8
0470	470	1000	3.9	6.0 (12.0)	5.4 (10.8)	4.9 (9.8)	3.6	1.5	3.0
0490	490	700	3.7	2.2 (4.4)	1.8 (3.6)	1.5 (3.0)	4.4	1.7	3.4
0505	505	1000	3.9	2.8 (5.6)	2.2 (2.2)	1.7 (3.4)	4.4	1.9	3.8
0530	530	1000	3.9	2.4 (4.8)	2.2 (4.4)	1.9 (3.8)	2.6	1.0	2.0

WFC High-Power | *continued*

Wavelength Code	Wavelength (nm)	I_{op} (mA)	V_{op} (V)	Typical Radiant Flux[1,2] (mW)					
				2-Wavelength		4-Wavelength		6 or 8-Wavelength	
				400µm 0.22NA fiber	400µm 0.39NA fiber	400µm 0.22NA fiber	400µm 0.39NA fiber	400µm 0.22NA fiber	400µm 0.39NA fiber
0560	560	700	3.9	1.5 (3.0)	1.3 (2.6)	1.0 (2.0)	2.4	1.1	2.2
0590	590	1000	3.9	1.3 (2.6)	1.2 (2.4)	1.1 (2.2)	9.4	4.2	8.4
0617	617	1000	3.9	5.2 (10.4)	4.7 (9.4)	4.2 (8.4)	11.0	5.0	10.0
0625	625	1000	3.9	6.1 (12.2)	5.5 (11.0)	5.0 (10.0)	9.4	4.2	8.4
0656	656	1000	2.7	5.2 (10.4)	4.7 (9.4)	4.2 (8.4)	1.6	0.5	1.0
0680	680	600	2.7	1.0 (2.0)	0.8 (1.6)	0.5 (1.0)	0.4	90uW	180uW
0700	700	500	2.1	0.4 (0.8)	0.2 (0.4)	90µW (180µW)	0.8	0.2	0.4
0720	720	600	2.2	0.6 (1.2)	0.4 (0.8)	0.2 (0.4)	4.4	1.9	3.8
0740	740	1000	2.9	2.4 (4.8)	2.2 (4.4)	1.9 (3.8)	2.2	0.7	1.4
0780	780	800	2.5	1.6 (3.2)	1.1 (2.2)	0.7 (1.4)	1.6	0.5	1.0
0810	810	800	2.2	1.0 (2.0)	0.8 (1.6)	0.5 (1.0)	5.8	2.6	5.2
0850	850, 3W	1000	3	4.8 (9.6)	4.3 (8.6)	3.9 (7.8)	4.4	1.9	3.8
0870	870	700	2	2.4 (4.8)	2.2 (4.4)	1.9 (3.8)	5.8	2.6	5.2
0940	940	1000	2.1	3.2 (6.4)	2.9 (5.8)	2.6 (5.2)	0.2	80uW	160uW
0980	980	500	1.4	0.3 (0.6)	0.1 (0.2)	80µW (160µW)	-	-	-
6500	glacier white 6,500K	1000	3.6	-	-	-	-	-	-
5500	cool white 5,500K	1000	3.9	-	-	-	-	-	-
4000	warm white 4,000K	1000	3.9	-	-	-	4.3 (8.6)	3.8 (7.6)	-

[1] Measured with a 400µm core 0.22 numerical aperture (NA) fiber. Output optical power scales approximately linearly with fiber core area and NA^2.
[2] Due to variations in the manufacturing process and operating parameters such as temperature and current, the actual output of any given LED may vary. Specifications are intended to be used as a guideline.

02

WFC Standard Fiber-Coupled LED

- Multiwavelength with up to 8 wavelengths in one unit
- Combined single fiber output
- Interchangeable fiber with SMA receptacle
- Cooling fan for maximum intensity stability
- Standard Configuration

Wavelength Code	Wavelength (nm)	I_{op} (mA)	V_{op} (V)	Typical Radiant Flux[1] (mW)	
				2-Wavelength	4-Wavelength
0365	365	1000	3.65	1.7	0.8
0380	380	1000	3.2	1.1	0.4
0385	385	1000	3.65	2.3	1.1
0390	390	1000	3.1	2.1	0.8
0395	395	1000	3.1	2.3	1.1
0400	400	1000	3.8	1.1	0.5

WFC Standard | *continued*

Wavelength Code	Wavelength (nm)	I_{op} (mA)	V_{op} (V)	Typical Radiant Flux[1] (mW)	
				2-Wavelength	4-Wavelength
0405	405	1000	3	2.8	1
0410	410	1000	3	2.8	1
0415	415	1000	3	2.7	0.9
0420	420	1000	3.8	1.8	0.5
0425	425	1000	3	2.4	0.9
0455	455	1000	3.9	2.7	1.3
0470	470	1000	3.9	2.9	1.4
0490	490	700	3.7	1	0.3
0505	505	1000	3.9	1.4	0.6
0530	530	1000	3.9	0.8	0.4
0560	560	700	3.9	0.7	0.3
0590	590	1000	3.9	0.6	0.3
0617	617	1000	3.9	2.5	1.2
0625	625	1000	3.9	2.5	1.2
0656	656	1000	2.7	2.5	1.2
0680	680	600	2.7	0.5	0.2
0700	700	500	2.1	0.2	90μW
0720	720	600	2.2	0.3	0.1
0740	740	1000	2.9	1.2	0.7
0780	780	800	2.5	0.7	0.3
0810	810	800	2.2	0.5	0.2
0850	850	1000	2.1	1.5	0.7
0870	870	700	2	1.1	0.5
0940	940	1000	2.1	1.5	0.7
0980	980	500	1.4	0.1	70μW
6500	glacier white 6,500K	1000	3.6	1.2	0.6
5500	cool white 5,500K	1000	3.9	1.2	0.6
4000	warm white 4,000K	1000	3.9	1.2	0.6

[1] Measured with a 400μm-core 0.22 numerical aperture (NA) fiber. Optical output power scales approximately linearly with fiber core area and NA[2].
[2] Due to variations in the manufacturing process and operating parameters such as temperature and current, the actual output of any given LED may vary. Specifications are intended to be used as a guideline.

In Vivo Optogenetics Starter Kits

Expand your experimental repertoire into optogenetic manipulation of biological/neural processes with our *in vivo* optogenetics starter kit. Each kit includes a 470nm high-power LED, light weight 200μm fiber optic patch cable with optional rotary joint, and fiber optic cannulas. This kit enables researchers to get started right away with their experiments, while leveraging the adaptability of Mightex's BLS-Series platform for flexibility down the road. Easily add in another wavelength LED or even a multiwavelength LED unit.

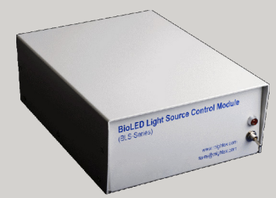

+

+

01

BLS-SA02-US Software Controller (or BLS-3000-2 Manual Controller)

Type B 470nm Fiber-Coupled LED

Rotary joint Patch cord

Starter Kit Contents

PERFORMANCE SPECIFICATIONS — WITH ROTARY JOINT

Models	OGK-0470-0200-37-250-BLSSA02-RJ	OGK-0470-0200-37-250-BLS3000-RJ	OGK-0470-0200-37-125-BLS-SA02-RJ	OGK-0470-0200-37-125-BLS3000-RJ
LED Controller	BLS-SA02-US	BLS-3000-2	BLS-SA02-US	BLS-3000-2
Cannula Ferrule Size | mm	Φ2.5	Φ2.5	Φ1.25	Φ1.25
Cannula Output Power[1] | mW	4.4	4.4	4.0	4.0
Variation in Output Power During Rotation	±2%			
Light Source	BLS-FCS-0470-101, 470nm Fiber-Coupled LED			
Fiber Core Size | μm	Φ200			

[1] Output power measured at the cannula at maximum driving current. For BLS-SA02-US LED controller, maximum driving current achieved using Intellipulsing

PERFORMANCE SPECIFICATIONS — WITHOUT ROTARY JOINT

Models	OGK-0470-0200-37-250-BLSSA02	OGK-0470-0200-37-250-BLS3000	OGK-0470-0200-37-125-BLS-SA02	OGK-0470-0200-37-125-BLS3000
LED Controller	BLS-SA02-US	BLS-3000-2	BLS-SA02-US	BLS-3000-2
Cannula Ferrule Size | mm	Φ2.5	Φ2.5	Φ1.25	Φ1.25
Cannula Output Power[1] | mW	7.6	7.6	6.8	6.8
Light Source	BLS-FCS-0470-101, 470nm Fiber-Coupled LED			
Fiber Core Size | μm	Φ200			

[1] Output power measured at the cannula at maximum driving current. For BLS-SA02-US LED controller, maximum driving current achieved using Intellipulsing

Fiber patch cords are also available as stand alone items. Each optogenetics patch cable features an SMA-connector on one end and either a 2.5mm or 1.25mm ceramic ferrule on the other. For experiments with awake and non-head fixed animals it is recommended to choose models with a built-in ultra low friction rotary joint to allow the live animal to have unhindered movement. Mightex's rotary joints have incredibly low power variation (less than 2%) during rotation.

FIBER OPTIC CABLES & ACCESSORIES

Fiber Patch Cord P/N	Fiber Core Diameter (µm)	Fiber NA	Rotary Joint	Ceramic Ferrule Diameter (mm)	Fiber Length (m)
FPC-0200-22-01SMA-125C	Φ200	0.22	No	Φ1.25	1
FPC-0200-22-01SMA-250C	Φ200	0.22	No	Φ2.5	1
FPC-0200-37-01SMA-125C	Φ200	0.37	No	Φ1.25	1
FPC-0200-37-01SMA-250C	Φ200	0.37	No	Φ2.5	1
FPC-RJ-0200-22-03SMA-125C	Φ200	0.22	Yes	Φ1.25	3
FPC-RJ-0200-22-03SMA-250C	Φ200	0.22	Yes	Φ2.5	3
FPC-RJ-0200-37-03SMA-125C	Φ200	0.37	Yes	Φ1.25	3
FPC-RJ-0200-37-01-SMA-250C	Φ200	0.37	Yes	Φ2.5	3
FFB-RJ-02-0200-37-03SMA[a]	Φ200	0.37	Yes	Φ1.25	3
FPC-RJ-H-200-37-03SMA-250C[b]	Φ200	0.37	Yes	Φ2.5	3
FPC-RJ-H-0200-37-03SMA-125C[b]	Φ200	0.37	Yes	Φ1.25	3
FPC-0200-50-01SMA-125C	Φ200	0.5	No	Φ1.25	1
FPC-0200-50-01SMA-250C	Φ200	0.5	No	Φ2.5	1
FPC-0400-50-01SMA-125C	Φ400	0.5	No	Φ1.25	1
FPC-0400-50-01SMA-250C	Φ400	0.5	No	Φ2.5	1
FPC-RJ-0200-50-03SMA-125C	Φ200	0.5	Yes	Φ1.25	3
FPC-RJ-0200-50-03SMA-250C	Φ200	0.5	Yes	Φ2.5	3
FPC-RJ-0400-50-03SMA-125C	Φ400	0.5	Yes	Φ1.25	3
FPC-RJ-0400-50-03SMA-250C	Φ400	0.5	Yes	Φ2.5	3

[a] Furcated fiber bundle with rotary joint. 1m length each leg (200µm core, 0.37NA each). Total length 3m long. Ideal for bilateral stimulation.
[b] Rotary Joint Multimode Fiber Patchcord, 0.37 NA, 1000µm Core, SMA on one end, 0.37 NA, 200µm core, ceramic ferrule on other end. For Type-H FCS light sources.

FIBER OPTIC CANNULAS

Fiber Implant P/N	NA	Ferrule Diameter	Protusion Length (mm)
CNL-200-37-05-125C	0.37	1.25	5
CNL-200-37-05-250C	0.37	2.5	5
CNL-200-37-10-125C	0.37	1.25	10
CNL-200-37-10-250C	0.37	2.5	10
CNL-200-50-05-125C	0.5	1.25	5
CNL-200-50-05-250C	0.5	2.5	5
CNL-200-50-10-125C	0.5	1.25	10
CNL-200-50-10-250C	0.5	2.5	10

FIBER OPTIC CANNULAS | *continued*

Fiber Implant P/N	NA	Ferrule Diameter	Protusion Length (mm)
CNL-400-50-05-125C	0.5	1.25	5
CNL-400-50-05-250C	0.5	2.5	5
CNL-400-50-10-125C	0.5	1.25	10
CNL-400-50-10-250C	0.5	2.5	10

FIBER OPTIC MATING SLEEVES

Mating Sleeve P/N	Description
ACC-FPC-SLV125	Mating Sleeve for Φ 1.25 mm ferrule or cannula
ACC-FPC-SLV250	Mating Sleeve for Φ 2.50 mm ferrule or cannula

Lightguide-Coupled LED Sources

Mightex GCS-series high power LED sources are designed for high-efficiency coupling of LED light into a liquid lightguide (LLG) or a fiber optic bundle. Virtually all lightguides with core diameters ranging from 3mm to 8mm can be used with the GCS series light source. Please note that lightguides are sold separately. The GSC series also features a locking electrical connector for secured connections. GCS series LEDs are designed as a universal light source for general lab use applications. The one-piece machined aluminum alloy housing features integrated heatsinks and multiple mounting holes. GCS-series multi-chip LED emitters are also available (Type B). Some of these 7W to 15W LEDs have total optical power exceeding 1W, quadrupling the power of a single-chip LED (Type A). Models with higher powers (i.e. Type B with 7W and higher) feature a cooling fan, and have a different form factor compared to other models. Power supply for the cooling fan is included. To drive a GCS LED source, one can use a wide range of LED controllers Mightex has to offer.

01

Type-A GCS Lightguide-Coupled LED

- Passive cooling with integrated heat sink
- Compact, machined metal housing
- Interchangeable liquid lightguides
- Multiple mounting features for lab applications

Part Number[1]	Description	Nominal Wavelength (nm)	I_{op} (mA)	V_{op} (V)	Typical Radiant Flux[2,3] (mW)
GCS-0310-03-xxxxx	DUV 310nm	310	350	5.8	18
GCS-0325-03-xxxxx	DUV 325nm	325	500	5.4	9
GCS-0340-02-xxxxx	DUV 340nm	340	500	4.3	12
GCS-0365-04-xxxxx	UV 365nm	365	1000	3.65	300
GCS-0380-03-xxxxx	UV 380nm, 3W	380	1000	3.2	80
GCS-0385-04-xxxxx	UV 385nm	385	1000	3.65	300
GCS-0390-03-xxxxx	UV 390nm	390	1000	3.1	165
GCS-0395-03-xxxxx	UV 395nm	395	1000	3.1	180
GCS-0400-03-xxxxx	UV 400nm, 3W	400	1000	3.1	175
GCS-0405-03-xxxxx	UV 405nm	405	1000	3	215
GCS-0410-03-xxxxx	410nm	410	1000	3	210
GCS-0415-03-xxxxx	415nm	415	1000	3	210
GCS-0430-02-xxxxx	430nm	430	500	3.8	130
GCS-0455-03-xxxxx	Royal Blue	455	1000	3	300
GCS-0470-04-xxxxx	Blue, 4W	470	1000	3.9	130
GCS-0471-04-xxxxx	Blue	471	350	3	95
GCS-0490-01-xxxxx	490nm	490	350	3.5	85
GCS-0505-04-xxxxx	Cyan	505	1000	3.9	30
GCS-0530-03-xxxxx	Green	530	1000	2.85	120
GCS-0560-02-xxxxx	560nm,broadband	560	700	2.9	120
GCS-0590-03-xxxxx	Amber	590	1000	3.2	35

Type-A GCS | *continued*

Part Number[1]	Description	Nominal Wavelength (nm)	I_{op} (mA)	V_{op} (V)	Typical Radiant Flux[2,3] (mW)
GCS-0617-03-xxxxx	Red-Orange	617	1000	3	100
GCS-0625-03-xxxx	Red	625	1000	3	100
GCS-0700-01-xxxx	700nm	700	500	2.1	35
GCS-0720-01-xxxx	720nm	720	600	2.2	50
GCS-0740-03-xxxx	740nm	740	1000	2.9	130
GCS-0810-02-xxxx	810nm	810	800	2.2	80
GCS-0850-03-xxxx	850nm	850	1000	3	150
GCS-0870-01-xxxx	870nm	870	700	1.9	75
GCS-0910-02-xxxx	910nm	910	1000	1.9	80
GCS-0940-02-xxxx	940nm	940	1000	2.4	125
GCS-0980-01-xxxx	980nm	980	500	1.4	20
GCS-3000-03-xxxx	Warm White	3,000K	1000	2.8	80
GCS-4000-04-xxxx	Warm White	4,000K	1000	3.9	95
GCS-5500-04-xxxx	Cool White	5,500K	1000	3.9	95
GCS-6500-04-xxxx	Glacier White	6,500K	1000	3.6	95

[1] xxxxx is the Lightguide Adaptor code. Please see Table on page 54.
[2] Measured at the exiting end of a 1 meter long, 3mm-core, 0.59 numerical aperture (NA) liquid lightguide.
[3] Due to variations in the manufacturing process and operating parameters such as temperature and current, the actual output of any given LED may vary. Specifications are intended to be used as a guideline.

02

Type-B GCS Lightguide-Coupled LED

- Active cooling with integrated fan
- High-power (>7W models)
- Compact, machined metal housing
- Interchangeable liquid lightguides
- Multiple mounting features for lab applications

Part Number[1]	Description	Nominal Wavelength (nm)	I_{op} (mA)	V_{op} (V)	Typical Radiant Flux[2,3] (mW)
GCS-0365-13-xxxxx	UV 365nm, 13W	365	3500	3.85	950
GCS-0385-07-xxxxx	UV 385nm, 7W	385	500	15	330
GCS-0385-11-xxxxx	UV 385nm, 11W	385	700	15.5	410
GCS-0385-13-xxxxx	UV 385nm, 13W	385	3500	3.75	1180
GCS-0470-15-xxxxx	Blue, 15W	470	1000	15	400
GCS-0505-12-xxxxx	Cyan	505	1000	12.2	200
GCS-0530-15-xxxxx	Green, 15W	530	1000	15	180
GCS-0617-10-xxxxx	Red-Orange, 10W	617	1000	10.8	175
GCS-0625-07-xxxxx	Red, 7W	625	700	9.6	400
GCS-3000-12-xxxxx	Warm White, 12W	3,000K	1000	12	240
GCS-5500-12-xxxxx	Cool White, 12W	5,500K	1000	12	300
GCS-6500-15-xxxxx	Glacier White, 15W	6,500K	1000	15	300

[1] xxxxx is the Lightguide Adaptor code. Please see Table 2 on page 54.
[2] Measured at the exiting end of a 1 meter long, 3mm-core, 0.59 numerical aperture (NA) liquid lightguide.
[3] Due to variations in the manufacturing process and operating parameters such as temperature and current, the actual output of any given LED may vary. Specifications are intended to be used as a guideline.
* When ordering an LED controller for a Type B LED, please make sure to upgrade the AC/DC power adaptor from the standard 12V to 24V.

03

Type-H GCS Lightguide-Coupled LED

- Active cooling with integrated fan
- Super-high power (>38W models)
- Compact, machined metal housing
- Interchangeable liquid lightguides
- Multiple mounting features for lab applications

Part Number[1]	Description	Nominal Wavelength (nm)	I_{op} (mA)	V_{op} (V)	Typical Radiant Flux[2,3] (mW)
GCS-0365-76-xxxxx	UV 365nm, 80W	365	18	4.2	2600
GCS-0405-65-xxxxx	UV 405nm, 65W	405	18	3.6	1600
GCS-0470-50-xxxxx	Blue, 50W	470	13	3.8	2000
GCS-0470-61-xxxxx	Blue, 60W	470	18	3.4	2400
GCS-0525-60-xxxxx	Green, 60W	525	13	4.6	800
GCS-0525-80-xxxx	Green, 80W	525	18	4.4	950
GCS-0560-68-xxxxx	560nm Broadband, 70W	560	18	3.8	1700
GCS-0625-38-xxxx	Red, 38W	625	13	2.9	700
GCS-0625-42-xxxx	Red, 42W	625	18	2.3	840
GCS-0730-77-xxxx	NIR, 80W	730	18	5.9	1100
GCS-0850-68-xxxx	NIR, 70W	850	18	3.75	2100
GCS-6500-33-xxxx	Glacier White, 30W	6,500K	9	3.7	1200
GCS-6500-65-xxxx	Glacier White, 65W	6,500K	18	3.7	2200

[1] xxxxx is the Lightguide Adaptor code. Please see Table below.
[2] Measured at the exiting end of a 1 meter long, 3mm-core, 0.59 numerical aperture (NA) liquid lightguide. Maximum CW output achievable with a BLS-13000-1E or BLS-18000-1 control module accordingly.
[3] Due to variations in the manufacturing process and operating parameters such as temperature and current, the actual output of any given LED may vary. Specifications are intended to be used as a guideline.

TABLE - LIGHTGUIDE ADAPTORS

Adaptor Code	Ferrule Diameter (mm)	Ferrule Length (mm)
A0510	5	≥10
A0610	6	≥10
A0710	7	≥10
A0810	8	≥10
A0815	8	≥15

Multiwavelength Lightguide-Coupled LEDs

Mightex offers high-power and versatile multiwavelength lightguide-coupled LED solutions. This system follows Mightex's unique modular system design. High-power collimated LEDs are combined together using high efficiency beam combiners to direct the illumination from multiple LEDs into a single, common output. At the output the light is coupled into a liquid lightguide by adding a lightguide adaptor. The modular based setup allows users to assemble an LED solution featuring two (2) or more wavelengths. By using beam combiners and dichroics, this setup allows users to rapidly switch (order of µs) between wavelengths, and/or output multiple wavelengths simultaneously. Furthermore, the utilization of dichroics allows these capabilities to be achieved without any mechanical moving parts involved. The modular system is also designed with flexibility and reconfigurability in mind. For example, a three-wavelength system can easily be expanded into a four wavelength by adding another LED and beam combiner to the setup.

EXAMPLE CONFIGURATION

Beam-combined super high-power LCS Series Collimated LEDs coupled to microscope's epi-illuminator port via a liquid lightguide, collimator and microscope adaptor.

COMPONENTS

1. LCS-Series Collimated LEDs
2. Beam Combiner
3. Lightguide Adaptor
4. Lightguide
5. Lightguide Collimator + Microscope Adaptor
6. LED Controllers

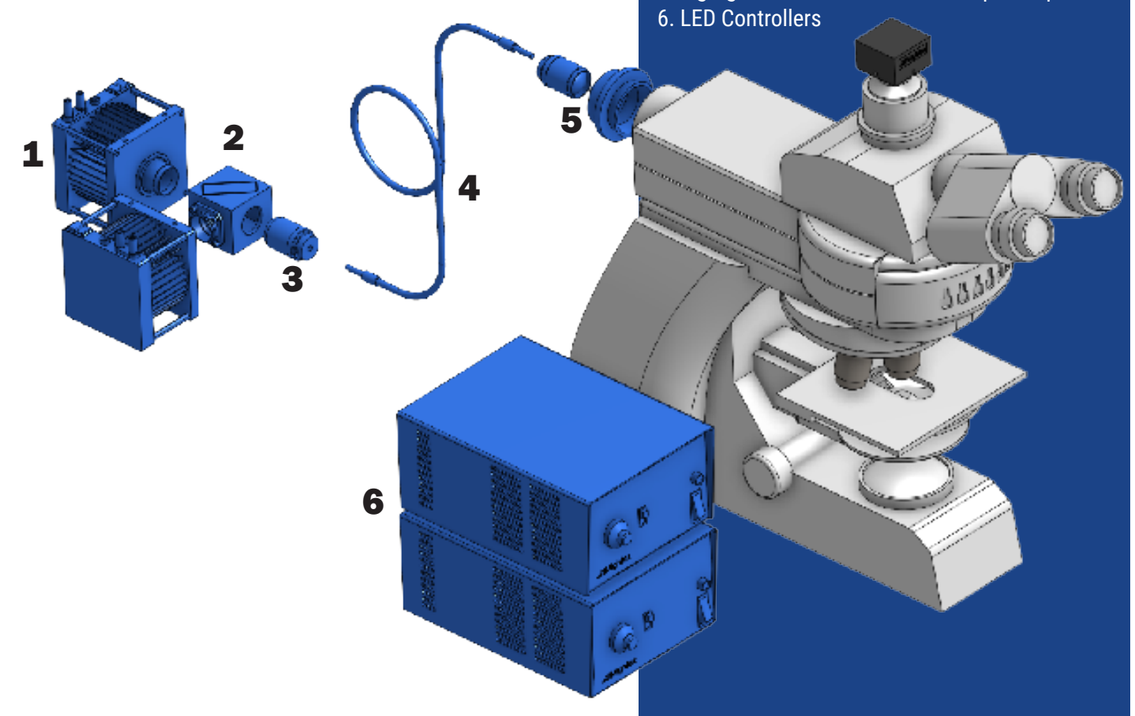

Precision LED Spotlights

Mightex precision LED spotlights contain state-of-the-art high-power LED emitters and a proprietary high-NA multi-element aspherical optical system. The result is a high-power, uniform illumination spot with a highly-delineated edge. Mightex PLS-series precision LED spotlights are general purpose light sources that can be used where uniform and high-intensity illumination is required. The projection lens at the front of the spotlight can be slid and locked to focus the illumination pattern at different working distances. With the standard projection lens the spot diameter is linearly proportional to the working distance.The LED emitters are mounted directly on the metal base of the light source which also features an integrated heatsink. This configuration minimizes thermal resistance between the LED emitter and the heatsink resulting in better heat dissipation. PLS-series multi-chip LED emitters (i.e. Type B) are also available. Some of these 7W to 15W LEDs have total optical power exceeding 500mW, doubling the power of a single-chip LED. Such Type B models with higher powers (7W and higher) feature a cooling fan, and have a different form factor compared to Type A models. Power supply for the cooling fan is included in the price of the Type B precision LED spotlights.

PLS Standard-Range LEDs

PLS high-uniformity, precision standard-range LEDs have a minimum working distance of 100mm, being able to produce a 30mm diameter spot at such distance. Spot diameter scales linearly with working distance.

PLS Close-Range LEDs

PLS high-uniformity, precision close-range LEDs have a minimum working distance of 75mm, being able to produce a 10mm diameter spot at such distance. These LEDs also have a maximum working distance of 100mm, producing a spot 17mm in diameter.

01

Type-A PLS Standard-Range Spotlight LED

- Passive cooling with integrated heatsink
- Adjustable Focus
- Compact, machined metal housing
- Uniform illumination spot with a highly delineated edge
- Multiple mounting features for lab applications

Part Number	Wavelength (nm)	I_{op} (mA)	V_{op} (V)	Typical Output Power[1] (mW)
BLS-PLS-0340-030-02-S	340	500	4.3	11
BLS-PLS-0365-030-04-S	365	1000	3.65	250
BLS-PLS-0380-030-03-S	380	1000	3.2	65
BLS-PLS-0385-030-04-S	385	1000	3.65	250

Type-A PLS Standard Range | *continued*

Part Number	Wavelength (nm)	I_{op} (mA)	V_{op} (V)	Typical Output Power[1] (mW)
BLS-PLS-0390-030-03-S	390	1000	3.1	140
BLS-PLS-0395-030-03-S	395	1000	3.1	150
BLS-PLS-0400-030-S	400	350	3.5	50
BLS-PLS-0400-030-03-S	400	1000	3.1	150
BLS-PLS-0400-030-04-S	400	1000	3.5	380
BLS-PLS-0405-030-03-S	405	1000	3	180
BLS-PLS-0410-030-03-S	410	1000	3	175
BLS-PLS-0415-030-03-S	415	1000	3	120
BLS-PLS-0430-030-02-S	430	500	3.8	100
BLS-PLS-0455-030-S	455	1000	3	260
BLS-PLS-0470-030-S	470	1000	3.9	110
BLS-PLS-0471-030-02-S	471	350	3	75
BLS-PLS-0490-030-01-S	490	350	3.5	80
BLS-PLS-0505-030-S	505	1000	3.9	65
BLS-PLS-0530-030-S	530	1000	2.85	100
BLS-PLS-0560-030-02-S	560 broadband	700	2.9	95
BLS-PLS-0590-030-S	590	1000	3.9	35
BLS-PLS-0617-030-S	617	1000	3.9	80
BLS-PLS-0625-030-S	625	1000	3.9	150
BLS-PLS-0656-030-S	656	1000	3.9	180
BLS-PLS-0680-030-S	680	600	2.7	20
BLS-PLS-0700-030-01-S	700	500	2.1	27
BLS-PLS-0720-030-01-S	720	600	2.2	39
BLS-PLS-0740-030-S	740	1000	2.5	100
BLS-PLS-0780-030-S	780	800	2.5	60
BLS-PLS-0810-030--02-S	810	800	2.2	65
BLS-PLS-0850-030-S	850	1000	2.1	85
BLS-PLS-0870-030-01-S	870	700	1.9	60
BLS-PLS-0910-030-02-S	910	1000	1.9	60
BLS-PLS-0940-030-S	940	700	1.5	16
BLS-PLS-0980-030--01-S	980	500	1.4	16
BLS-PLS-3000-030-S	Warm white 3,000K	1000	2.8	70
BLS-PLS-4000-030-S	Warm white 4,000K	1000	3.9	85
BLS-PLS-5500-030-S	Cool white 5,500K	1000	3.9	85
BLS-PLS-6500-030-S	Glacier white 6,500K	1000	3.6	100

[1] Due to variations in the manufacturing process and operating parameters such as temperature and current, the actual output of any given LED may vary. Specifications are intended to be used as a guideline.

02

Type-B PLS Standard-Range Spotlight LED

- Active cooling with integrated fan
- Adjustable Focus
- High-power (>7W models)
- Uniform illumination spot with a highly delineated edge
- Multiple mounting features for lab applications

Part Number	Wavelength (nm)	I_{op} (mA)	V_{op} (V)	Typical Output Power[1] (mW)
BLS-PLS-0365-030-13-S	365	3500	3.85	720
BLS-PLS-0385-030-07-S	385	500	15	300
BLS-PLS-0385-030-11-S	385	700	15.5	375
BLS-PLS-0385-030-13-S	385	3500	3.75	900
BLS-PLS-0400-030-17-S	400	1000	16.6	400
BLS-PLS-0470-030-15-S	470	1000	15	450
BLS-PLS-0505-030-12-S	505	1000	12.2	185
BLS-PLS-0530-030-15-S	530	1000	15	200
BLS-PLS-0540-030-14-S	540 broadband	3000	4.6	260
BLS-PLS-0590-030-05-S	590	500	9.5	130
BLS-PLS-0617-030-10-S	617	1000	10.8	200
BLS-PLS-0625-030-07-S	625	700	9.6	315
BLS-PLS-0656-030-07-S	656	700	9.6	420
BLS-PLS-0740-030-10-S	740	1000	9.5	300
BLS-PLS-3000-030-12-S	Warm white 3,000K	1000	12	320
BLS-PLS-5500-030-12-S	Cool white 5,500K	1000	12	400
BLS-PLS-6500-030-15-S	Glacier white 6,500K	1000	15	400

* When ordering an LED controller for a Type B LED, please make sure to upgrade the AC/DC power adaptor from the standard 12V to 24V.
[1] Due to variations in the manufacturing process and operating parameters such as temperature and current, the actual output of any given LED may vary. Specifications are intended to be used as a guideline.

03

Type-H PLS Standard-Range Spotlight LED

- Active cooling with integrated fan
- Adjustable Focus
- Super high-power (>38W models)
- Uniform illumination spot with a highly delineated edge
- Multiple mounting features for lab applications

Part Number	Wavelength (nm)	I_{op} (A)	V_{op} (V)	Typical Output Power[1] (mW)
PLS-0365-030-76-S	365	18	4.2	2200
PLS-0405-030-65-S	405	18	3.6	1400
PLS-0470-030-50-S	470	13	3.8	1850
PLS-0470-030-61-S	470	18	3.4	2150

Type-H PLS Standard Range | *continued*

Part Number	Wavelength (nm)	I_{op} (A)	V_{op} (V)	Typical Output Power[1] (mW)
PLS-0525-030-60-S	525	13	4.6	715
PLS-0525-030-79-S	525	18	4.3	850
PLS-0560-030-68-S	560 broadband	18	3.8	1800
PLS-0625-030-38-S	625	13	2.9	605
PLS-0625-030-42-S	625	18	2.3	720
PLS-0730-030-77-S	730	18	5.9	2100
PLS-0850-030-68-S	850	18	3.75	4400
PLS-6500-030-33-S	Glacier white 6,500K	9	3.7	1100
PLS-6500-030-65-S	Glacier white 6,500K	18	5.9	2000

[1] Due to variations in the manufacturing process and operating parameters such as temperature and current, the actual output of any given LED may vary. Specifications are intended to be used as a guideline.

04

Type-A PLS Close-Range Spotlight LED

- Passive cooling with integrated heatsink
- Adjustable Focus
- Compact, machined metal housing
- Uniform illumination spot with a highly delineated edge
- Multiple mounting features for lab applications

Part Number	Wavelength (nm)	I_{op} (mA)	V_{op} (V)	Typical Output Power[1] (mW)
BLS-PLS-0340-010-02-C	340	500	4.3	11
BLS-PLS-0365-010-04-C	365	1000	3.65	180
BLS-PLS-0380-010-03-C	380	1000	3.2	65
BLS-PLS-0385-010-04-C	385	1000	3.65	250
BLS-PLS-0390-010-03-C	390	1000	3.1	140
BLS-PLS-0395-010-03-C	395	1000	3.1	150
BLS-PLS-0400-010-03-C	400	1000	3.1	150
BLS-PLS-0400-010-04-C	400	1000	3.5	380
BLS-PLS-0405-010-03-C	405	1000	3.1	180
BLS-PLS-0410-010-03-C	410	1000	3.1	175
BLS-PLS-0415-010-03-C	415	1000	3.1	120
BLS-PLS-0430-010-02-C	430	500	3.8	100
BLS-PLS-0455-010-C	455	1000	3	260
BLS-PLS-0470-010-C	470	1000	3.9	110
BLS-PLS-0471-010-02-C	471	350	3	75
BLS-PLS-0490-010-01-C	490	350	3.5	80
BLS-PLS-0505-010-C	505	1000	3.9	65
BLS-PLS-0530-010-C	530	1000	2.85	100
BLS-PLS-0560-010-02-C	560 broadband	700	2.9	95
BLS-PLS-0590-010-C	590	1000	3.9	35

Type-A PLS Close-Range | *continued*

Part Number	Wavelength (nm)	I_{op} (mA)	V_{op} (V)	Typical Output Power[1] (mW)
BLS-PLS-0617-010-C	617	1000	3.9	80
BLS-PLS-0625-010-C	625	1000	3.9	90
BLS-PLS-0656-010-C	656	1000	3.9	180
BLS-PLS-0680-010-02-C	680	600	2.7	20
BLS-PLS-0700-010-01-C	700	500	2.1	27
BLS-PLS-0720-010-01-C	720	600	2.2	39
BLS-PLS-0740-010-03-C	740	1000	2.5	100
BLS-PLS-0780-010-C	780	800	2.5	60
BLS-PLS-0810-010-02-C	810	800	2.2	65
BLS-PLS-0850-010-C	850	1000	2.1	85
BLS-PLS-0870-010-01-C	870	700	1.9	60
BLS-PLS-0910-010-02-C	910	1000	1.9	60
BLS-PLS-0940-010-C	940	700	1.5	50
BLS-PLS-0980-010-01-C	980	500	1.4	16
BLS-PLS-3000-010-C	Warm white 3,000K	1000	2.8	70
BLS-PLS-4000-010-C	Warm white 4,000K	1000	3.9	85
BLS-PLS-5500-010-C	Cool white 5,500K	1000	3.9	85
BLS-PLS-6500-010-C	Glacier white 6,500K	1000	3.6	100

[1] Due to variations in the manufacturing process and operating parameters such as temperature and current, the actual output of any given LED may vary. Specifications are intended to be used as a guideline.

05

Type-B PLS Close-Range Spotlight LED

- Active cooling with integrated fan
- Adjustable Focus
- High-power (>7W models)
- Uniform illumination spot with a highly delineated edge
- Multiple mounting features for lab applications

Part Number	Wavelength (nm)	I_{op} (mA)	V_{op} (V)	Typical Output Power[1] (mW)
BLS-PLS-0365-010-13-C	365	3500	3.85	720
BLS-PLS-0385-010-07-C	385	500	15	300
BLS-PLS-0385-010-11-C	385	700	15.5	375
BLS-PLS-0385-010-13-C	385	3500	3.75	900
BLS-PLS-0400-010-17-C	400	1000	16.6	400
BLS-PLS-0470-010-15-C	470	1000	15	450
BLS-PLS-0505-010-12-C	505	1000	12.2	185
BLS-PLS-0530-010-15-C	530	1000	15	200
BLS-PLS-0540-010-14-C	540 broadband	3000	4.6	260
BLS-PLS-0590-010-05-C	590	500	9.5	130
BLS-PLS-0617-010-10-C	617	1000	10.8	200
BLS-PLS-0625-010-07-C	625	700	9.6	155

Type-B PLS Close-Range | *continued*

Part Number	Wavelength (nm)	I_{op} (mA)	V_{op} (V)	Typical Output Power[1] (mW)
BLS-PLS-0656-010-07-C	656	700	9.6	420
BLS-PLS-0740-010-10-C	740	1000	9.5	300
BLS-PLS-3000-010-12-C	Warm white 3,000K	1000	12	320
BLS-PLS-5500-010-12-C	Cool white 5,500K	1000	12	400
BLS-PLS-6500-010-15-C	Glacier white 6,500K	1000	15	400

* When ordering an LED controller for a Type B LED, please make sure to upgrade the AC/DC power adaptor from the standard 12V to 24V.
[1] Due to variations in the manufacturing process and operating parameters such as temperature and current, the actual output of any given LED may vary. Specifications are intended to be used as a guideline.

06

Type-H PLS Close-Range Spotlight LED

- Active cooling with integrated fan
- Adjustable Focus
- Super high-power (>38W models)
- Uniform illumination spot with a highly delineated edge
- Multiple mounting features for lab applications

Part Number	Wavelength (nm)	I_{op} (A)	V_{op} (V)	Typical Output Power[1] (mW)
PLS-0365-010-76-C	365	18	4.2	640
PLS-0405-010-65-C	405	18	3.6	420
PLS-0470-010-50-C	470	13	3.8	630
PLS-0470-010-61-C	470	18	3.4	750
PLS-0525-010-60-C	525	13	4.6	240
PLS-0525-010-79-C	525	18	4.4	280
PLS-0560-010-68-C	560 broadband	18	3.8	950
PLS-0625-010-38-C	625	13	2.9	200
PLS-0625-010-42-C	625	18	2.3	240
PLS-0730-010-77-C	730	18	5.9	650
PLS-6500-010-33-C	Glacier white 6,500K	9	3.7	400
PLS-0650-010-65-C	Glacier white 6,500K	18	3.7	680

[1] Due to variations in the manufacturing process and operating parameters such as temperature and current, the actual output of any given LED may vary. Specifications are intended to be used as a guideline.

Fiber-Coupled Laser Sources

Mightex's fiber-coupled laser sources are designed to produce high power and high intensity output of illumination through an optical fiber patchcord. Our laser sources are configurable to contain up to 2 different wavelengths that share the same fiber-optic output. Laser intensity can be controlled in two different modes:

1. **Manual Knob Control Mode:** 10-turn dial knobs are present for each wavelength channel.
2. **Analog Input mode:** each channel can be controlled with 0-5V signal. Maximum modulation frequency achieved in this mode is 100 kHz.

With many safety features, including a power switch, key switch, emergency switch and interlock, Mightex's laser sources are optimal for high intensity illumination applications.

LSR Fiber-Coupled Lasers

- Single fixed fiber, 2.5m in length
- Manual knobs with 10-turn dial for each channel
- Analog mode 0-5V input for each channel
- Maximum modulation frequency of 100kHz
- Multiple safety features

Part number	Typical Output Power[1] | **mW**					
	405nm	463nm	465nm	520nm	635nm	637nm
LSR-040-0405	500	-	-	-	-	-
LSR-040-0463	-	2200	-	-	-	-
LSR-040-0465	-	-	3200	-	-	-
LSR-040-0520	-	-	-	500	-	-
LSR-040-0635	-	-	-	-	500	-
LSR-040-0637	-	-	-	-	-	4000
LSR-040-0405-0463	450	2000	-	-	-	-
LSR-040-0405-0635	450	-	-	-	450	-
LSR-040-0463-0635	-	2000	-	-	450	-

[1] Measurement from a 400µm-core, 0.22NA fiber patchcord.

Microscope Illuminators

Mightex microscope illuminators are complete optical solutions used to couple our various light sources to your microscope. They are designed to readily fit into the infinity optical path of your microscope to provide imaging and stimulation capabilities, depending on the illuminator. Mightex has developed a complete system of components and adaptors for users to easily mount our illuminators onto any of their existing microscopes, including both upright and inverted microscopes. Since our illuminators are designed to fit into the infinity path, the most common way to mount them is by using a beam combiner along with an adaptor that matches the exact make/model of the user's existing microscope.

MODELS

Infinity Path Expander

Mightex's IPX expands an infinity-path port on a microscope into a maximum of 4 ports. There are two models of IPX expanders: (1) IPX4, which has 4 integrated ports; and (2) IPX2, which starts with 2 ports, but has a modular design and can be scaled up to 4 ports. Both IPX expanders are compatible with all Mightex Polygon models as well as with all Mightex's and any 3rd party widefield epi-fluorescent illumination sources via standard 3mm core liquid lightguide. It also supports cameras and laser scanners via appropriate adaptors.For more details, please see page 10.

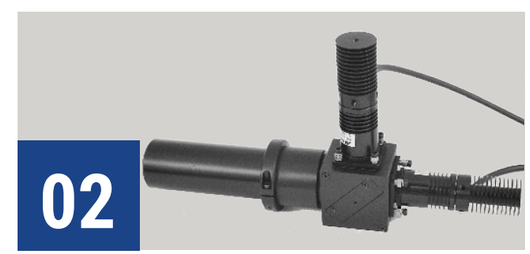

Microscope Illumination Tube (MIT)

The Mightex Microscope Illumination Tube is designed for coupling up to 4 collimated LED (LCS) light sources into the infinity optical path of any commercial microscope, providing wide-field illumination for imaging. Mightex provides 2 different models of the MIT with different optical lengths. The first model is designed for 1 beam combiner allowing up to 2 LCS sources (as seen in the side picture). Alternatively, the second model is designed for 2 beam combiners allowing up to 4 LCS sources.

Lightguide-Coupled Epi-Illuminator (EPI)

Mightex's Lightguide-coupled Epi-illuminator provides fluorescent imaging capability to any commercial microscope system. It is usually coupled to our OASIS stimulation and imaging systems (OASIS Implant, Micro and Macro). It accepts a standard 3mm liquid lightguide, which gives the user the versatility to use Mightex's lightguide-coupled LED sources or any 3rd party light source.

Publications using Mightex's LEDs

Below is a select list of recent peer-reviewed scientific publications from Mightex customers that include experiments performed with our Mightex light sources. Please find a complete updated list of publications on our website including all of the 100+ publications.

1. S. Kh. Batygov, M. N. Brekhovskikh, L. V. Moiseeva, V. V. Vinokurova, N. Yu. Kirikova, V. A. Kondratyuk & V. N. *Makhov Optical Properties of Fluorozirconate Glasses Doped with Chromium Ions.* (2023) **Russian Journal of Inorganic Chemistry.**
2. Shuofeng Liang, Shuxiu Li, Chenrui Yuan, Dachuan Zhang, Jiahui Chen, and Si Wu *Polyacrylate Backbone Promotes Photoinduced Reversible Solid-To-Liquid Transitions of Azobenzene-Containing Polymers.* (2023) **Macromolecules.**
3. Yuval Harari,Chandra Shakher Pathak and Eran Edri *Molecular relays in nanometer-scale alumina: effective encapsulation for water-submersed halide perovskite photocathodes.* (2023) **Nanoscale.**
4. Sagil James & Joel Zarate *Preliminary study on volumetric 3D printing using visible light.* (2023) **The International Journal of Advanced Manufacturing Technology.**
5. Xinyu Xie, Fuqiang Hu, Dr. Yuqiao Zhou, Zhihao Liu, Xin Shen, Jielin Fu, Prof. Dr. Xiaohu Zhao, Prof. Dr. Zhipeng Yu *Photoswitchable Oxidopyrylium Ylide for Photoclick Reaction with High Spatiotemporal Precision: A Dynamic Switching Strategy to Compensate for Molecular Diffusion.* (2023) **Angewandte Chemie.**
6. Ishita Chakraborty a 1, Ming-Chung Wu b c d 1, Sz-Nian Lai e, Chao-Sung Lai *Self-powered broadband photodetection with mixed-phase black TiO2-assisted output boosting of a biobased triboelectric nanogenerator.* (2023) **Chemical Engineering Journal.**
7. James A. Jones, Matthew H. Higgs, Erick Olivares, Jacob Peña and Charles J. Wilson *Spontaneous Activity of the Local GABAergic Synaptic Network Causes Irregular Neuronal Firing in the External Globus Pallidus.* (2023) **Journal of Neuroscience.**
8. Yichi Zhang, Kaiqi Long, Weiping Wang *Facile Preparation and Photoactivation of Prodrug-Dye Nanoassemblies.* (2023) **Medicine.**
9. Margarita Anisimova, Bas van Bommel, Rui Wang, Marina Mikhaylova, Jörn Simon Wiegert, Thomas G Oertner, Christine E Gee *Spike-timing-dependent plasticity rewards synchrony rather than causality.* (2023) **Cerebral Cortex.**
10. Gregory E. Alberto, David C. Klorig, Allison T. Goldstein, Dwayne W. Godwin *Alcohol withdrawal produces changes in excitability, population discharge probability, and seizure threshold.* (2023) **Alcohol.**
11. N. M. Khaidukov, K. S. Nikonov, M. N. Brekhovskikh, N. Yu. Kirikova, V. A. Kondratyuk & V. N. Makhov *Synthesis and Luminescent Properties of Multicomponent Garnets Y3MgGa3SiO12, Y3MgGa2AlSiO12, and Y3MgGaAl2SiO12 Doped with Cr3+ Ions.* (2023) **Russian Journal of Inorganic Chemistry.**
12. Adeline Haobing Wang, Rebecca Brown, Julia J Bryant, Sergio Leon-Saval *Focal ratio degradation in optical fibres for the Hector integral field units.* (2023) **Monthly Notices of the Royal Astronomical Society.**
13. Arij Farhat a, Marine Tassé a, Mathilde Bocé a, Dominique de Caro a, Isabelle Malfant a, Patricia Vicendo b, Anne-Françoise *Mingotaud First example of photorelease of nitric oxide from ruthenium nitrosyl-based nanoparticles.* (2023) **Chemical Physics Letters.**
14. Guo Jiao Hou, Elisa García-Tabarés, Iván García, Ignacio Rey-Stolle *High-low refractive index stacks as antireflection coatings on triple-junction solar cells.* (2023) **Photovoltaics.**
15. Grigory Arzumanya, Kahramon Mamatkulov,Yersultan Arynbek,Darya Zakrytnaya,Anka Jevremović and Nina Vorobjeva *Radiation from UV-A to Red Light Induces ROS-Dependent Release of Neutrophil Extracellular Traps.* (2023) **International Journal of Molecular Science.**
16. Camille Courtine, Inès Hamouda, Samuel Pearson, Laurent Billon, Pierre Lavedan, Sonia Ladeira, Jean-Claude Micheau, Véronique Pimienta, Erwan Nicol , Nancy Lauth de Viguerie, Anne-Françoise Mingotaud *Photoswitchable assembly of long-lived azobenzenes in water using visible light.* (2023) **Journal of Colloid and Interface Science.**
17. Anna Törteli, Réka Tóth, Sarah Berger, Sarah Samardzic, Ferenc Bari, Ákos Menyhárt, and Eszter Farkas *Spreading depolarization causes reperfusion failure after cerebral ischemia.* (2023) **Journal of Cerebral Blood Flow & Metabolism.**
18. Jonathan Thomas Elliott, Eric Henderson, Samuel S. Streeter, Valentin Demidov, Xinyue Han, Yue Tang, J. Scott Sottosanti, Logan Bateman, Petr Brůža, Shudong Jiang, I. Leah Gitajn *Fluorescence-guided and molecularly guided debridement: identifying devitalized and infected tissue in orthopaedic trauma.* (2023) **Molecular-Guided Surgery: Molecules.**
19. Daniela Neuhofer and Peter Kalivas *Differential Modulation of GABAergic and Glutamatergic Neurons in the Ventral Pallidum by GABA and Neuropeptides.* (2023) **eNeuro.**
20. Charles J. Wilson and James A. Jones *Propagation of Oscillations in the Indirect Pathway of the Basal Ganglia.* (2023) **Journal of Neuroscience.**
21. Clayton M. Geipel, Brian T. Bojko, Christopher J. Pfützner, Brian T. Fisher, Ryan F. Johnson *Regression of solid polymer fuel strands in opposed-flow combustion with gaseous oxidizer.* (2023) **Proceedings of the Combustion Institute.**
22. Camille Courtine, Pierre-Louis Brient, Inès Hamouda, Nicolas Pataluch, Pierre Lavedan, Jean-Luc Putaux, Camille Chatard, Céline Galès, Anne-Françoise Mingotaud, Nancy Lauth de Viguerie, Erwan Nicol *Tetrafluorinated versus hydrogenated azobenzene polymers in water: Access to visible-ligh stimulus at the expense of responsiveness.* (2023) **Journal of Photochemistry and Photobiology A: Chemistry.**
23. Barbara C. Niort, Alice Recalde,Caroline Cros and Fabien Brette *Critical Link between Calcium Regional Heterogeneity and Atrial Fibrillation Susceptibility in Sheep Left Atria.* (2023) **Journal of Clinical Medicine.**

24. Yen-Yu Fu, Jia-Yu Lin, and Yang-Fang Chen *Optically and Electrically Controllable Light-Emitting Nonvolatile Resistive Switching Memory.* (2023) **ACS Applied Electronic Materials.**
25. Enqi Bu, Xiaowei Chen, Carlos López-Cartes, Fernando Cazaña, Antonio Monzón, Javier Martínez-López, Juan José Delgado *Effect of the TiO2-carbon interface on charge transfer and ethanol photo-reforming.* (2023) **Catalysis Today.**
26. Hideaki Mamaoto, F.Paul Spitzner, Taiki Takemuro Victor Buendia, Hakuba Murota, Carla Morante, Tomohiro Konno, Shigeo Sato, Ayumi Hirano-Iwata, Anna Levina, Viola, Priesemann, Miguel A.Munoz, Johannes Zierenberg, and Jordi Soriano *Modular architecture facilitates noise-driven control of synchrony in neuronal networks.* (2023) **Science Advances.**
27. Takuma Sumi, Hideaki Yamamoto, Yuichi Katori, and Ayumi Hirano-Iwata *Biological neurons act as generalization filters in reservoir computing.* (2023) **PNAS.**
28. Louis Conrad Winkler, Jonas Kublitski, Johannes Benduhn, Karl Leo *Photomultiplication Enabling High-Performance Narrowband Near-Infrared Organic Photodetectors.* (2023) **Advanced Electronic Materials.**
29. Shoko Hososhima, Rei Abe-Yoshizumi, Hideki Kandori *Chapter Thirteen - Functional assay of light-induced ion-transport by rhodopsins.* (2023) **Methods in Enzymology.**
30. Nowrin Ahmed and Denis Paré *The Basolateral Amygdala Sends a Mixed (GABAergic and Glutamatergic) Projection to the Mediodorsal Thalamic Nucleus.* (2023) **JNeurosci.**
31. Jeffrey E. Markowitz, Winthrop F. Gillis, Maya Jay, Jeffrey Wood, Ryley W. Harris, Robert Cieszkowski, Rebecca Scott, David Brann, Dorothy Koveal, Tomasz Kula, Caleb Weinreb, Mohammed Abdal Monium Osman, Sandra Romero Pinto, Naoshige Uchida, Scott W. Linderman, Bernardo L. Sabatini & Sandeep Robert Datta *Spontaneous behaviour is structured by reinforcement without explicit reward.* (2023) **Nature.**
32. Boris Gourévitch, Teresa Pitts, Kimberly Iceman, Mitchell Reed, Jun Cai, Tianci Chu, Wenxin Zeng, Consuelo Morgado-Valle & Nicholas Mellen *Synchronization of inspiratory burst onset along the ventral respiratory column in the neonate mouse is mediated by electrotonic coupling.* (2023) **BMC Biology.**
33. Adam Mani, Xinzhu Yang, Tiffany A. Zhao, Megan L. Leyrer, Daniel Schreck & David M. Berson *A circuit suppressing retinal drive to the optokinetic system during fast image motion.* (2023) **Nature Communications.**
34. Dariia U. Musaeva, Alexey N. Kopylov, Alexander V. Syuy, Valentyn S. Volkov, Nikita D. Mitiushev, Olga S. Pavlova, Yury A. Pirogov ,Andrey N. Baranov and Victor Yu. Timoshenko *Gadolinium-Doped Carbon Nanoparticles with Red Fluorescence and Enhanced Proton Relaxivity as Bimodal Nanoprobes for Bioimaging Applications.* (2023) **Applied Sciences.**
35. Adrian K. Rylski, Tejas Maraliga, Yudian Wu, Elizabeth A. Recker, Anthony J. Arrowood, Gabriel E. Sanoja, and Zachariah A. Page *Digital Light Processing 3D Printing of Soft Semicrystalline Acrylates with Localized Shape Memory and Stiffness Control.* (2023) **ACS Applied Materials & Interfaces.**
36. Dylan Brault, Thomas Olivier, Nicolas Faure, Sophie Dixneuf, Chloé Kolytcheff, Elodie Charmette, Ferréol Soulez & Corinne Fournier *Multispectral in-line hologram reconstruction with aberration compensation applied to Gram-stained bacteria microscopyl.* (2023) **Nature.**
37. Moawiah M. Naffaa, Rehan R. Khan,Chay T. Kuo, Henry H. Yin *Cortical regulation of neurogenesis and cell proliferation in the ventral subventricular zone.* (2023) **Cell.**
38. Michael Okebiorun, Cameron Waite, Dalton Miller, Kenneth A. Cornell, Jim Browning *Selective Optical Imaging for Detection of Bacterial Biofilms in Tissues.* (2023) **Journal of Imaging.**
39. A. A. Fronya, S. V. Antonenko, N. V. Karpov, N. S. Pokryshkin, A. S. Eremina, A. A. Garmash, N. I. Kargin, S. M. Klimentov, V. Yu. Timoshenko, A. V. Kabashin *Pulsed laser deposition in He-N2 gaseous mixtures for the synthesis of photoluminescent Si and Ge nanoparticles for bioimaging.* (2023) **Nanoscale and Quantum Materials.**
40. Tzu-Yang Huang, Zijian Cai, Matthew J. Crafton, Lori A. Kaufman, Zachary M. Konz, Helen K. Bergstrom, Elyse A. Kedzie, Han-Ming Hao, Gerbrand Ceder, Bryan D. McCloskey *Quantitative Decoupling of Oxygen-Redox and Manganese-Redox Voltage Hysteresis in a Cation-Disordered Rock Salt Cathode*. (2023) **Advanced Energy Materials.**
41. Dhananjay Mishra, Krishnaiah Mokurala, Ajit Kumar, Seung Gi Seo, Hyeon Bin Jo, Sung Hun Jin *Light-Mediated Multi-Level Flexible Copper Iodide Resistive Random Access Memory for Forming-Free, Ultra-Low Power Data Storage Application.* (2023) **Advanced Energy Materials.**
42. Yung-Chi Huang, Jinyue Luo, Alexandra B. Byrne, Steven W. *Flavell A single neuron in C. elegans orchestrates multiple motor outputs through parallel modes of transmission.* (2023) **Cell.**
43. Ugur Dag, Ijeoma Nwabudike, Di Kang, Emma Towlson,Steven W. Flavell *Dissecting the functional organization of the C. elegans serotonergic system at whole-brain scale.* (2023) **Cell.**
44. Kathrin Frey, Lucia Rohrer, Fabian Frommelt, Meret Ringwald, Anton Potapenko, Sandra Goetze, Arnold von Eckardstein, Bernd Wollscheid "Mapping the dynamic high-density lipoprotein synapse. (2023) **Atherosclerosis.**
45. Hamilton White, Vanessa Kamara, Veronika Gorski, Molly Busby, Dirk R. Albrecht *Automated Multimodal Stimulation and Simultaneous Neuronal Recording from Multiple Small Organisms.* (2023) **Neuroscience.**
46. Shoko Hososhima, Shinji Ueno, Satoshi Okado, Ken-ichi Inoue, Yumeka Yamauchi, Keiichi Inoue, Hiroko Terasaki, Hideki Kandori & Satoshi P. Tsunoda *A light-gated cation channel with high reactivity to weak light. (*2023) **Nature.**
43. Owen Y. Chao, Salil Saurav Pathak, Hao Zhang, George J. Augustine, Jason M. Christie, Chikako Kikuchi, Hiroki Taniguchi & Yi-Mei Yang *Social memory deficit caused by dysregulation of the cerebellar vermis.* (2023) **Nature.**
44. Katelyn Mathisates, Afia Ibnat Kohon, Stephen Black, and Brian Meckes *Light-Controlled Cell–Cell Assembly Using Photocaged Oligonucleotides.* (2023) **ACS Publications.**
45. Huan Sheng, Chao Lei, Yu Yuan, Yali Fu, Dongyang Cui, Li Yang, Da Shao, Zixuan Cao, Hao Yang, Xinli Guo, Chenshan Chu, Yaxian Wen, Zhangyin Cai, Ming Chen, Bin Lai & Ping Zheng *Nucleus accumbens circuit disinhibits lateral hypothalamus glutamatergic neurons contributing to morphine withdrawal memory in male mice.* (2023) **Nature.**

46. Hanna den Bakker, Marie Van Dijck, Jyh-Jang Sun, Fabian Kloosterman *Sharp-wave-ripple-associated activity in the medial prefrontal cortex supports spatial rule switching.* (2023) **Cell.**
47. Abdulkadir Mohamed, Iro Malekou, Timothy Sim, Cahir J. O'Kane, Yousef Maait, Benjamin Scullion, Liria M. Masuda-Nakagawa *Mushroom body output neurons MBON-a1/a2 define an odor intensity channel that regulates behavioral odor discrimination learning in larval Drosophila*. (2023) **Frontier.**
48. Roberto de la Torre-Martinez, Maya Ketzef & Gilad Silberberg *Ongoing movement controls sensory integration in the dorsolateral striatum.* (2023) **Nature.**
49. Zachariah Bertels, Elizaveta Mangutov, Kendra Siegersma, Haley C. Cropper, Alycia Tipton, Amynah A. Pradhan *PACAP-PAC1 receptor inhibition is effective in opioid induced hyperalgesia and medication overuse headache models.* (2023) **Cell.**
50. Sebastián Loyola,Tycho M Hoogland, Vincenzo Romano, Mario Negrello, Chris I De Zeeuw *How inhibitory and excitatory inputs gate output of the inferior olive. (*2023) **eLife.**
51. Yvonne Johansson, Maya Ketzef *Sensory processing in external globus pallidus neurons.* (2023) **Cell.**
52. Geng Pan, Ruonan Li, Guozhong Xu, Shijun Weng, Xiong-li Yang, Limin Yang, Bing Ye *Cross-modal modulation gates nociceptive inputs in Drosophila.* (2023) **Cell.**
57. Tania Mariastella Caputo,Angela Maria Cusano,Sofia Principe,Paola Cicatiello,Giorgia Celetti,Anna Aliberti,Alberto Micco,Menotti Ruvo,Maria Tagliamonte,Concetta Ragone,Michele Minopoli, Maria Vincenza Carriero, Luigi Buonaguro &Andrea Cusano "Sorafenib-Loaded PLGA Carriers for Enhanced Drug Delivery and Cellular Uptake in Liver Cancer Cells". (2023) **International Journal of Nanomedicine.**
58. Conte L.O., Dominguez C.M., Checa-Fernandez A., Santos A. Vis LED Photo-Fenton Degradation of 124-Trichlorobenzene at a Neutral pH Using Ferrioxalate as Catalyst. (2022) **International Journal of Environmental Research and Public Health.**
59. Kuzmiak-Glancy S., Glancy B., Kay M.W. Ischemic damage to every segment of the oxidative phosphorylation cascade elevates ETC driving force and ROS production in cardiac mitochondria. (2022) **Am J Physiol Heart Circ Physiol.**
60. Amariei G., Valenzuela L., Iglesias-Juez A., Rosal R., Visa M. ZnO-functionalized fly-ash based zeolite for ciprofloxacin antibiotic degradation and pathogen inactivation. (2022) **Journal of Environmental Chemical Engineering.**
61. Ball J.M., Chen S., Li W. Mitochondria in cone photoreceptors act as microlenses to enhance photon delivery and confer directional sensitivity to light. (2022) **Science Advances.**
62. Baleisyte A., Schneggenburger R., Kochubey O. Stimulation of medial amygdala GABA neurons with kinetically different channelrhodopsins yields opposite behavioral outcomes. (2022) **Cell Reports.**
63. Inbar K., Levi L.A., Bernat N., Odesser T., Inbar D., Kupchik Y.M. Cocaine Dysregulates Dynorphin Modulation of Inhibitory Neurotransmission in the Ventral Pallidum in a Cell-Type-Specific Manner. (2020) **Journal of Neuroscience.**
64. Levi L.A., Inbar K., Nachshon N., Bernat N., Gatterer A., Inbar D., Kupchik Y.M. Projection-Specific Potentiation of Ventral Pallidal Glutamatergic Outputs after Abstinence from Cocaine. (2020) **Journal of Neuroscience.**
65. Betolngar D.B., Mota E., Fabritius A., Nielsen J., Hougaard C., Christoffersen C.T., Yang J., Kehler J., Griesbeck O., Castro L.R.V., Vincent P. Phosphodiesterase 1 Bridges Glutamate Inputs with NO- and Dopamine-Induced Cyclic Nucleotide Signals in the Striatum. (2020) **Cerebral Cortex.**
66. Karube F., Takahashi S., Kobayashi K., Fujiyama F. Motor Cortex can Directly Drive the Globus Pallidus Neurons in a Projection Neuron Type-Dependent Manner in the Rat. (2019) **eLife.**
67. St. Laurent R. & Kauer J. Synaptic Plasticity at Inhibitory Synapses in the Ventral Tegmental Area Depends upon Stimulation Site. (2019) **eNeuro.**
68. Antinucci P., Folgueira M., Bianco I.H. Pretectal Neurons Control Hunting Behaviour (2019) **eLife.**
69. Wilson T.D., Valdivia S., Khan A., Ahn H., Adke A.P., Gonzalez S.M., Sugimura Y.K., Carrasquillo Y. Dual and Opposing Functions of the Central Amygdala in the Modulation of Pain. (2019) **Cell Reports.**
70. Tenedini F.M., González M.S., Hu C., Pedersen L.H., Petruzzi M.M., Spitzweck B., Wang D., Richter M., Petersen M., Szpotowicz E., Schweizer M., Sigrist S.J., de Anda F.C., Soba P. Maintenance of cell type-specific connectivity and circuit function requires Tao kinase. (2019) **Nature Communications.**
71. Abdelfattah A.S., Kawashima T., Singh A., Novak O., Liu H., Shuai Y., Huang Y., Campagnola L., Seeman S.C., Yu J., Zheng J., Grimm J.B., Patel R., Friedrich J., Mensh B.D., Paninski L., Macklin J.J., Murphy G.J., Podgorski K., Lin B., Chen T., Turner G.C., Liu Z., Koyama M., Svoboda K., Ahrens M.B., Lavis L.D., Schreiter E.R. Bright and photostable chemigenetic indicators for extended in vivo voltage imaging. (2019) **Science.**
72. Pribic M.R., Black A.H., Beale A.D., Gauvin J.A., Chiang L.N., Rose J.K. Association of Two Opposing Responses Results in the Emergence of a Novel Conditioned Response. (2022) **Frontiers in Behavioral Neuroscience.**
73. Yaghmazadeh O., Vöröslakos M., Alon L., Carluccio G., Collins C., Sodickson D.K., Buzsáki G. Neuronal activity under transcranial radio-frequency stimulation in metal-free rodent brains in-vivo. (2022) **Communications Engineering.**
74. Foster D.A.N., Hwang D.K. Microfluidic flow assembly system with magnetic clamp for unlimited geometry in millimetric hydrogel film patterning. (2022) **Applied Materials Today**
75. Inbar K., Levi L.A., Kupchik Y.M. Cocaine induces input and cell-type-specific synaptic plasticity in ventral pallidum-projecting nucleus accumbens medium spiny neurons. (2022) **Neuropsycopharmacology.**
76. Kaberniuk A.A., Baloban M., Monakhov M.V., Shcherbakova D.M., Verkhusha V.V. Single-component near-infrared optogenetic systems for gene transcription regulation. (2021) **Nature Communications.**
77. Hososhima S., Kandori H., Tsunoda S.P. Ion transport activity and optogenetics capability of light-driven Na+-pump KR2. (2021) **PLOS One.**
79. Ahmed N., Headley D.B., Paré D. *Optogenetic study of central medial and paraventricular thalamic projections to the basolateral amygdala*. (2021) **Journal of Neurophysiology.**

80. Um K.B., Hahn S., Kim S.W., Lee Y.J., Birnbaumer L., Kim H.J., Park M.K. *TRPC3 and NALCN channels drive pacemaking in substantia nigra dopaminergic neurons.* (2021) **eLife.**
81. Covian R., Edwards L., He Y., Kim G., Houghton C., Levine R.L., Balaban R.S. Energy homeostasis is a conserved process: Evidence from Paracoccus denitrificans' response to acute changes in energy demand. (2021) **PLOS One.**
82. Yang S., Constantin O.M., Sachidanandan D., Hofmann H., Kunz T.C., Kozjak-Pavlovic V., Oertner T.G., Nagel G., Kittel R.J., Gee C.E., Gao S. *PACmn for improved optogenetic control of intracellular cAMP.* (2021) **BMC Biology.**
83. Ji N., Madan G.K., Fabre G.I., Dayan A., Baker C.M., Kramer T.S., Nwabudike I., Flavell S.W. *A neural circuit for flexible control of persistent behavioral states.* (2021) **eLife.**
84. Margiotta J.F., Smith-Edwards K.M., Nestor-Kalinoski A., Davis B.M., Albers K.M., Howard M.J. *Synaptic Components, Function and Modulation Characterized by GCaMP6f Ca2+ Imaging in Mouse Cholinergic Myenteric Ganglion Neurons.* (2021) **Frontiers in Physiology.**
85. Ketzef M., Silberberg G. *Differential Synaptic Input to External Globus Pallidus Neuronal Subpopulations In Vivo.* (2021) **Neuron.**
86. Pouchelon G., Dwived D., Bollmann Y., Agba C.K., Xu Q., Mirow A.M.C., Sehyun Kim, Yanjie Qiu, Elaine Sevier, Kimberly D. Ritola, Rosa Cossart, Gord Fishell. *The organization and development of cortical interneuron presynaptic circuits are area specific*. (2021) **Cell Reports**
87. Shin Y.J., Shafranek R.T., Tsuic J.H., Walcott J., Kim D. *3D bioprinting of mechanically tuned bioinks derived from cardiac decellularized extracellular matrix.* (2021) **Acta Biomaterialia.**
88. Alegre-Cortés J., Sáez M., Montanari R., Reig R. *Medium spiny neurons activity reveals the discrete segregation of mouse dorsal striatum.* (2021) **eLife.**
89. Han X., Su Y., White H., O'Neill K.M., Morgan N.Y., Christensen R., Potarazu D., Vishwasrao H.D., Xu S., Sun Y., Huang S., Moyle M.W., Dai Q., Pommier Y., Giniger E., Albrecht D.R., Probst R., Shroff H. A polymer index-matched to water enables diverse applications in fluorescence microscopy. (2021) **Lab on a Chip.**
90. Brennan E.K.W., Sudhakar S.K., Jedrasiak-Cape I., John T.T., Ahmed O.J. *Hyperexcitable Neurons Enable Precise and Persistent Information Encoding the Superficial Retrospinal Cortex.* (2020) **Cell Reports.**
91. Katz M., Corson F.,Singhal A.,Liang Y., Shaham S. *Glutamate spillover in C. elegans triggers repetitive behavior through presynaptic activation of MGL-2/mGluR5.* (2019) **Nature Communications.**
92. Bigelow J., Morrill R.J., Dekloe J., Hasenstaub A.R. *Movement and VIP Interneuron Activation Differentially Modulate Encoding in Mouse Auditory Cortex.* (2019) **eNeuro.**
93. Liu Y., Ohshiro T., Sakuragi S., Koizumi K., Mushiake H., Ishizuka T., Yawo H. *Optogenetic Study of the Response Interaction Among Multi-Afferent Inputs in the Barrel Cortex of Rats.* (2019) **Scientific Reports.**
94. Tiroshi & Goldberg J.A. *Population Dynamics and Entrainment of Basal Ganglia Pacemakers are Shaped by their Dendritic Arbors.* (2019) **PLOS Computational Biology.**
95. Hashimotodani Y., Karube F., Yanagawa Y., Fujiyama F., Kano M. *Supramammillary Nucleus Afferents to the Dentate Gyrus Co-release Glutamate and GABA and Potentiate Granule Cell Output.* (2018) **Cell Reports.**
99. Goodwill H.L., Manzano-Nieves G., LaChance P., Teramoto S., Lin S., Lopez C., Stevenson R.J., Theyel B.B., Moore C.I., Connors B.W., Bath K.G. *Early Life Stress Drives Sex-Selective Impairment in Reversal Learning by Affecting Parvalbumin Interneurons in Orbitofrontal Cortex of Mice.* (2018) **Cell Reports.**
100. Glantz S.T., Berlew E.E., Jaber Z., Schuster B.S., Gardner K.H., & Chow B.Y. *Directly Light-Regulated Binding of RGS-LOV Photoreceptors to Anionic Membrane Phospholipids.* (2018) **PNAS.**
101. Burgos A., Honjo K., Ohyama T., Qian C.S., Shin G.J., Gohl D.M., Silies M., Tracey W.D., Zlatic M., Cardona A., Grueber W.B. *Nociceptive interneurons control modular motor pathways to promote escape behavior in Drosophila* (2018) **eLife.**
102. Tastekin I., Khandelwal A., Tadres D., Cardona A., Louis M. *Sensorimotor pathway controlling stopping behavior during chemotaxis in the Drosophila melanogaster larva.* (2018) **eLife.**
103. Wiegert J.S., Pulin M., Gee C.E., & Oertner T.G. *The Fate of Hippocampal Synapses Depends on the Sequence of Plasticity-Inducing Events.* (2018) **eLife.**
104. Crandall S.R., Patrick S.L., Cruikshank S.J., Connors B.W. *Infrabarrels Are Layer 6 Circuit Modules in the Barrel Cortex that Link Long-Range Inputs and Outputs.* (2017) **Cell Reports.**
105. Higgs M.H. & Wilson C.J. *Measurement of Phase Resetting Curves Using Optogenetic Barrage Stimuli.* (2017) **Journal of Neuroscience Methods.**
106. Wright P.W., Brier L.M., Bauer A.Q., Baxter G.A., Kraft A.W., Reisman M.D., Bice A.R., Snyder A.Z., Lee J., Culver J.P. *Functional connectivity structure of cortical calcium dynamics in anesthetized and awake mice.* (2017) **PLOS One.**
107. Heinsbroek J.A., Neuhofer D.N., Griffin III W.C., Siegel G.S., Bobadilla A., Kupchik Y.M., Kalivas P.W. *Loss of Plasticity in the D2-Accumbens Pallidal Pathway Promotes Cocaine Seeking.* (2017) **Journal of Neuroscience.**
108. Morrill R.J. & Hasenstaub A.R. *Visual Information Present in Infragranular Layers of Mouse Auditory Cortex.* (2017) **Journal of Neuroscience.**
110. Zhao Y., Zhang J., Yang H., Cui D., Song J., Ma Q., Luan W., Lai B., Ma L., Chen M. & Zheng P. *Memory Retrieval in addiction: a Role for miR-105-Mediated Regulation of D1 Receptors in mPFC Neurons Projecting to the Basolateral Amygdala.* (2017) **BMC Biology.**
111. Abe K. & Yawo H. *Optogenetic Conditioning of Paradigm and Pattern Discrimination in the Rat Somatosensory System.* (2017) **PLOS One.**
112. Ketzef M., Spigolon G., Johansson Y., Bonito-Oliva A., Fisone G., & Silberberg G. *Dopamine Depletion Impairs Bilateral Sensory Processing in the Striatum in a Pathway-Dependent Manner.* (2017) **Neuron.**
113. Neske G.T. & Connors B.W. *Synchronized Gamma-Frequency Inhibition in Neocortex Depends on Excitatory-Inhibitory Interactions but not Electrical Synapses.* (2016) **Journal of Neurophysiology.**
114. Phillips E.A.K. & Hasenstaub A.R. *Asymmetric Effects of Activating and Inactivating Cortical Interneurons.* (2016) **eLife.**
115. Seybold B.A., Phillips E.A.K., Schreiner C.E., & Hasenstaub A.R. *Inhibitory Actions Unified by Network Integration.* (2015). **eLife.**
116. Joanna Ptasinski, Iam-Choon Khoo and Yeshaiahu Fainman *Phototuning Liquid Crystals for Photonic Integrated Circuit Applications.* (2015) **Iraqui Journal of Applied Physics.**
117. S Pierrick Guiral, Jean Marc Galvan, Guo Neng Lu, Patrice Jalade, Denis Dauvergne *Failure Detection Method for GaN-Based Dosimetric Systems.* (2015) **Key Engineering Materials.**
118. Jeeun Kang, Jin Ho Chang, Brian C. Wilson, Israel Veilleux, Yanhui Bai; Ralph DaCosta, Kang Kim, Seunghan Ha, Jong Gun Lee, Jeong Seok Kim, Sang-Goo Lee, Sun Mi Kim, Hak Jong Lee,Tai-Kyong Song *A prototype hand-held tri-modal instrument for in vivo ultrasound, photoacoustic, and fluorescence imaging.* (2015) **AIP Publishing.**

LED CONTROLLERS

An vital component in any illumination system is the LED controller. Mightex's world class design team has thoughtfully designed a portfolio of high performance, easy-to-use LED controllers, to make sure our customers can get the most from their LED system. Mightex's BLS-Series controllers offer excellent output current stability, along with very fast modulation frequencies (Up to 100kHz). Each BLS-Series Controller features BNC connections for all analog or TTL inputs/outputs and a safe, turn-key push-pull connectors for an easy connection with any Mightex LED.

Software & TTL LED Controllers

The BLS-SA and BLS-PL series LED controllers allow users the drive LEDs with a TTL trigger or with their PC through a Windows-based operation software featuring an intuitive, yet powerful, graphic user interface. Users can choose between a 2-channel and 4-channel model to drive multiple LEDs with different wavelengths and formats simultaneously. Furthermore, multiple control modules can be 'stacked' in software to support situations where more than 4 LEDs are required.

The controllers feature a linear design that eliminates light intensity ripples and oscillations often observed when low-cost buckpuck nonlinear drivers are used. Clean and highly repeatable current output is critical to quantitative experiments. The time resolution of the control module is 20μs and light intensity can be adjusted with 0.1% increments. Each driving channel on the control module has its own TTL trigger input. Rising edge, falling edge, and follower mode are supported in the trigger mode.

In addition to driving LEDs in a constant waveform mode (CW mode), these controllers also feature pulse mode to support applications where precisely-timed and high-intensity light pulses are required. For example, in optogenetics experiments to activate ChR2 or inhibit NpHR, pulses of <10ms are often used. To meet these requirements, Mightex has developed a proprietary "IntelliPulsing" technology to allow BLS-LEDs to output significantly higher power in pulse mode than what the LEDs are rated for in CW mode.

The control module can be operated without being connected to a computer. Once pulse sequences are programmed they can be stored into the control module (through software). A TTL trigger signal can then initiate the user-programmed pulse sequences. A software development kit (SDK) is also provided for user integration into environments such as LabView and MATLAB.

01

BLS-SA02-US

02

BLS-SA04-US

PERFORMANCE SPECIFICATIONS

Models[1]	BLS-SA02-US	BLS-SA04-US
Number of Channels	2	4
Power Supply Input Voltage, V_{dc} | V	9 - 24	
Per Channel Driving Current | mA	0 ~ 1,000[a] 0 ~ 3,500[b]	
Output Current Resolution | mA	12	
External Trigger	TTL	
Trigger Connector	BNC	
Trigger Input High Level | V	3.3 ~ 10.0	
Trigger Input Low Level | V	0.8 (Max)	
Timing Resolution | µs	20	
# of Data Points for Waveform Definition	2	
Trigger Pulse Width | µs	100 (Minimum)	
Maximum Trigger Delay | µs	25	
Optical Head Connector	2-pin Aero Connector	
Host Interface	USB or RS232, selectable	
On-Device Memory	Yes	
Device per Computer	Up to 16	

[1] Proper heat dissipation should be provided to the LED controller in order to prevent overheating, which may lead to self-shutdown by the LED controller for protection purposes. In addition, the total output current of all channels should not exceed the capacity of the power adaptor.
[2]Maximum Output Voltage V_{max} is 0.5V less than the Power Supply Input Voltage (V_{dc}). For instance, with a Power Supply Input Voltage of V_{dc} = 24V, the Maximum Output Voltage V_{max} would be 23.5V.
[a] Under normal mode.
[b] Under strobe or trigger mode.

Manual & Analog LED Controllers

Mightex BLS-Series manual and analog controllers feature the latest technology for LED drivers. Customers can choose between four different models depending on the LED(s) they are operating: (1) the BLS-1000-2, (2) the BLS-3000-2, (3) the BLS-13000-1E, and (4) the BLS-18000-1, with the last two designed specifically to operate Mightex's Type H super high-power LEDs. All BLS-Series controllers feature a linear design that eliminates light intensity ripples and oscillations often observed when low-cost buckpuck nonlinear drivers are used. These controllers are also capable of achieving extremely fast modulation frequencies. The BLS-1000-2 for example is capable of a maximum modulation frequency of 100kHz in analog mode. When the controller is set to "trigger" mode, the output current is fully controlled by the user's analog control signal (0-5V). The output current can also be controlled with high precision manual knobs. The control mode is selected with a slide switch on the front panel. The controller also provides maximum current selection DIP switches on the rear panel which allows the user to set the maximum current of the channel to either 500mA, 750mA and 1000mA for BLS-1000-2, and either 1,000mA, 2,000mA and 3,000mA for BLS-3000-2.The factory default is set to 500mA for BLS-1000-2 and 1,000mA for BLS-3000-2, respectively. BLS-13000-1E and BLS-18000-1 have only one maximum current setting - 13,000mA and 18,000 mA respectively.

BLS-1000-2

BLS-3000-2

BLS-13000-1E

BLS-18000-1

PERFORMANCE SPECIFICATIONS

Models	BLS-1000-2	BLS-3000-2	BLS-13000-1E	BLS-18000-1
Current Accuracy | mA	±3%			
Number of Channels	2		1	
Power Supply Input Voltage (V_{dc}) | V	9-12[a]	9	48	12
Power Supply Input Current (I_{dc}) | A	> Total/combined channel current[b]		2.5	13.75
Maximum Output Voltage (V_{max}) | V	V_{dc} - 4.5V	V_{dc} - 4V	5.5	7.5
Maximum Per Channel Output Current (I_{max}) | mA	1000	3000	13000	18000
Maximum Per Channel Output Power (P_{max}) | W	20	15	72	135
Max Modulation Frequency | KHz	100	50	3	
External Analog Input[c] | V	0-5			

[a] When forward voltage of LED load is greater than 8V, 24V DC input might be used.
[b] External analog voltage source should have 8+ mA of current driving capability.
[c] The input current should be greater than the combined output current of the two channels.

DIMENSIONS

Models	Weight |g	Size (lxwxh) |mm
BLS-1000-2 | BLS-3000-2	600	160x157x68
BLS-13000-1E | BLS-18000-1	1300	221x156x96

MICROSCOPY CAMERAS

Cameras serve a crucial role across many bioscience fields. Mightex offers several excellent cost effective microscopy camera choices. Our general purpose CMOS camera with standard C-Mount interface is a strong choice for bright-field applications and teaching labs. Fluorescence CCD cameras are excellent for both imaging and as a measurement tool for most fluorescence microscopy applications. Engineered by our team of leading optical and electronic engineers, Mightex CCD cameras are well-priced, reliable, and have excellent performance, ensuring that our customers get the most value from their camera.

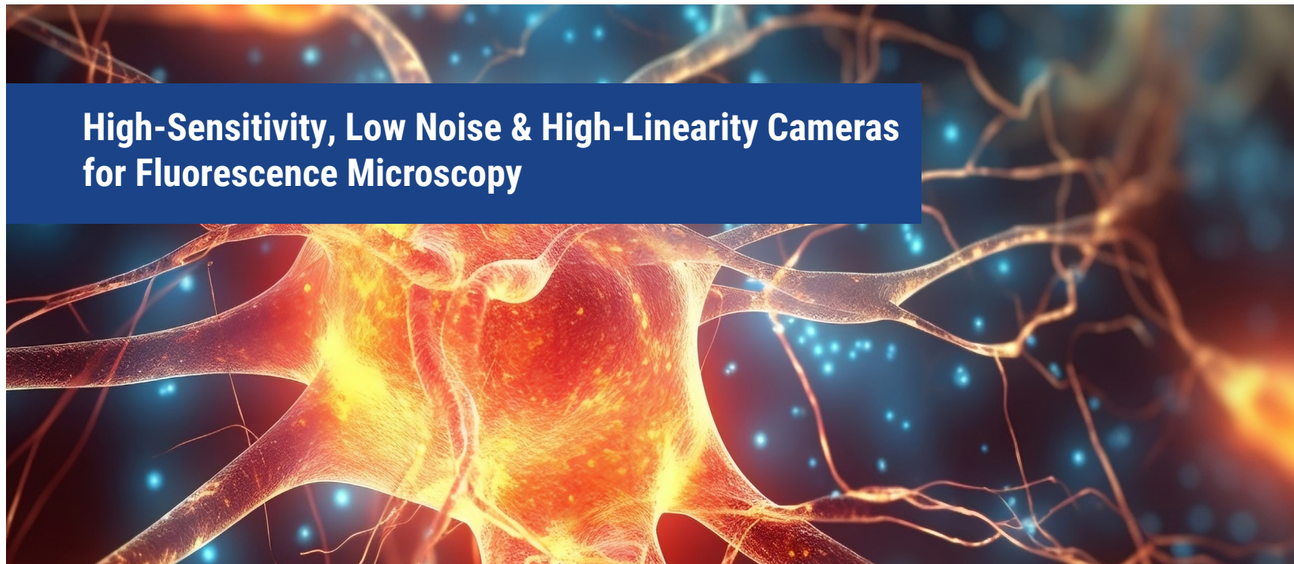

CMOS General Microscopy Cameras

The SCE-series is Mightex's entry level general purpose microscopy camera. The SCE Series is a low cost imaging solution featuring a 1/3" 1.3 MP CMOS sensor with 5.2µm x 5.2µm size pixels. SCE series camera has a 20fps frame rate at full resolution, and higher frame rates can be achieved in ROI mode. Applications include transmitted light microscopy and wide-field imaging in research or teaching lab environments. The low cost of the SCE-series camera makes it a great choice as a general purpose microscopy camera.

01

SCE-B013-U

APPLICATIONS
- Transmitted light microscopy
- Live cell imaging
- Teaching lab equipment

Models	SCE-B013-U
Number of GPIOs	4
Resolution	1,280 x 1,024
CMOS Chip	½" (5:4) Micron MT9M001, Rolling Shutter
Pixel Size | µm	5.2 x 5.2
Active Imager Size | mm	6.66 x 5.32
Dynamic Range | dB	68
Sensor SNR | dB	45
Responsivity | V/lux-sec	2.1
Frame Rates* (@48MHz Clock) | fps	20 @1280 x 1024 31 @1024 x 768 45 @800 x 600 52 @752 x 480 52 @640 x 480 120 @320 x 240
Shutter Speed (Exposure Time) | ms	1 ~ 750
Hardware Gains	0.125x ~ 8x
Trigger Cable	
Strobe Out	Yes
Lens Mount	CS-mount or C-mount
Built-in Filters	IR-cut (factory standard), IR-pass or No filter
Power Consumption | W	< 1.0

* Actual achievable frame rate depends on exposure time, as well as available resources of the host PC system.

DIMENSIONS

Models	Weight (excluding lens) |g	Size (hxwxd) |mm	
		CS-mount	C-mount
SCE series	120	45x45x23	45x45x28

SYSTEM REQUIREMENTS

Processor	Pentium III 900 MHz or better, or a compatible processor
Operating System	Windows XP, Vista, 7, 8, and 10
RAM	256MB or greater
Hard Disk Space	30MB for software installation, plus additional space for storing captured images
Display	24 bit True Colour
USB2.0 Host Controller	Intel Integrated USB2.0 Host Controller is recommended

CCD Microscopy Cameras

Mightex C-series CCD USB 2.0 area cameras provide higher sensitivity than CMOS cameras. They are are optimized for fluorecensce imaging, and they can also be used for a wide variety of other microscopy applications where quality, ease of use, and cost-effectiveness are crucial. These cameras have external trigger-in and strobe-out. A USB command set protocol is provided for non-Windows based applications. A Linux driver is also available upon request.

01

CGE-B013-U/CGE-C013-U

02

CXE-B013-U/CXE-C013-U

APPLICATIONS

- Live cell fluorescent imaging
- Fluorescent protein imaging
- Ratiometric imaging
- Immunofluorescence imaging
- Phase contrast, DIC & bright-field

PERFORMANCE SPECIFICATIONS

Models	CXE-B013-U	CXE-C013-U	CGE-B013-U	CGE-C013-U
Number of GPIOs	4	4	4	4
Resolution	1,392 x1,040		1,280 x 960	
CCD Chip	2/3" Sony ICX285AL Global Shutter	2/3" Sony ICX285AQ Global Shutter	1/3" Sony ICX445AL Global Shutter	1/3" Sony ICX445AK Global Shutter
Bit | bit	8 or 12			
Pixel Size | µm	6.45 x 6.45		3.75 x 3.75	
Active Imager Size | mm	(Diagonal) 11.0		6.26 x 5.01	
Scanning System	Progressive			
On-Board Memory | MB	N/A			
Frame Rates* (@28MHz Clock) | fps	15 @1392 x 1040 29 @696 x 520 (2x2 Bin) 37 @464 x 344 (3x3 Bin) 49 @348 x 256 (4x4 Bin) 49 @348 x 256 (1:4 Skip)		20 @1280 x 960 38 @640 x 480 (2x2 Bin) 53 @424 x 320 (3x3 Bin) 66 @320 x 240 (4x4 Bin) 66 @320 x 240 (4x4 Bin2)	
Sub Resolutions	696 x 520(2x2 Bin) 464 x 344 (3x3 Bin) 348 x 256 (4x4 Bin) 348 x 256 (1:4 Skip)		640 x 480(2x2 Bin) 424 x 320(3x3 Bin) 320 x 240(4x4 Bin) 320 x 240 (1:4 Bin2)**	
Shutter Speed (Exposure time) | ms	0.05~200,000			
Hardware Gains | dB	6 ~ 43		6 ~ 41	
Trigger Mode	With external trigger			
Trigger Cable	ACC-CAM-DIN8		ACC-CAM-CON8	
Trigger Delay | µs	< 25			
Strobe Out	Yes			
Lens Mount	C– mount or CS-mount (M12.5-mount or custom-defined lens mount supported)			
Built-in Filters	IR-cut (factory standard), or IR-pass, or no filter			
Power Consumption | W	< 1.8			

* Actual achievable frame rate depends on exposure time, as well as available resources of the host PC system.

DIMENSIONS

Models	Weight (excluding lens) |g	Size (hxwxd) |mm	
		CS-mount	C-mount
CGE series	115	45x45x30.5	45x45x35.5
CXE series	150	95x70x38.5	95x70x43.5

Mightex is empowering bioscience researchers with market-leading optical stimulation & imaging tools, enabling scientists to push the boundaries of life science research.

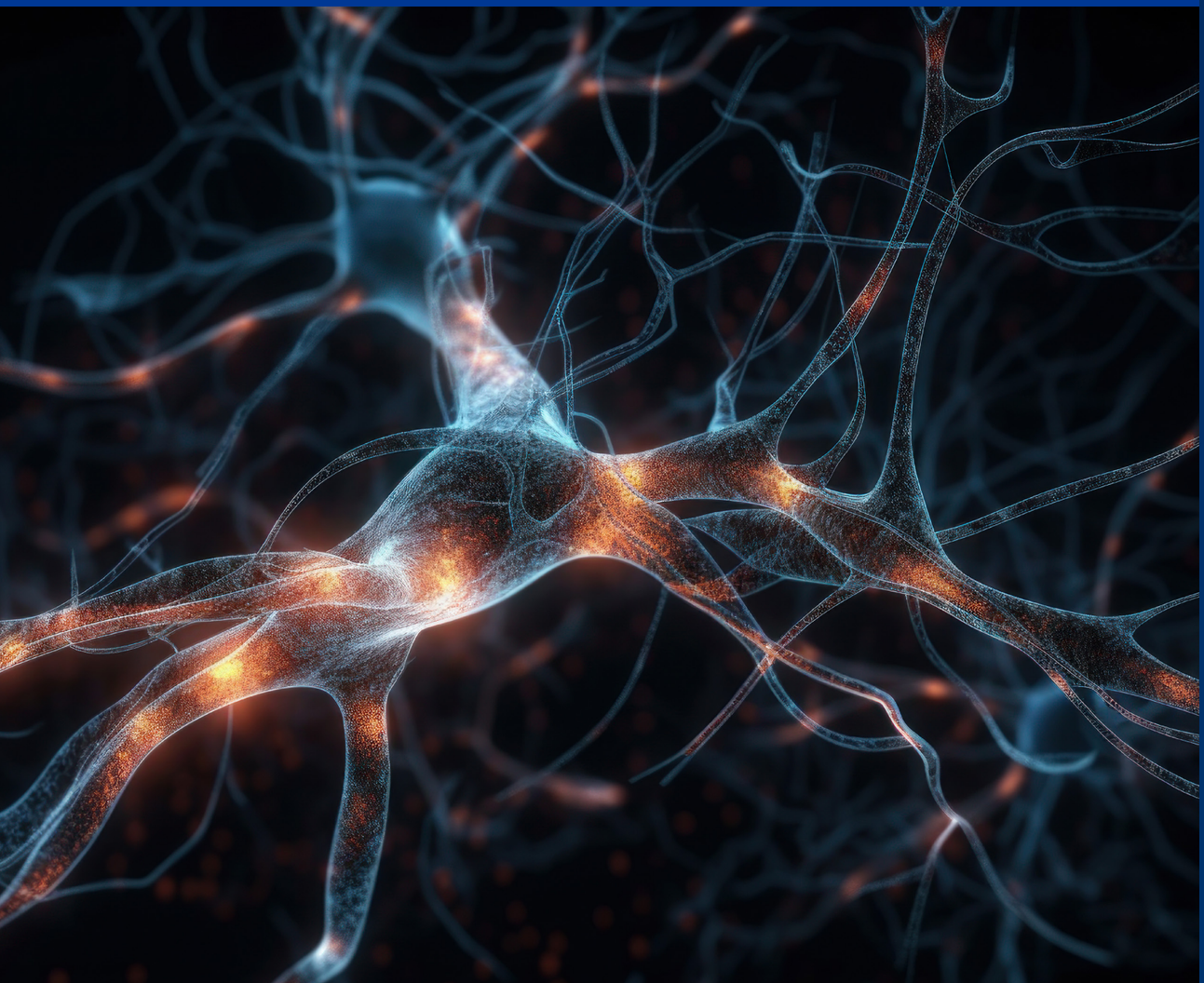

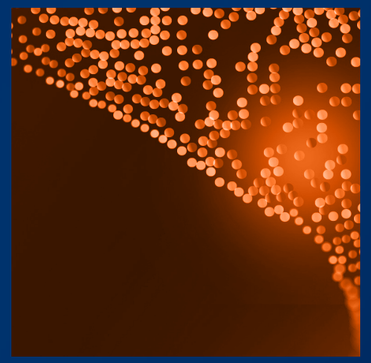

MIGHTEX

PAYMENT TERMS

US and Canadian customers are eligible for NET-30 terms upon credit approval. International customers require prepayment via credit card, wire transfer, or money order. Multiple payment methods are avaialble including VISA, MasterCard, Discover, American Express, PayPal and eCheck.

SHIPPING

All shipping is made from California, USA unless otherwise stated. A street address is required. If you have a post office box only, we will ship via US Postal Service.

QUOTATION

You may obtain an official quotation (including shipping cost) by contacting a sales representative. Please visit www.mightexbio.com to request a quote online or call us at 1-925-218-1885 to speak with a Mightex sales representative directly.

SPECIFICATIONS

Listed specifications are accurate as of the publication date, and they may change without prior notice due to product improvements and design changes.

POLICIES AND CONDITIONS

All Mightex Company policies including Cancellation and Return policy, Warranty Terms and Conditions, Sales Terms and Conditions, and Privacy policy are available online at

www.mightex.com

CONTACT US

CANADA OFFICE

111 Railside Road
Suite 201
Toronto, ON
M3A 1B2
1-416-840-4991

US OFFICE

1241 Quarry Lane
Suite 105
Pleasanton, CA
94566
1-925-218-1885

WWW.MIGHTEX.COM